Fall 1974

A study of the feasibility in obtaining the kinetics of various ordering phenomena of the iron aluminum system utilizing the Mössbauer effect

Lloyd Rollan Chapman

Department:

A STUDY OF THE FEASIBILITY IN OBTAINING THE KINETICS OF VARIOUS ORDERING PHENOMENA OF THE IRON ALUMINUM SYSTEM UTILIZING THE MÖSSBAUER EFFECT

BY

LLOYD ROLLAN CHAPMAN

A

PAPER

submitted to the faculty of the

UNIVERSITY OF MISSOURI AT ROLLA

in partial fulfillment of the work required for the

Degree of

MASTER OF SCIENCE IN METALLURGICAL ENGINEERING

Rolla, Missouri

1974

ABSTRACT

The determination of the kinetics of ordering for various ordering phenomena of the Iron-Aluminum system utilizing exclusively the Mössbauer effect technique is shown to be infeasible for all but a highly restrictive consideration from experimental as well as theoretical evidence. Also, the possible use of the Mössbauer effect for the analysis of other ordered systems is discussed.

An alternative method for the acquisition of the needed information utilizing diffraction and Mössbauer techniques is presented recognizing the need for a computer fitting analysis of the complex Mössbauer effect spectra. However, at this stage of investigation, no experimental work has been performed using the alternative method.

ACKNOWLEDGEMENTS

The author wishes to express his appreciation to Dr. H. P. Leighly Jr., Professor of Metallurgical Engineering, and Dr. Gary J. Long, Associate Professor of Chemistry, for their assistance throughout this investigation.

He also wishes to extend his gratitude to Dr. Manfred R. G. Wuttig, Professor of Metallurgical Engineering, for valuable suggestions and cooperation.

He also conveys his thanks to Mr. James T. Wrobleski for his valuable assistance with the computer fitting procedure and the operation of the Mössbauer spectrometer.

TABLE OF CONTENTS

LIST OF FIGURES

LIST OF TABLES

CHAPTER 1

INTRODUCTION TO THE MÖSSBAUER EFFECT

Alloying is an adulteration of a pure metal by another metal and the location of these foreign atoms in the crystal lattice of the host metal is of condern. If the foreign atoms merely replace atoms of the parent metal on some of the lattice sites, the alloy is known as a substitutional solid solution. For many years researchers supposed that the replacement of atoms of one element by those of another to form a primary substitutional solid solution did so by a purely random replacement. As theory progressed, the question of whether the atoms of different kinds may be distributed in an ordered distribution arose. Present knowledge verifies that there are indeed possible ordered distributions.

Presently there are two types of approaches for the study of the distribution of the atoms over the lattice points. The secondary approach observes changes of some physical property of the alloy upon its ordering. Dilatometry and electrical resistivity are the most commonly used secondary techniques. The primary approach involves the direct observation of the ordering process; of course, this cannot be accomplished presently, but there does exist pseudo primary approaches. Of these, diffraction techniques, electron microscopy and Mössbauer effect are the most commonly used.

Since 1923, X-Ray diffraction served as the major tool for the study of ordered systems; however, with the work of Rudolf L. Mössbauer

in 1957, a new tool for the study of atomic order became available, although not immediately recognized. Since the Mössbauer effect or the recoiless gamma ray fluorescence is utilized in the present study, the following discussion introduces the physical concepts of the Mössbauer effect and progresses to its application in the study of atomic order.

Mössbauer's discovery rests on the realization that some of the energies associated with nuclear events are not larger than those of lattice vibrations. The energies in question are those associated with the recoil imparted to a nucleus by the emission of a low energy gamma ray and are analogous to the recoil associated with the firing of a rifle. As expected, the nuclear recoil is a small energy and before Mössbauer's work the energy of a gamma ray was impossible to measure with sufficient precision to detect such a small energy difference. With the discovery of recoil free emission and resonant absorption of nuclear gamma rays in solids by Mössbauer, this energy difference could be measured. Before exploring the far reaching consequences of this discovery, a consideration will be made of the term 'resonant absorption' which appeared in the above discussion.

Acoustic resonance is easily demonstrated with two tuning forks having the same frequency. If one is struck, the other will also begin to vibrate because it is driven by the sound waves emanating from the first one.

At the beginning of this century resonance in atomic systems was demonstrated by R. W. Wood who used the yellow light emitted by sodium atoms; the sodium D lines which was produced by NaCl placed in a flame. Each of these D lines of definite frequency and wavelength may be considered as corresponding to a natural vibration frequency of the sodium

outer electrons. When the light from the sodium flame is focused on an evacuated bulb filled with sodium vapors, a yellow glow is observable. The sodium atoms in the bulb are acting in a manner similar to that of the second tuning fork where they are abstracting energy from the incident beam of yellow light and reradiating it in all directions, i.e., producing resonance fluorescence. If other atoms are not 'tuned' to the sodium D lines no effect will be observed.

From a quantum mechanical point of view, the characteristic light emitted by the sodium atoms may be considered the result of an electronic transition between the ground state and an excited state of the sodium atom. The energy difference between these two states is radiated as a photon of specific energy and resonant absorption results if the incident photon has just the correct energy to raise an atom of sodium vapor to an excited state.

Only a small extension of this concept is needed to ask whether the same experiment could also be performed with other electromagnetic radiation such as the gamma rays emitted by nuclei.

Investigating this possibility, consider a free nucleus of mass M with two energy levels A and B separated by an energy E_r. If the system decays brom B to A by emission of a gamma ray of energy E_g, momentum conservation demands that the momentum p of the gamma ray and the momentum P of the recoiling system be equil and opposite. The recoil energy of the emitting nuclei may be determined in terms of the gamma ray energy from the conservation of momentum. Actually, the recoil energy is very small compared to the gamma ray energy and from energy conservation this becomes apparent. Equations 1 and 2 illustrate these relationships.

As earlier stated, the fraction of the available energy which is

Eq 1

$$R_{\text{recoil energy}} = \frac{P^2}{2M} = \frac{p^2}{2M} = \frac{E_g^2}{2Mc^2}$$

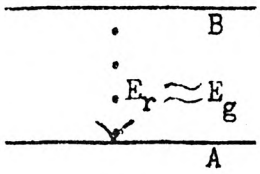

Eq 2

$E_r = E_g + R \qquad R << E_g$

$E_r \approx E_g$

Therefore $R \approx E_r^2 / 2Mc^2$

and $E_r << Mc^2$ therefore R (recoil energy) is very small.

lost to the emitting atoms as a recoil energy is small and before Mössbauer's work was impossible to measure. Nevertheless, the recoil energy lost does become significant when compared with the inherent width of the gamma ray, i.e., the precision with which its energy is defined by the properties of the nucleus. This finite width arises from the finite time, characterized by the halflife of the state which the nucleus spends in the excited state. In essence, it is a result of the uncertainity principle of energy and time. The uncertainity in energy corresponds to the width Γ of the excited nuclear state and appears also as the linewidth of the gamma ray, while the uncertainty in time corresponds to the meanlife τ of the excited nuclear state. A lifetime $\tau_{\frac{1}{2}} = 10^{-7}$ seconds (a typical value) results in a linewidth of 4.6×10^{-9} ev which is very much smaller than the energy lost in the nuclear recoil: 10^{-7} ev.

Eq 3

$$\Gamma \cdot \tau = \hbar \qquad \Gamma = \frac{0.0693\,\hbar}{\tau_{1/2}}$$

When an emitted gamma ray of energy E_g and momentum p strikes the absorber of mass M, which is initially at rest, the entire momentum p is

transferred to the absorber; the absorber thus recoils and the energy of recoil R is again given as before. In order to excite a level of energy E_r, the transition energy from state A to B, to achieve resonance absorption in the absorber, the incoming gamma ray must have an energy $E_r + R$ to compensate for the recoil of the absorber; however, only an energy $E_r - R$ is available for the excitation of internal degrees of freedom due to the recoil energy loss of the emitter. Resonance absorption can occur only if some of the incoming gamma rays possess enough energy to reach the state B and at the same time provide the energy R to the recoiling absorber. For resonance absorption to be

Figure 1

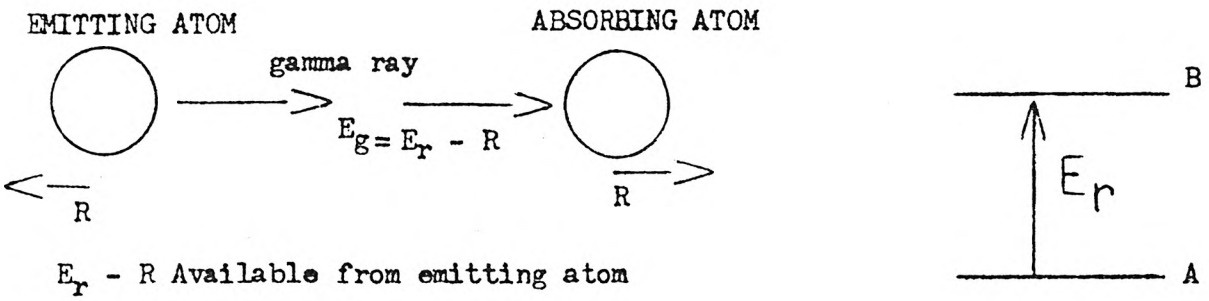

$E_r - R$ Available from emitting atom

$E_r + R$ Required to excite absorber to excited state

Equation 4

REQUIREMENT FOR RESONANCE ABSORPTION

$$2R \lesssim \Gamma$$

possible, the following relation expressed by equation 4 must be met in which case there is an overlap of the two spectra resulting in resonance absorption. For the nuclear gamma ray process considered, the absorption is not possible as illustrated by figure 2. For optical systems as with the sodium gas mentioned earlier, the condition for resonance absorption is generally met and is readily observable for optical

FIGURE 2

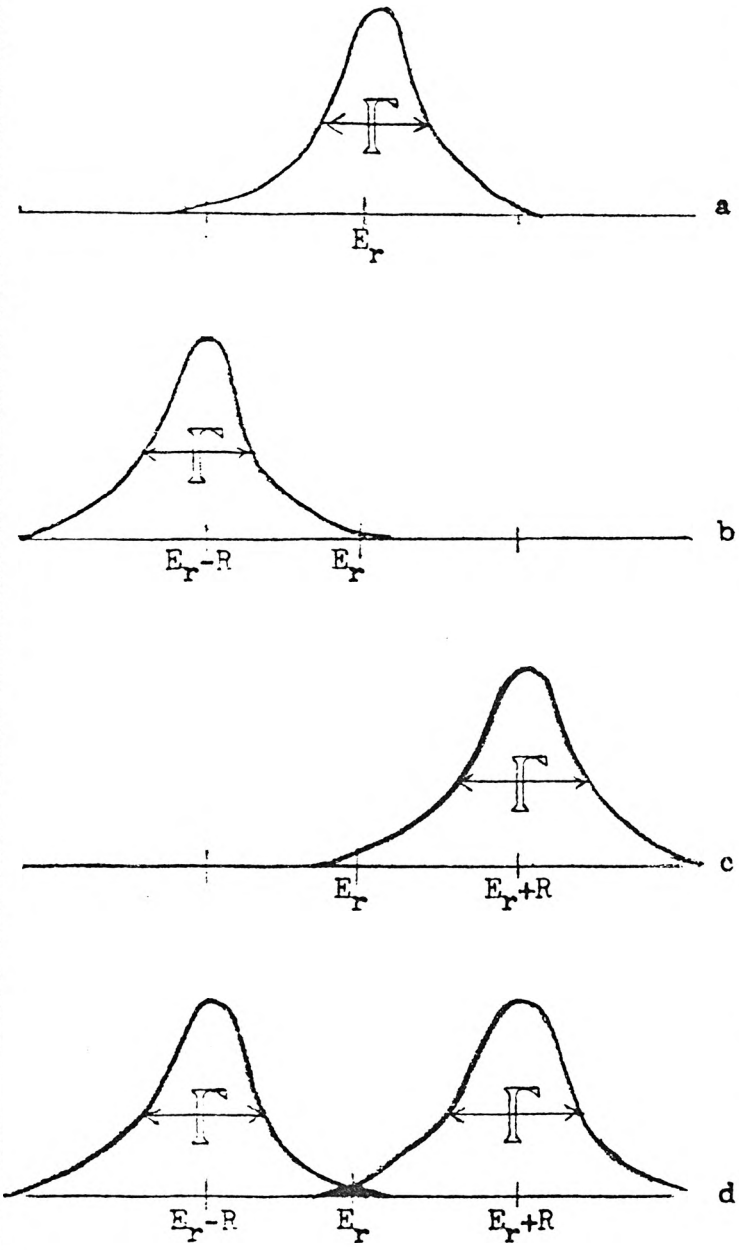

ENERGY DISTRIBUTION OF EXCITED STATE B GIVING THE LINEWIDTH Γ

ENERGY DISTRIBUTION OF GAMMA RAY EMITTED BY TRANSITION B→A

ENERGY SPECTRA NEEDED TO EXCITE STATE B IN TARGET

OVERLAP OF b and c

OVERLAP AREA IS RESPONSIBLE FOR RESONANCE ABSORPTION

THE CONDITION FOR OVERLAP AND THUS RESONANCE ABSORPTION IS:

$$2R \leq \Gamma$$

systems.

Previously, the emitting and the absorbing systems were assumed to be at rest; actually, source and target atoms are in thermal motion and this motion produces an additional separation of the emission and absorption lines called Doppler broadening. This broadening produces an added component to the recoil energy as shown in figure 3.

Figure 3

$E_g = E_r + R + \text{DOPPLER TERM}$

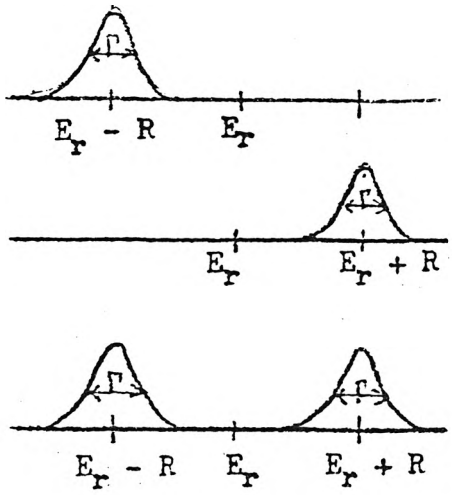

Doppler broadening causes further separation of absorption and emission lines

For the ideal observation of nuclear resonance absorption, the incoming gamma ray should possess an energy distribution of width identical to the width of the absorbing state and with its energy centered at E_r. This implies that (1) the recoil energy R is either negligible or has been compensated for, and that (2) emitting and absorbing states are identical and are not broadened by external influences. If these two conditions are met, the cross section for nuclear resonance absorption is large as illustrated in figure 4. In nuclear experiments both conditions may be fulfilled by several means.

Condition (1) is fulfilled upon the realization that a crystalline solid is a mechanical system whose vibrational properties must be described in quantum mechanical terms. The vibration of a lattice is

FIGURE 4

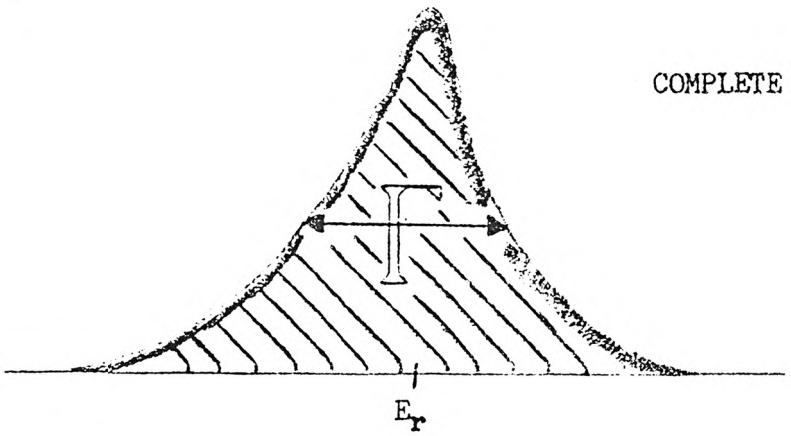

analogous to an oscillator and is characterized by the quantum numbers of its oscillation where the only possible changes in its state are an increase or decrease in one or more of the quantum numbers. The emission of a gamma ray is accompanied by the transfer of integral multiples of the phonon or lattice vibrational energy to the lattice; $(0,\pm h\nu,\pm 2h\nu,\ldots)$, and if an average is taken over many emission processes, the energy transferred per event is exactly the free-atom recoil energy.[1] The possibility of no energy transfer to the lattice exists and let f be the fraction of events which takes place without lattice excitation or zero phonon events. This recoil free fraction of the emitted gamma ray possess the full energy of the nuclear transition and therefore the required energy to excite the absorber nucleus to an excited state, i.e., E_r+R. Noting that n which is the quantum vibrational state of the lattice approaches zero at low temperatures, the recoil free fraction f increases; therefore, many experiments are performed at low temperatures. Condition (1) is currently satisfied.

EQUATION 5

$$f = 1 - \frac{R}{\hbar\omega}\left(1 + 2n\right)$$

The widths Γ of these gamma rays shown in figures 2 and 4 are so small that it is exceedingly unlikely that a gamma ray from a nuclear transition in one isotope can be resonantly absorbed by another. Mössbauer effect experiments are therefore carried out with sources and absorbers utilizing the same nuclear transition as depicted by figure 5. If this procedure is followed, then condition (2) is fulfilled.

FIGURE 5

Radioactive Source for use with Fe^{57} Absorber

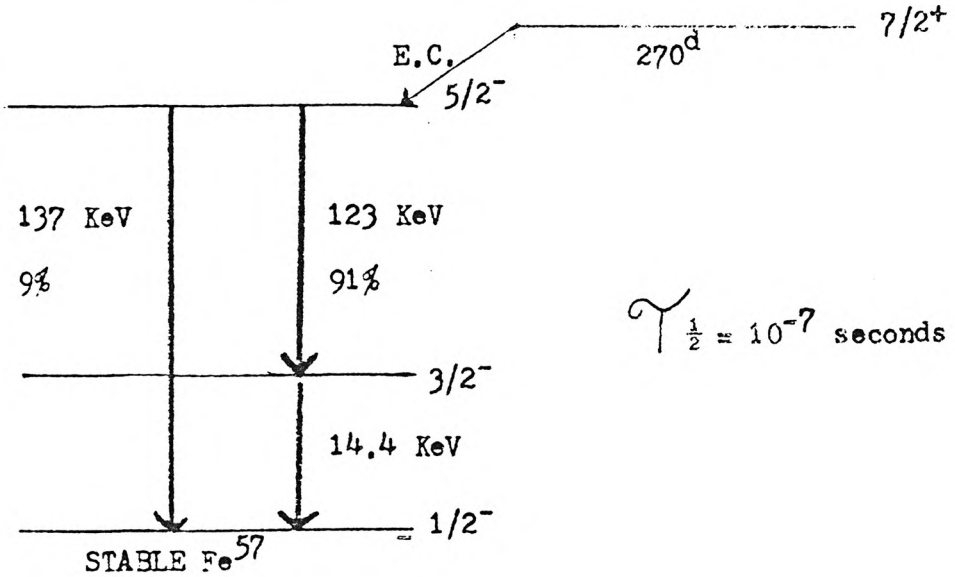

Co^{57} decays by electron capture to an excited state of Fe^{57} which then emits the Mössbauer gamma ray which interacts with the target containing Fe^{57}.

In the operation of an automatic Mössbauer effect spectrometer, the energy of the gamma ray of a radioactive source is Doppler modulated to sweep repeatedly across the region of resonant absorption of the absorber which contains nuclei of the same species. The gamma ray detector output is sorted into storage registers in a multichannel analyzer whose access is synchronized with the Doppler velocity of the source as illustrated by figure 6. The results are absorption spectra like those shown in figure 7 where the energy scale is usually repre-

FIGURE 6

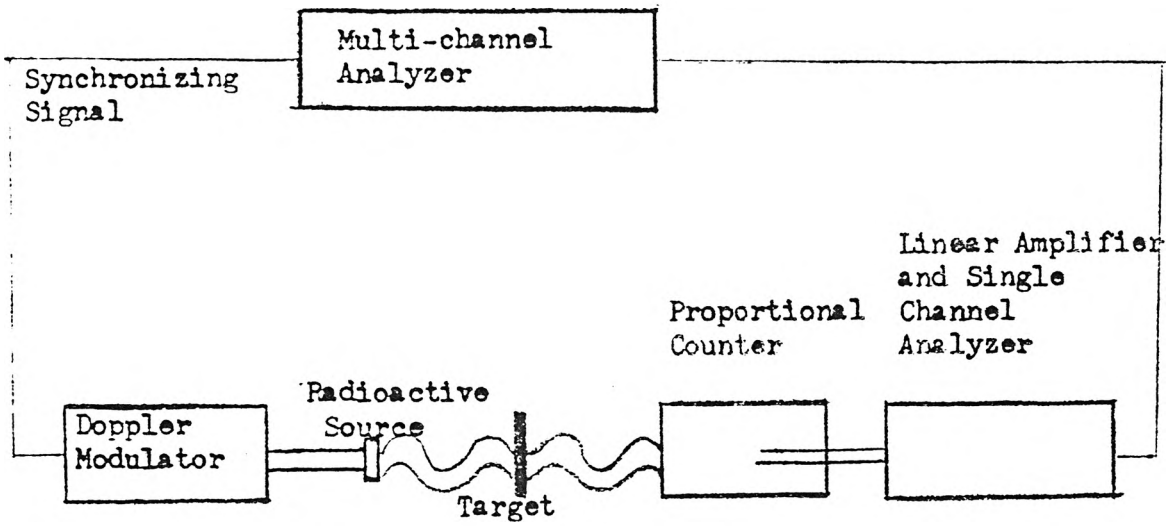

DIAGRAM OF THE MÖSSBAUER EFFECT SPECTROMETER

FIGURE 7

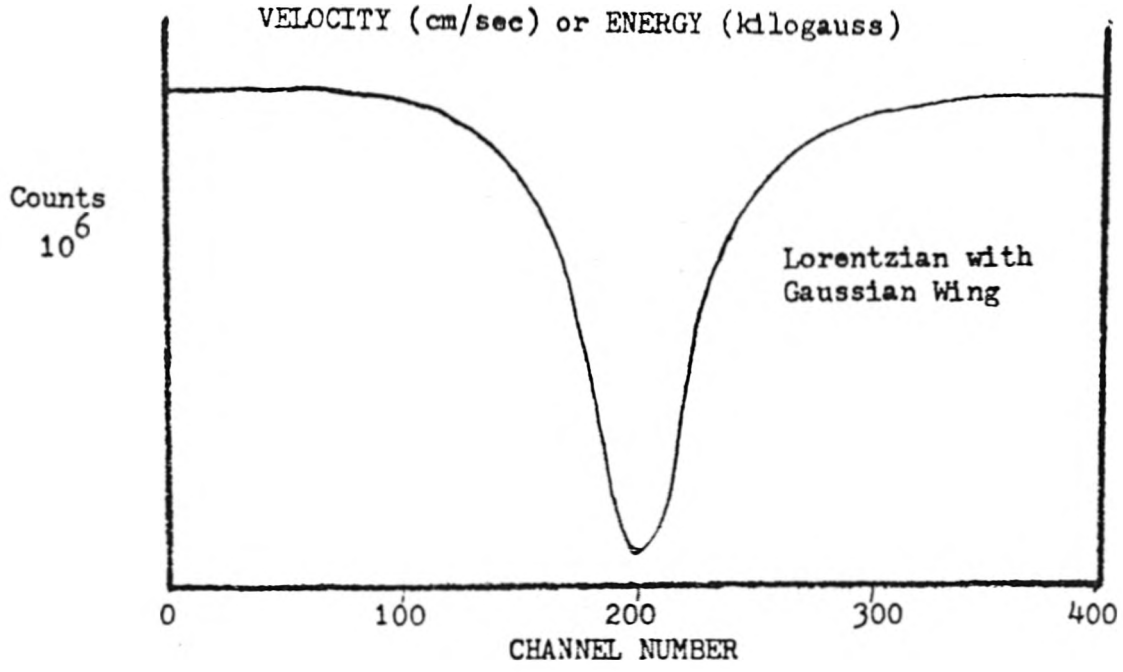

MÖSSBAUER EFFECT SPECTRUM

sented by the Doppler velocity. The Doppler velocity, $\vec{V}$, relationship to the energy shift δE is expressed by equation 6. The purpose of the Doppler modulation is to permit an examination of a region of the spectrum near the unperturbed energy of the gamma ray; thus allowing the spectrometer to map out the total energy absorption region as shown in figure 9.

EQUATION 6

$$\frac{\delta E}{E_r} = \frac{\vec{V}}{C}$$

The Mössbauer effect spectrometer enables the comparison of the nuclear transition energies in two materials with high precision. At first thought this does not appear to be a valuable accomplishment, unless the levels are split, because one tends to believe that the nuclear levels are themselves fixed in position. However, the nucleus is surrounded and penetrated by electronic charge with which it interacts electrostatically. A change in the s-electron density such as might arise from a change in valence will result in an altered Coulombic interaction which manefests itself as a shift of the nuclear levels. This effect is part of the elctric hyperfine splitting (hfs) i.e., the splitting of the lines of an atomic spectrum produced by the angular momentum of the nucleus of the atom and is called the Isomer Shift or Center Shift (C.S.). This shifting of the nuclear levels is conceptually seen by the following Mössbauer effect spectrum; figures 8 and 9.

The preceding discussion assumed the nucleus to be spherical and the charge density to be uniform. If these restrictions are relaxed,

FIGURE 8

ISOMER SHIFT AFFECT UPON THE MÖSSBAUER EFFECT SPECTRUM

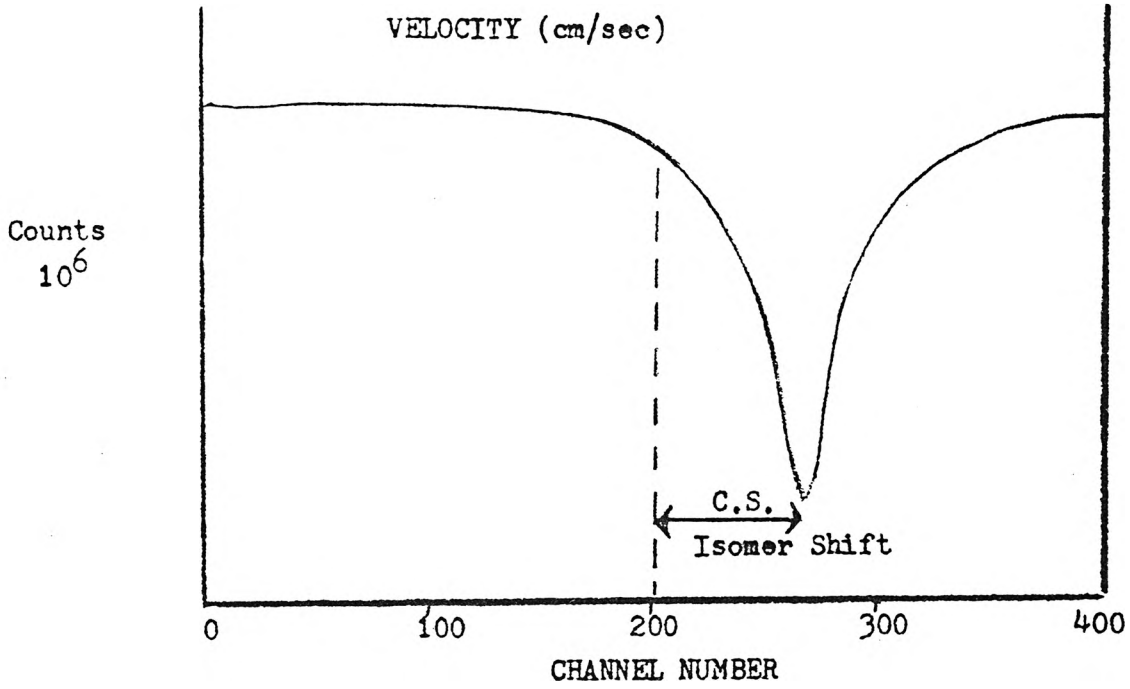

FIGURE 9

ISOMER SHIFT AFFECT UPON THE NUCLEAR ENERGY LEVELS

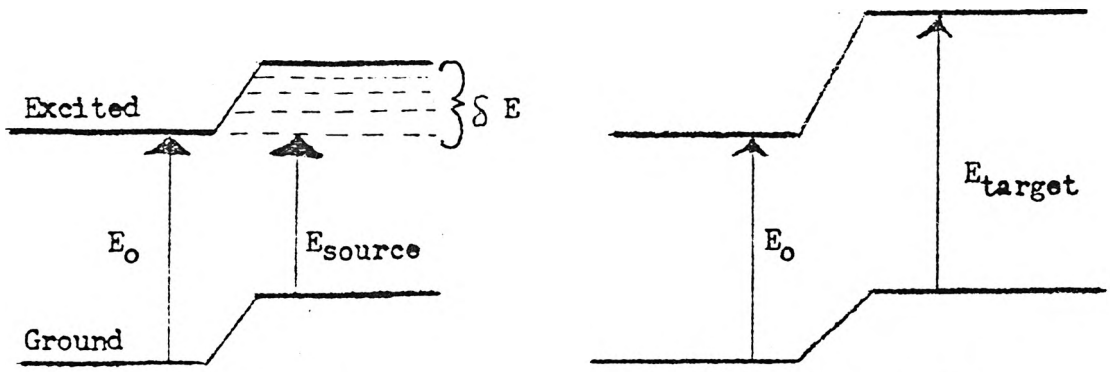

EMITTER or SOURCE ABSORBER or TARGET

ISOMER SHIFT = $E_{target} - E_{source}$

The Isomer Shift (or Center Shift C.S.) shifts nuclear levels without lifting the spin degeneracy.

higher order terms of the electrostatic interaction appear. These higher order terms do not shift the nuclear levels, they split them, i.e., they lift all or part of the degeneracy levels. This splitting results from the interaction of the nuclear quadrupole moment, Q, with the gradient of the electric field with changes in the crystal. A change in the local environment of the atom as illustrated by different degrees of order for an ordered system can cause such a change in the symmetry thereby invoking the higher order considerations. This property reflects the deviation of the nucleus from spherical symmetry and is known as the Quadrupole Splitting (QQ). The affect upon the Mössbauer effect spectrum is illustrated by figures 10 and 11.

The most familiar part of the hyperfine structure is the magnetic part arising from the interaction of the nuclear magnetic dipole moment with the magnetic field due to the atom's own electrons. This affect upon the Mössbauer effect spectrum is presented in figures 12 and 13.

The Mössbauer effect may be utilized to study the order of a system due to its sensitivity to the local electronic environment about an absorbing nuclide. Each different electronic environment about an absorbing nuclide will produce its own hyperfine splitting structure (hfs) characteristic of the local environment of the absorbing atom. Recognizing that an ordered structure possesses a definite atomic environment of other atoms at each degree of order and knowing that the structure of this environment will affect the electronic environment of the absorbing nuclide, the ordering of a system may be studied by observing the change of environment upon ordering as exhibited by the changing Mössbauer spectra.

FIGURE 10

QUADRUPOLE SPLITTING OF THE MÖSSBAUER EFFECT SPECTRUM

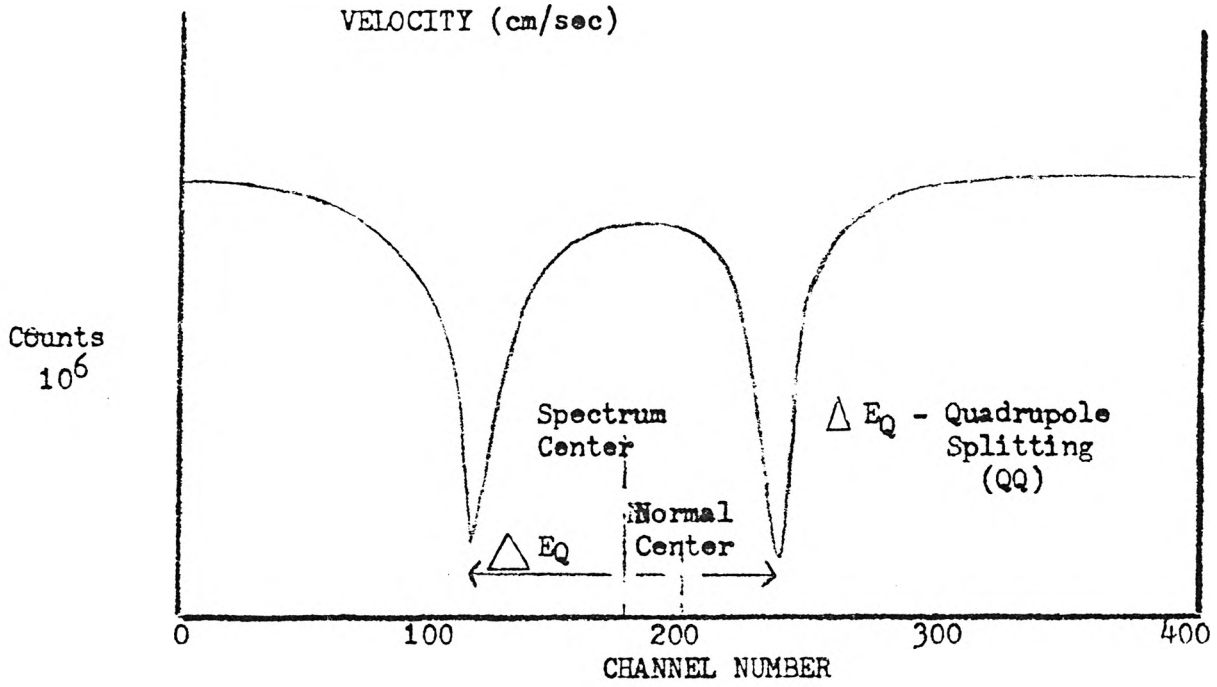

FIGURE 11

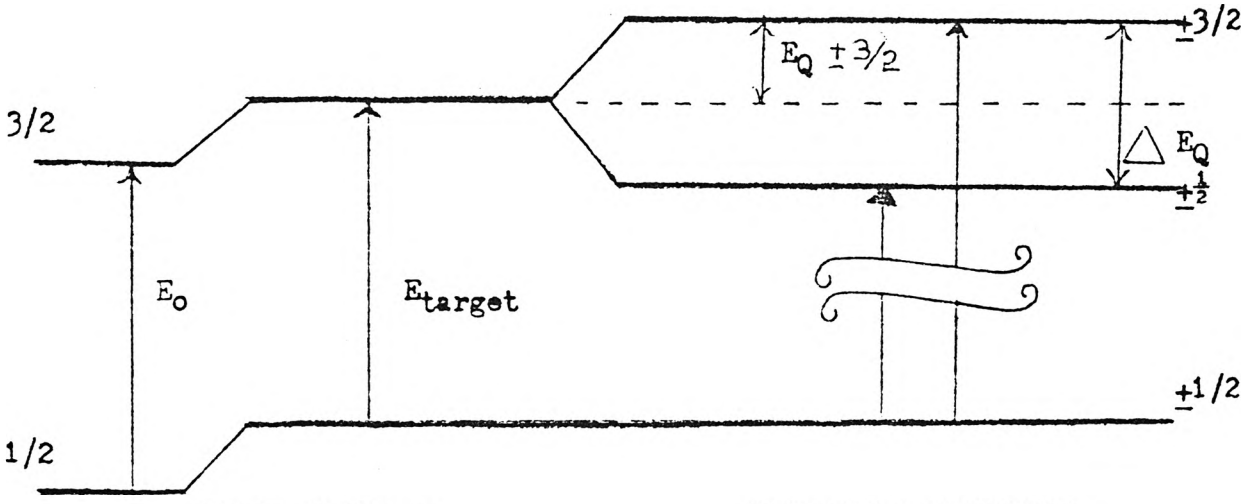

$\Delta E_Q = E_Q (3/2) - E_Q (1/2)$

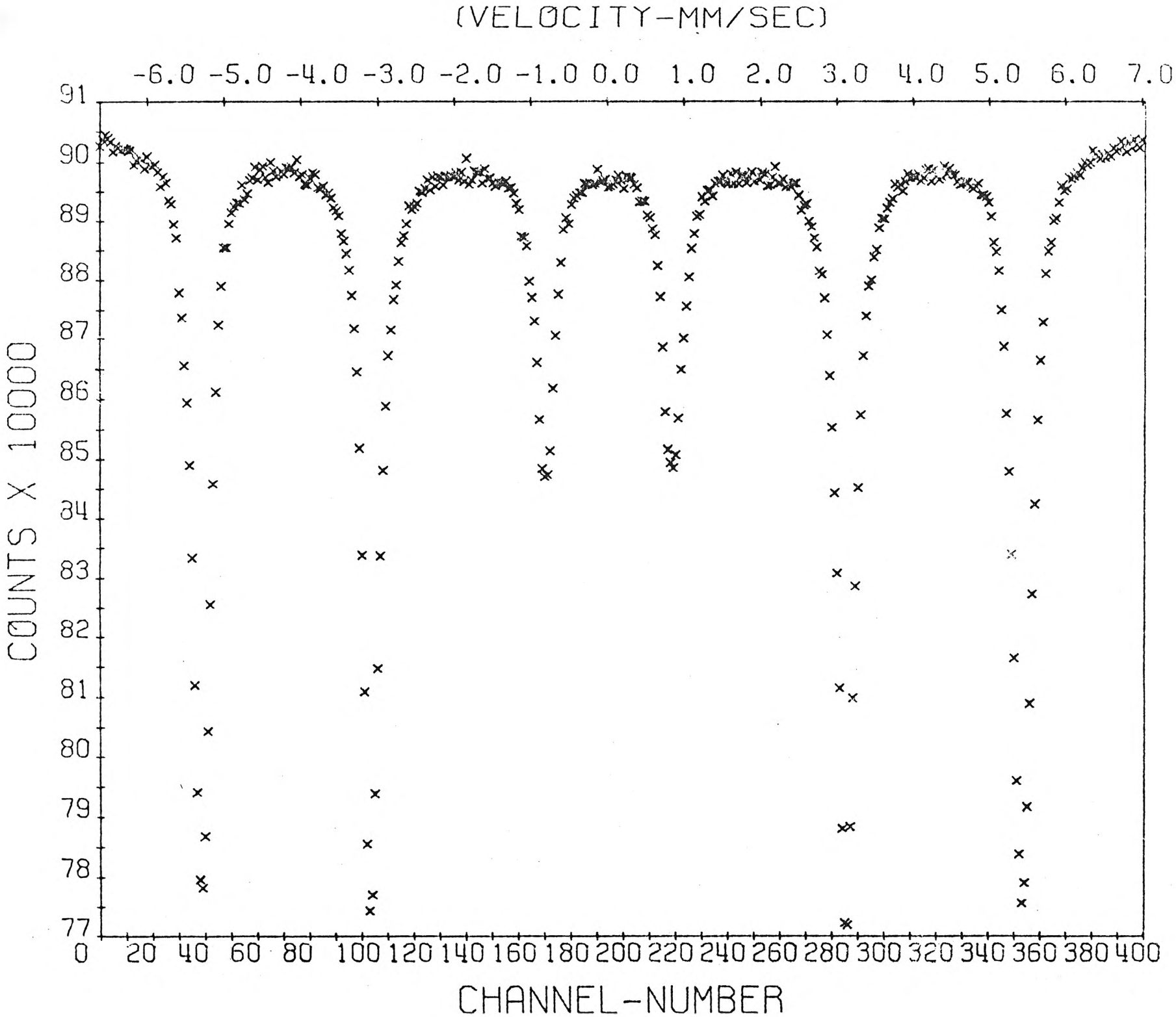
(VELOCITY-MM/SEC)
-6.0 -5.0 -4.0 -3.0 -2.0 -1.0 0.0 1.0 2.0 3.0 4.0 5.0 6.0 7.0
91
90
89
88
87
86
85
84
83
82
81
80
79
78
77
COUNTS X 10000
0 20 40 60 80 100 120 140 160 180 200 220 240 260 280 300 320 340 360 380 400
CHANNEL-NUMBER

FIGURE 12

FIGURE 13

THE MAGNETIC HYPERFINE SPLITTING of the GROUND and FIRST EXCITED STATE of Fe^{57}

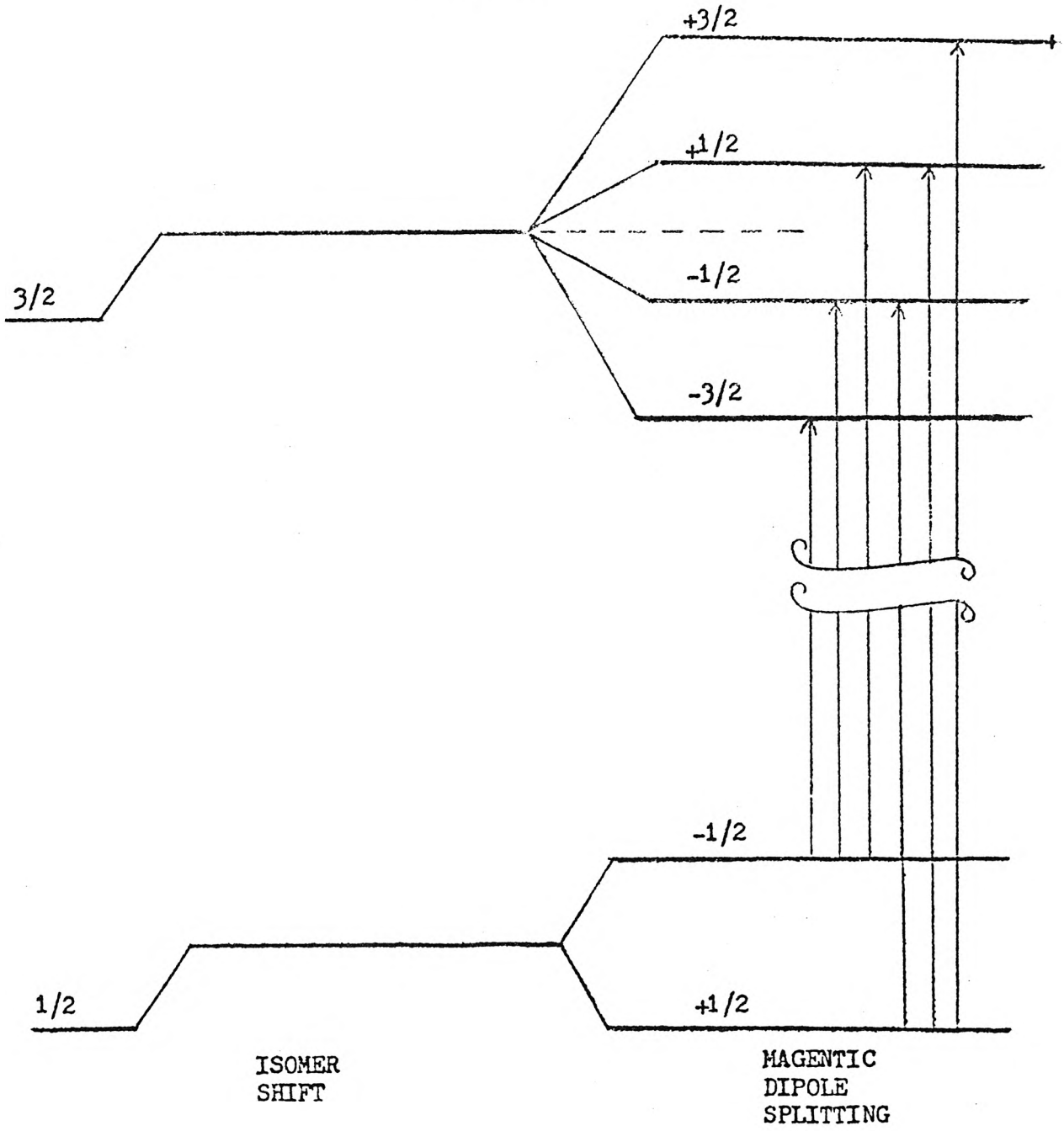

The six allowed Δ m= $\pm$1 transitions are indicated. These transitions are responsible for the six peaks of the Mössbauer effect spectrum.

CHAPTER 2

MÖSSBAUER EFFECT AND THE STUDY OF ATOMIC ORDER

The proceeding discussion introduces in general terms the resulting Mössbauer spectra for different states and degrees of order for an elementary type of ordered binary system. Following this discussion, the various ordering processes for the Fe-Al system are investigated in detail to ascertain the feasibility of utilizing the Mössbauer effect in obtaining the kinetics of ordering from various states and degrees of order.

A binary metal alloy consists of two or more metallic species combined homogeniously. Assuming a pure metal is adulterated by the addition of another metal thereby forming a binary system; an ordered solid solution comes into existance from such a mixing if dissimilar atoms are attracted by one type of atom more than similar ones. The resulting tendency is for one atom of one type to possess nearest neighbors of the other type.

There are two distinct types of order that may exist. For long range order the lattice can be regarded as being composed of two or more interpenetrating sub-lattices some of which contain most of the atoms of one type and the remaining containing most of the atoms of the other type. There is thus a coherent scheme of order extending over a large region of the lattice. This ordered lattice structure known as a superlattice is larger than the lattice of the disordered or random solution. This observation was alluded to above and comes about because in the

ordered structure, the true lattice vectors must join similar atoms and not merely similar lattice sites as is the case for a disordered random alloy. A 'perfect' superlattice is only possible at a critical and simple porportion of atoms. In practice, the atomic porportions at which superlattices have been observed are 1:1 as B2 order type and 3:1 as a DO_3 type of ordered structure. If the composition is changed from the critical porportion, the alloy will exhibit partial or imperfect order due to lattice sites being forced to accept the wrong type of atoms.

The distribution of atoms in an ordered substitutional solid solution generally depends upon temperature. Above a critical ordering temperature, T_c, the long range order is destroyed, for the ordering force is no longer strong enough to maintain the coherent scheme with the presence of intense thermal agitation. Despite the long range order being destroyed, short range order does persist in which small ordered groups of atoms continually form, break up and form again thereby producing an order over the short ranged distances. The change from an ordered to a disordered state upon heating or the reverse change on cooling, may exhibit a second order transition where the ordering process proceeds over a range of temperature; the beginning and end of the transition are but the extremes of a continious process.

Investigating such a transition upon cooling an alloy from above the critical temperature T_c, to well below T_c, produces a study of short range order and antiphase domains in the formation of long range order. Basically, the condition for order is that disimiliar atoms should attract each other preferentially and this can be satisfied to a large degree without having any long range order present; only small groups or domains of local order as illustrated below by figure 14. Experimentally,

FIGURE 14

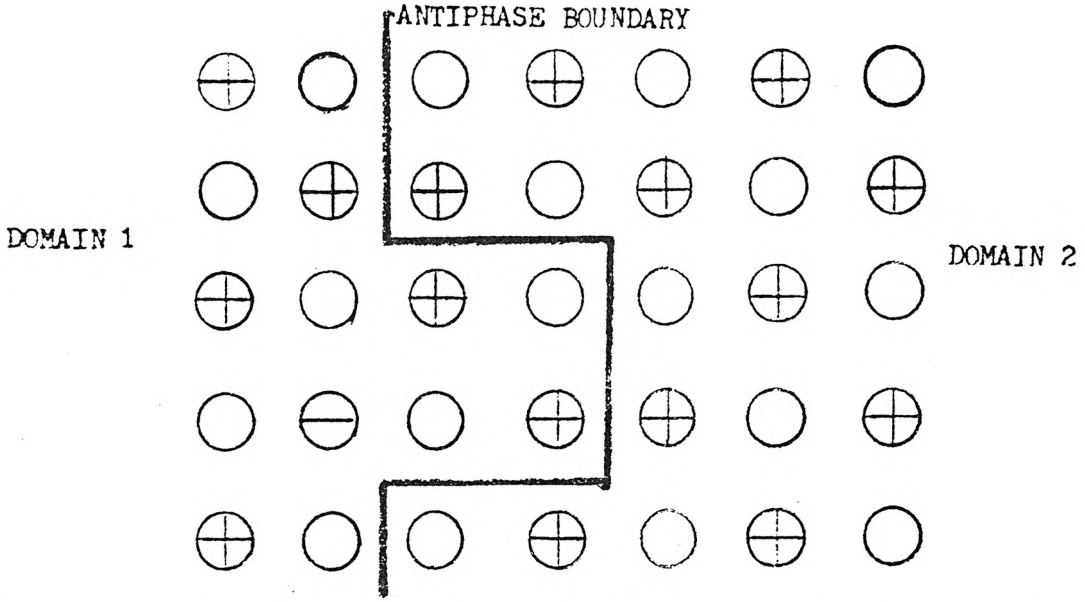

long range order is known to exist and arise from the fact that the domain boundaries are unstable at low temperatures. There is thus a tendency for the domains to grow absorbing each other and nearby disordered material thereby reducing the total area of domain boundaries in the alloy and also converting the short range order into long range order. The growth of a domain is analogous to the growth of a grain and may be expected to be correspondingly slow.

In order to specify the degree of long range order of the atoms over lattice points, a long range order parameter S is introduced and is defined by equation 7 where r_a is the fraction of A sites occupied by the 'correct' atoms, i.e., A atoms, and F_A is the fraction of A atoms in the alloy. When the long range order is perfect, $r_a = 1$ by definition, and therefore $S = 1.0$. When the atomic arrangement is completely random, $r_a = F_A$ and $S = 0.0$. Perfect order is such a structure that

EQUATION 7

$$S = \frac{r_a - F_A}{1 - F_A}$$

the alloy would need to be ordered at 0^{o} Kelvin; however, at low temperatures the diffusion rates are of such slowness as to prevent any extensive ordering of the system. Therefore, perfect order even at the critical composition may be concluded to be experimentally non-existant.

Presently the Mössbauer effect is used for the study of the long range order of many systems by incorporating the effect of the configuration of nearest neighbor atoms upon the absorbing nuclide's electronic invironment.(2,3,4).

Academically, consider an ordered BCC structure of FeCo possessing the CsCl ordered structure where the Mössbauer effect sensitive element Fe^{57} is located at the body centered position; the remainder of the lattice positions being occupied by Co atoms. The critical porportion is 1:1 or B2 type and the alloy is 50 at% Fe.

FIGURE 15

PERFECTLY ORDERED Fe-Co ALLOY

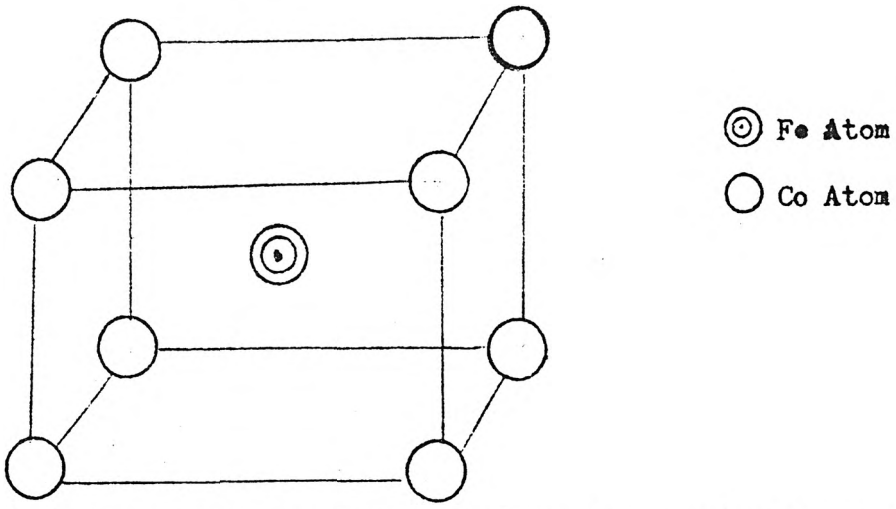

If 100% of the alloy is ordered with long range order parameter equal to unity, the Fe atoms possess 8 Co nearest neighbors or 0 Fe nearest neighbors ($0Fe_{nn}$). The natural occurance of Fe^{57} is 2.19% which implies that some unit cells are not Mössbauer effect sensitive;

nevertheless, the long range order structure is represented in view of statistical considerations. The resulting Mössbauer spectrum of this perfectly ordered structure would appear as a single component ($0Fe_{nn}$), 6 peak structure (due to the magnetic dipole interaction) with its own characteristic quadrupole splitting (QQ) and center shift (C.S.). Figure 16 illustrates this concept.

FIGURE 16

MÖSSBAUER SPECTRUM FOR PERFECTLY ORDERED Fe-Co ALLOY

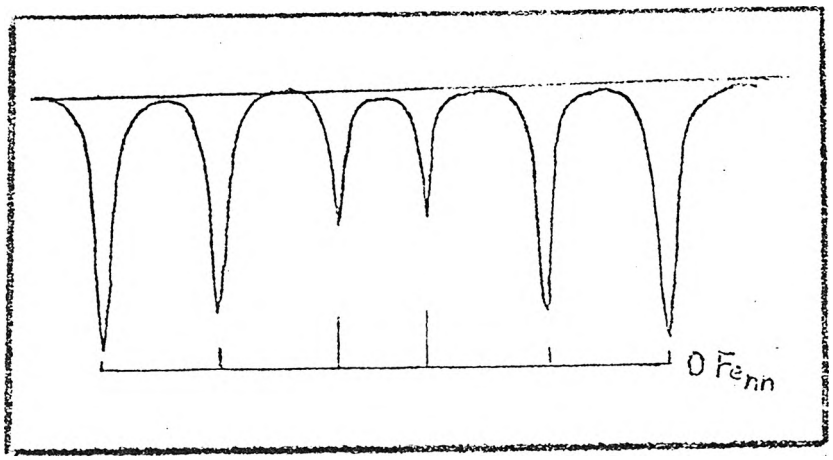

As earlier stated, the presence of perfectly ordered alloy is an impossibility. If the order parameter S is different from unity, the alloy will possess other iron nearest neighbor configurations other than the $0Fe_{nn}$ configuration component. For instance, suppose the alloy is known to have an equillibrium order degree of 0.98, which is a high degree of order but not perfect order, i.e., some Co atoms are replaced by Fe and some Fe atoms by Co atoms. There would now be probabilities for 0,1,2,3,4,5,6,7 and 8 Fe_{nn} components. Fortunantly, most of these components would have percentage effect probabilities close to zero;

i.e., the area under the component would be close to zero. Therefore, the Mössbauer effect spectrum would most likely appear as before which was illustrated by figure 16.

As the order degree decreases, the probabilities of the 1,2,3,4, 5,6,7 and 8 Fe_{nn} components become increasingly important. Assuming the 6,7 and 0 Fe_{nn} components are of importance i.e., percentage effect significantly greater than zero, the Mössbauer effect spectrum may appear as depicted by figure 18 consisting of 9 components of which only three are considered. Each component consists of 6 peaks and their own characteristic center shift and quadrupole splitting.

FIGURE 17

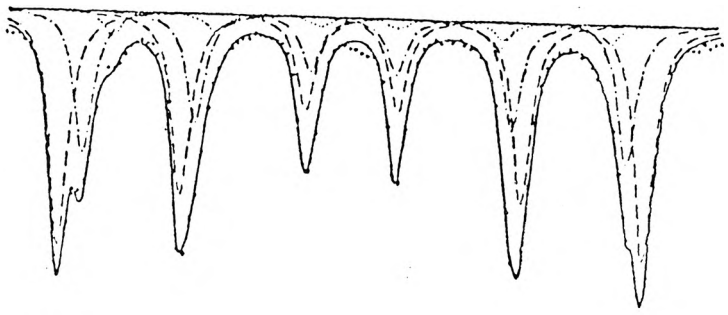

COMPUTER RESOLVED MOSSBAUER EFFECT SPECTRUM

– – – 0 Fe_{nn} ..... 7 Fe_{nn}

.-.-.- 6 Fe_{nn}

FIGURE 18

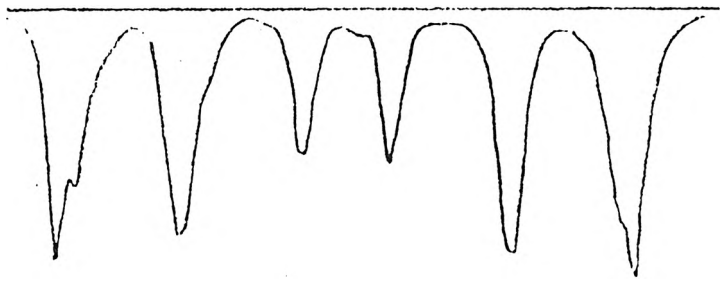

OBSERVED MOSSBAUER EFFECT SPECTRUM

Since the basic implications of the Mössbauer have been investigated, a detailed and systematic study of an ordered system, the Fe-Al system, will be undertaken. Specifically, the feasibility of obtaining the kinetics of ordering of the DO_3 ordered structure from the disordered α structure of the Fe-Al system from the utilization of the Mössbauer effect will be of interest. The concepts thus learned will be applied to other ordering phenomena of the Fe-Al system to determine their feasibility in obtaining their kinetics of ordering.

Elucidation of the true nature of the Fe-Al equilibrium diagram has proven to be a challenging problem as evidenced by the fact that six quite different versions of the iron rich portions have been published since 1958.[5] The first equilibrium diagram shown by figure 19 was obtained by dilatometric studies and presented by H. J. McQueen and G. C. Kuczynski[6] in 1959. This equilibrium diagram, however, has been shown to be in error in light of new information. A second equilibrium deagram, figure 20, was proposed by L. Rimlinger[7] in 1965 based upon X-Ray diffraction analysis and dilatometry. The equilibrium diagram invisions single phase fields of the ordered phases of the types FeAl (B2), Fe_3Al (DO_3) and the disordered BCC Fe-Al solid solution disordered phase α separated from one another in every case by large two phase regions. The implication is that the order transitions are of first order; however, theoretical considerations show that the transitions are actually second order or higher.[5] A further and most likely a more correct revision of the Fe-Al equilibrium diagram of state was presented by P. R. Swann, et al., in 1969; figure 21. Their revision was based upon observations utilizing transmission electron microscopy and their equilibrium diagram will be used for all future references.

FIGURE 19

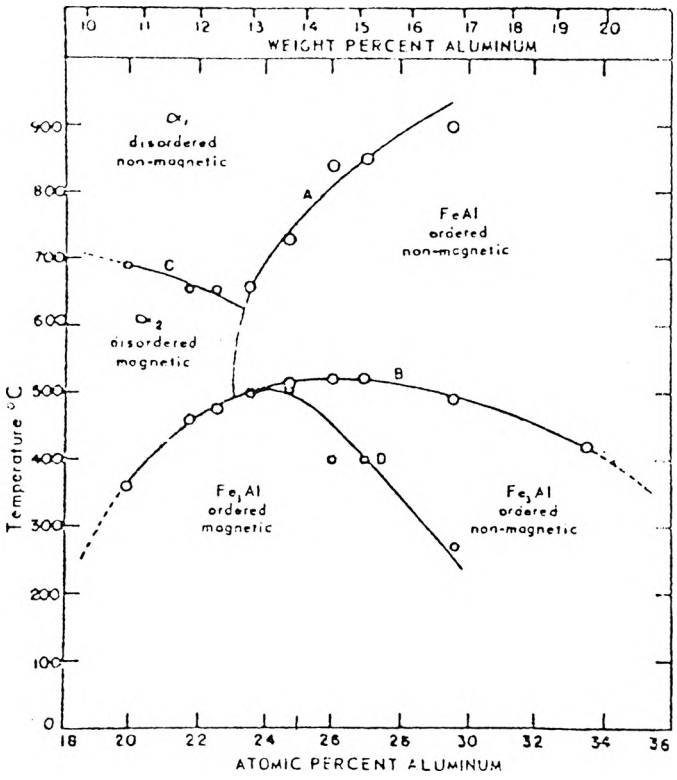

Constitution diagram of iron-rich Fe-Al alloys in the solid-solution range as determined by McQueen and Kuczynski (6)

FIGURE 20

The iron-rich portions of the Fe-Al equilibrium diagram proposed by Rimlinger (7)

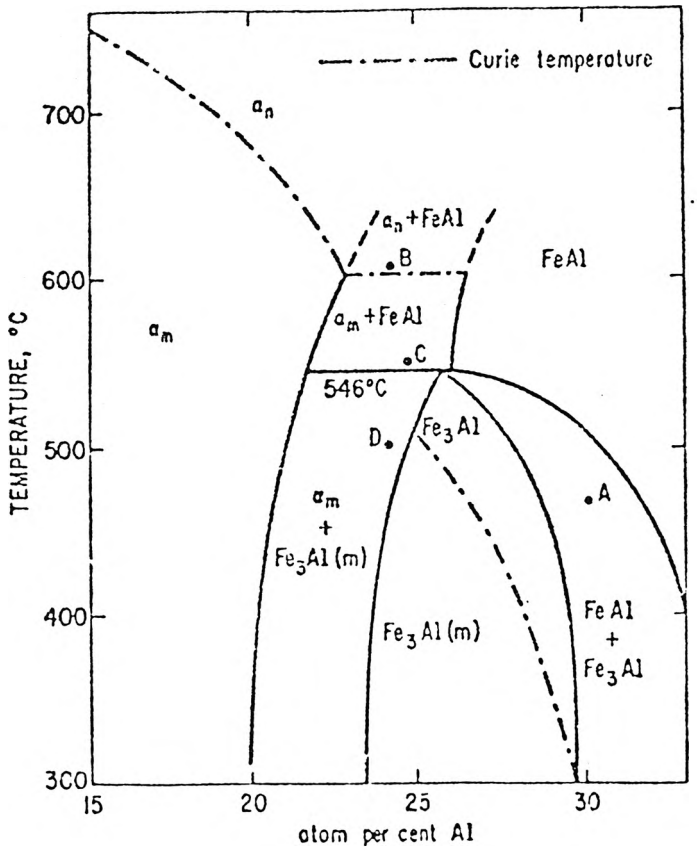

FIGURE 21

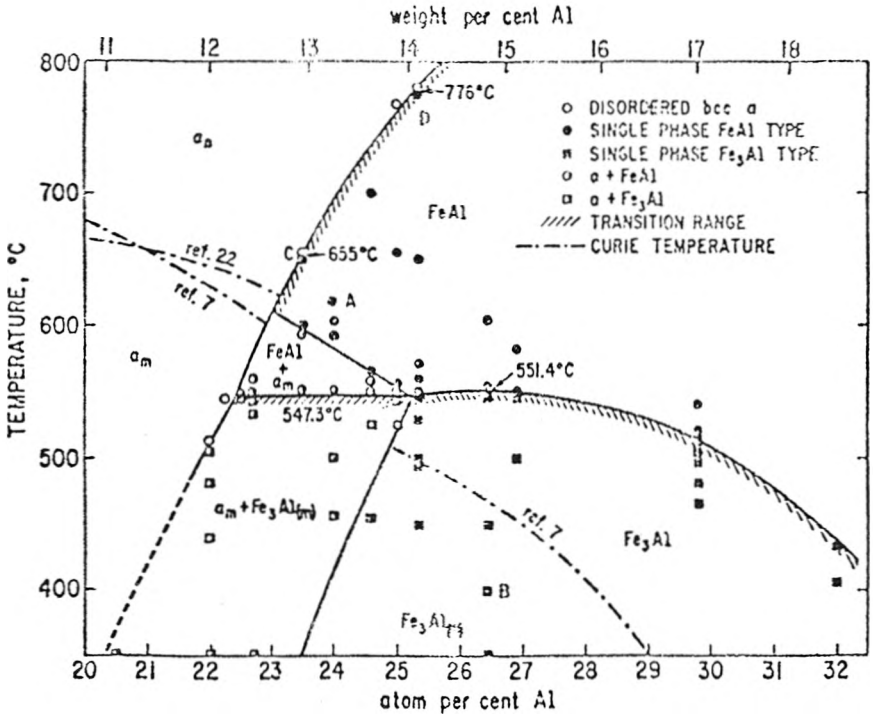

The iron-rich portions of the Fe-Al equilibrium diagram proposed by Swann et al. (5)

FIGURE 22

Fe-Al EQUILIBRIUM DIAGRAM

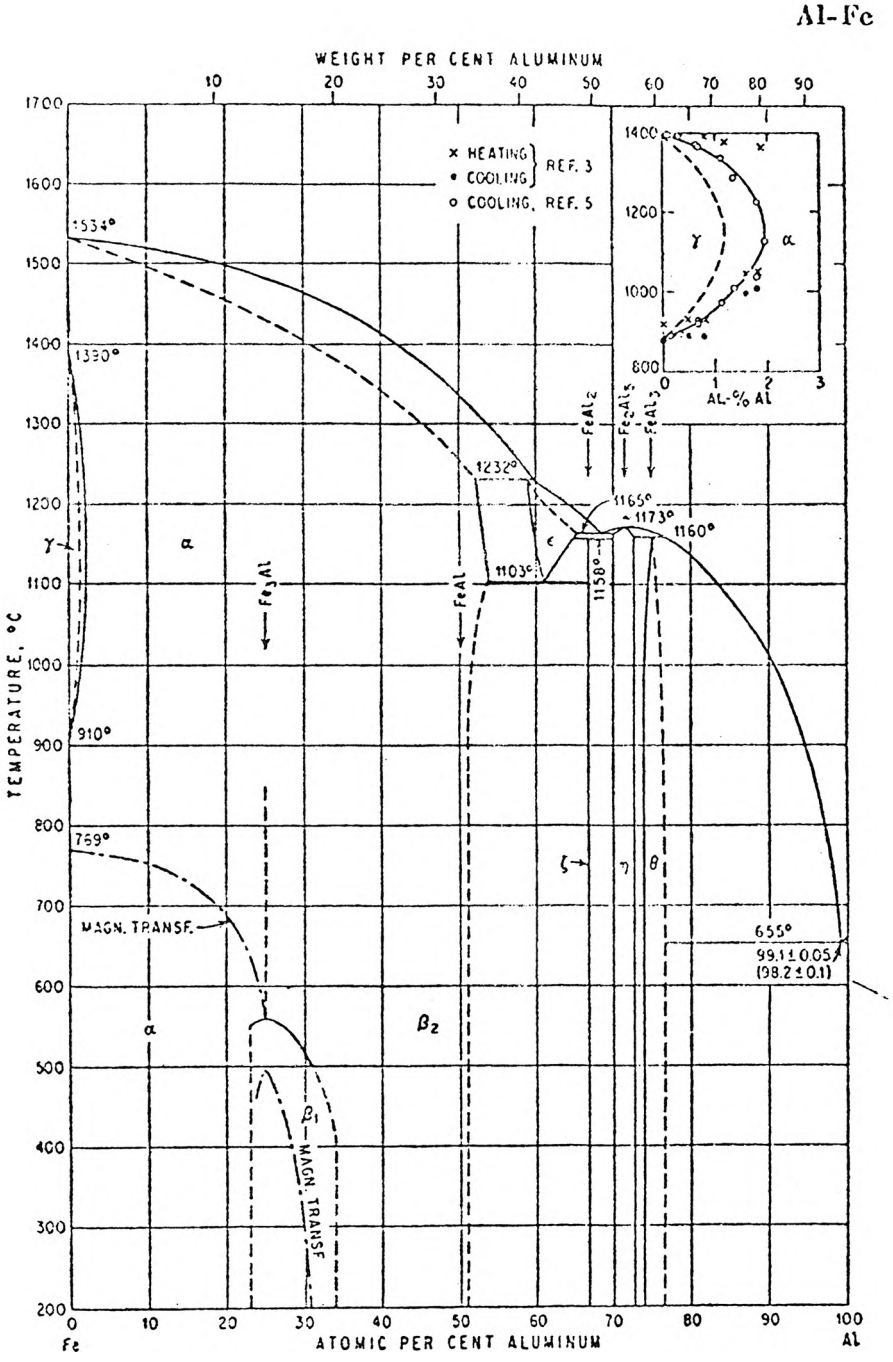

The equilibrium diagram for the Fe-Al system shows three types of order; a B2 structure as FeAl at high temperatures, a DO_3 structural type existing as Fe_3Al at lower temperatures and a disordered random phase denoted as α . As a first order approxiamation, the α phase may be considered as a solid solution of iron and aluminum possessing a BCC structure whose lattice positions occupancy is considered random with respect to iron and aluminum atoms.

For the illustration of the B2 and DO_3 ordered structures, consider a unit cell which consists of three kinds of sublattice sites, α , β , and γ . At 25 at% Al, the stoichiometric composition of Fe_3Al,

FIGURE 23

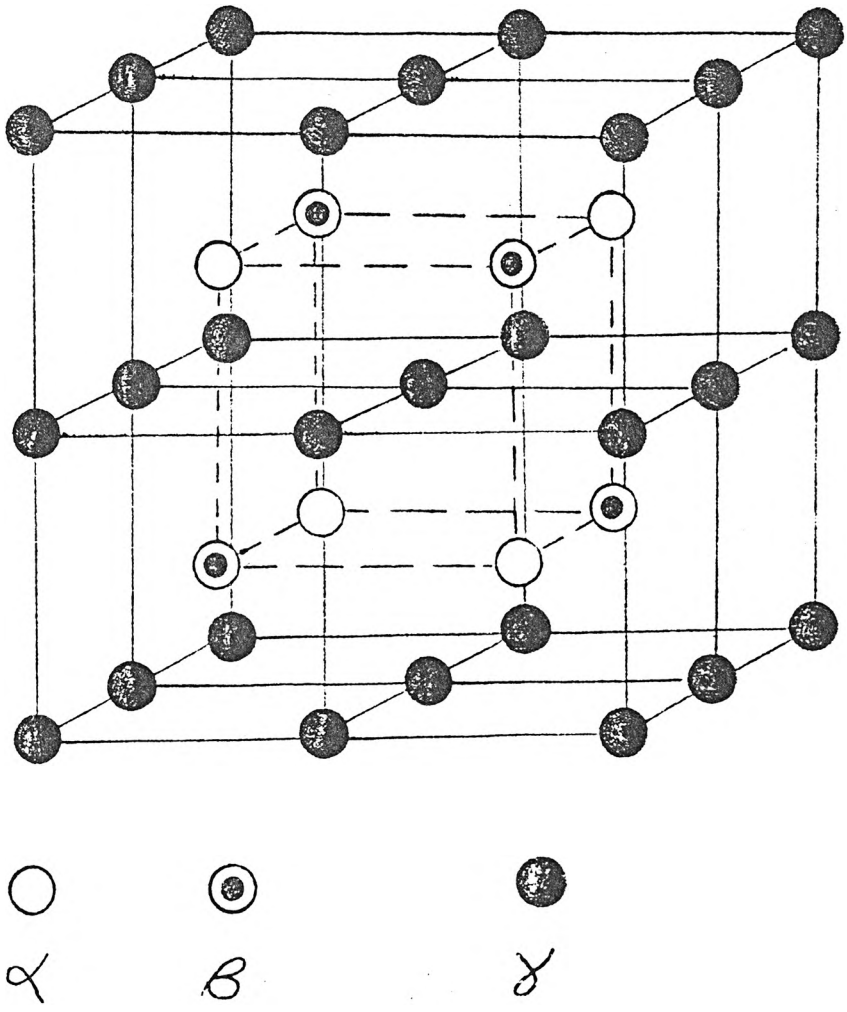

the perfectly ordered structure possesses the above superlattice whose sublattices are occupied in the following manner: β lattices being occupied by Al atoms and α and γ sites by Fe atoms. The perfectly ordered structure produces two types of Fe nearest neighbors; the Fe atom in the γ sites possesses 4 Fe_{nn} and the Fe atom in the α site possesses 8 Fe_{nn} in a ratio of 2/3 : 1/3 respectively.

The FeAl order structure possesses sublattices that are occupied in the following manner for the stoichiometric composition of 50 at% Al: α and β lattices are occupied by Al atoms and the γ sites by Fe atoms thereby causing the Fe atoms to possess 0 Fe_{nn}. If the Al composition is reduced to 25 at% Al, the α and β sites become randomly occupied with Fe and Al atoms while the γ sites remain occupied by Fe atoms.

The point of interest for this investigation is to obtain the kinetics of ordering for the DO_3, Fe_3Al, structure from the disordered random phase α . The experimental response was to utilize a stoichiometric, 25 at% Al sample that would be quenched from 1100°C within the disordered α region to room temperature thereby retaining the high temperature state. Subsequent isothermal anneals as a function of time would be performed at 200, 240, 260,and 300°C until equillibrium was reached. Subsequent Mössbauer spectra were to be obtained for each step of the annealing procedure for each temperature and then analyzed using the computer least-squares fitting procedure outlined by Bent,[8] et al., in order to acquire the percent change of the 4,8 and 6 Fe_{nn} components with ordering. From this percent change as a function of anneal time, the rate or kinetics of this ordering process could be ascertained.

However, many complications arose that were not anticipated and the consideration of the feasibility in utilizing exclusively the

Mössbauer spectrometer in ascertaining the ordering kinetics become of importance. The feasibility in utilizing the Mössbauer spectrometer depends upon the compensation of the following complications.

1. Difficulty of producing a workable computer fitting procedure yielding the percentage effect for each iron nearest neighbor configuration for each constituent.
2. Consideration of antiphase boundaries.
3. The recognition of the Mössbauer spectrometer averaging the Fe_{nn} components arising from different phases.
4. The retention of unwanted high temperature states during quenching.
5. Recognition that the ordered domains are of different Al composition than the surrounding disordered matrix.
6. Extraneous considerations as directional magnetic properties exhibited due to rolling, spectra peak broadening due to the finite thickness of the foil specimens, possibility of secondary extraneous phases not predicted, and finally the possibility of supersaturation of Al due to quenching from a high temperature state.

These complications will be elaborated upon with the proceding discussions of the different states and types of ordering phenominon of the Fe-Al ordered system.

Building upon the concepts associated with a 22 at% Al alloy, a belief existed that in performing a room temperature water quench, the quenching rate would be rapid enough to prevent any DO_3 ordering during quenching and also retain the high temperature disordered α phase at room temperature. Since a definite time is required for atoms to rearrange themselves, the change in order does not respond instantly to a change in temperature. At temperatures where diffusion is very slow, it is possible for non-equilibrium states of order to persist for indefinitely long periods of time. To verify that a room temperature agitated water quench did suppress the formation of DO_3 order during the quench, an ice water and room temperature agitated quench from 1100°C

was performed on 0.007 inch thick specimens. The specimens were subsequently chemically thinned to 0.002 inches to avoid line broadening of their Mössbauer effect spectrums which were obtained. If a difference exists between the two spectra, the possibility of the DO_3 order not being suppressed is a real consideration. As illustrated by figures 25 and 26 there is indeed a difference.

This previously mentioned difference is attributed to the formation of very fine ordered DO_3 domains during the quench. Also, the investigations performed by D. Watanabe[9] has demonstrated that the DO_3 domains thus initially formed upon the first increment of anneal are of the equilibrium degree of order and subsequently grows upon isothermal annealing to the equilibrium amount of DO_3 structure as exhibited by the equilibrium order phase diagram for that particular temperature. An isothermal anneal sequence is presented by figure 26 for a 22 at% Al alloy heat treated at 200°C.

The original thinking considered only the 4 and 8 Fe_{nn} components for the well ordered specimens, which are characteristic of the ordered system. The 6 Fe_{nn} component was believed to be characteristic of the disordered state; however, theoretical calculations were made of the probability of various configurations of Fe atoms in alloys of different compositions with different degrees of order. Based upon these calculations, other Fe_{nn} components were found to be of extreme importance especially at low degrees of order. The following discussion elaborates upon this concept.

Referring to the unit cell shown earlier by figure 23 describing the Fe_3Al or DO_3 type of order for the 25 at% Al alloy; the α and γ sites are occupied by Fe atoms and the β nodes by Al atoms. Based upon the work of S. A. Losiyevskaya and R. N. Kuz'min[10], the long range order

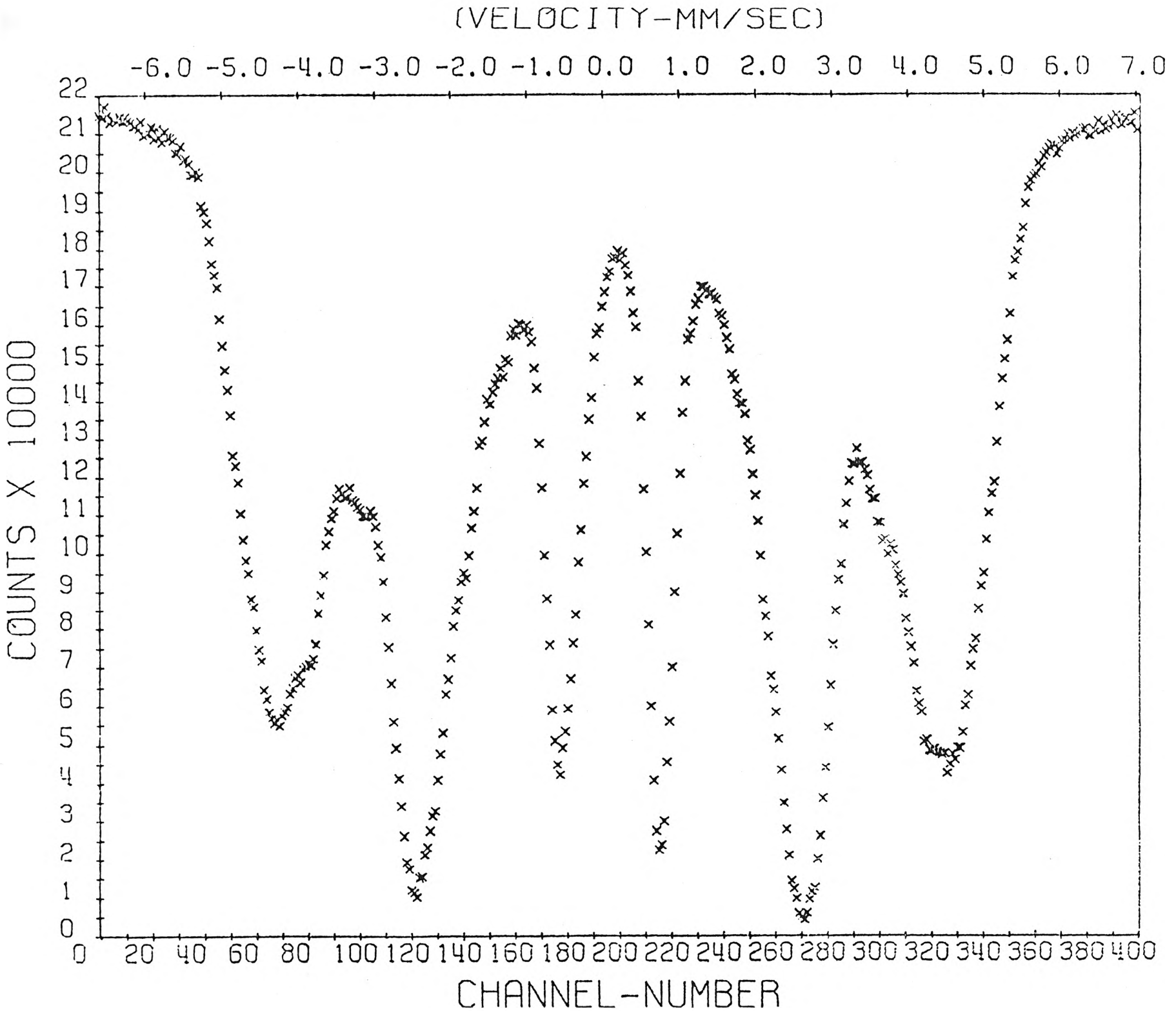

FIGURE 24 ROOM TEMPERATURE WATER QUENCH

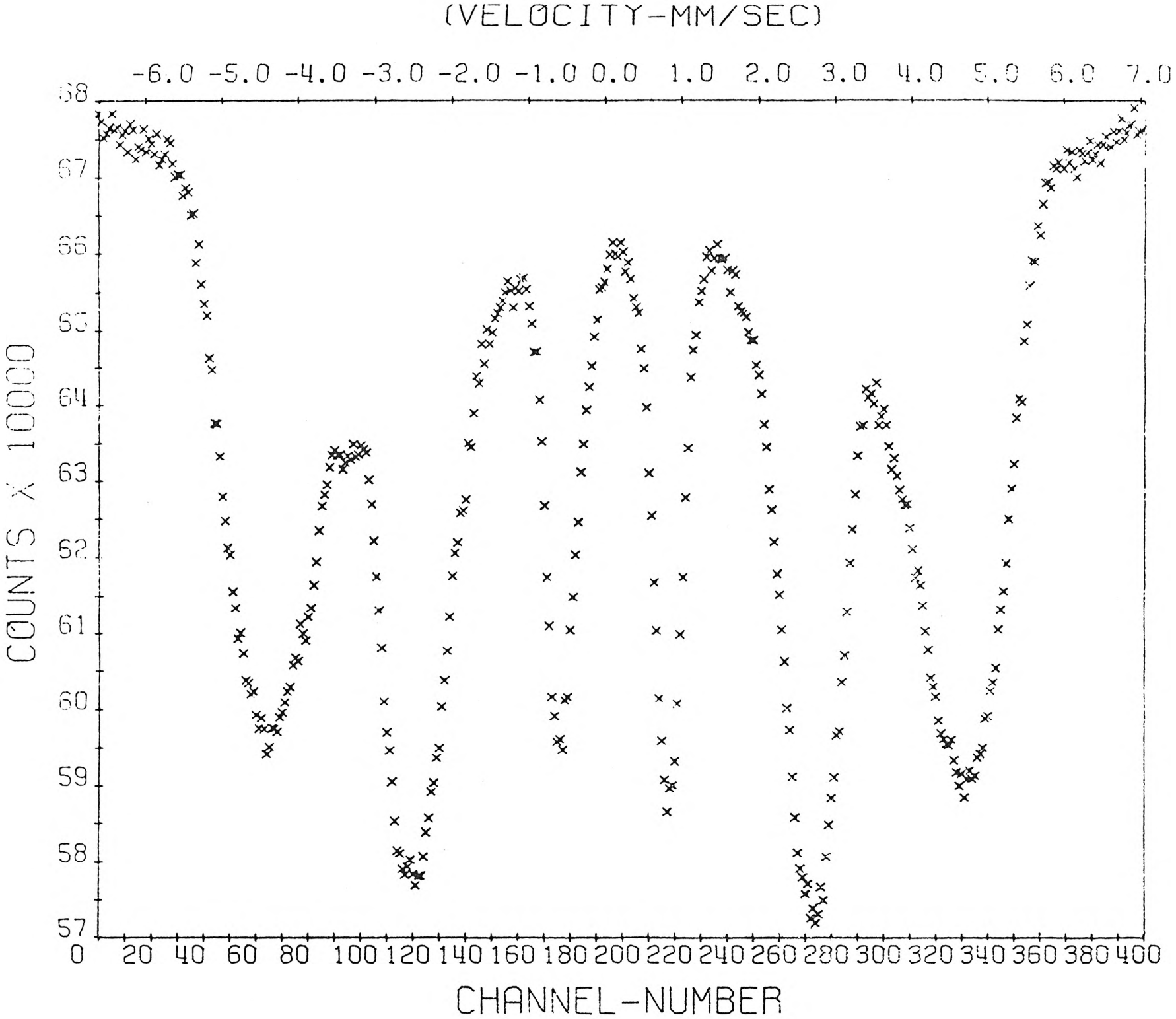

FIGURE 25

BRINE QUENCHED

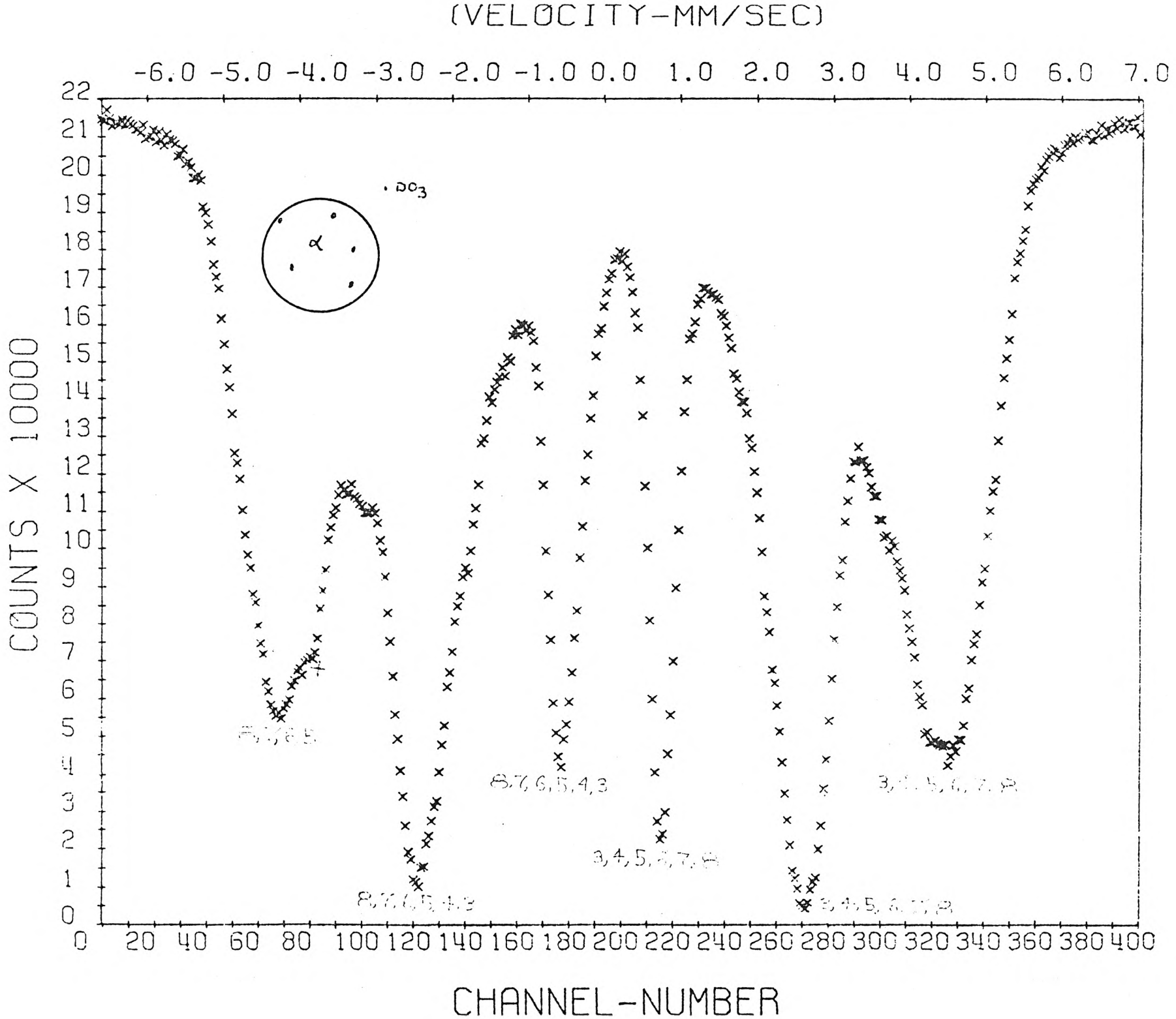

FIGURE 26 WATER QUENCHED FROM 1100°C

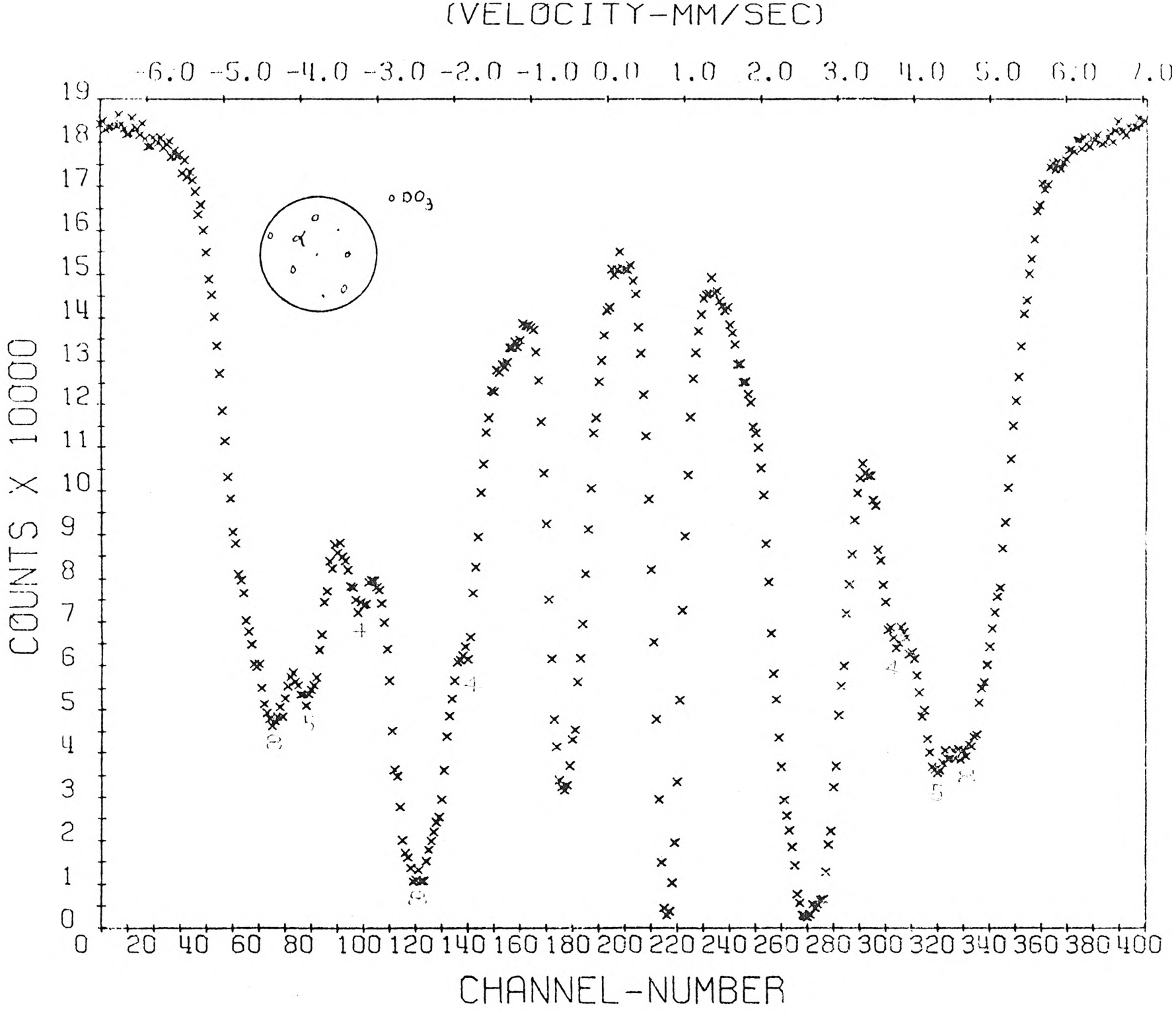

FIGURE 26

ANNEALED AT 200°C for 1 Hr.

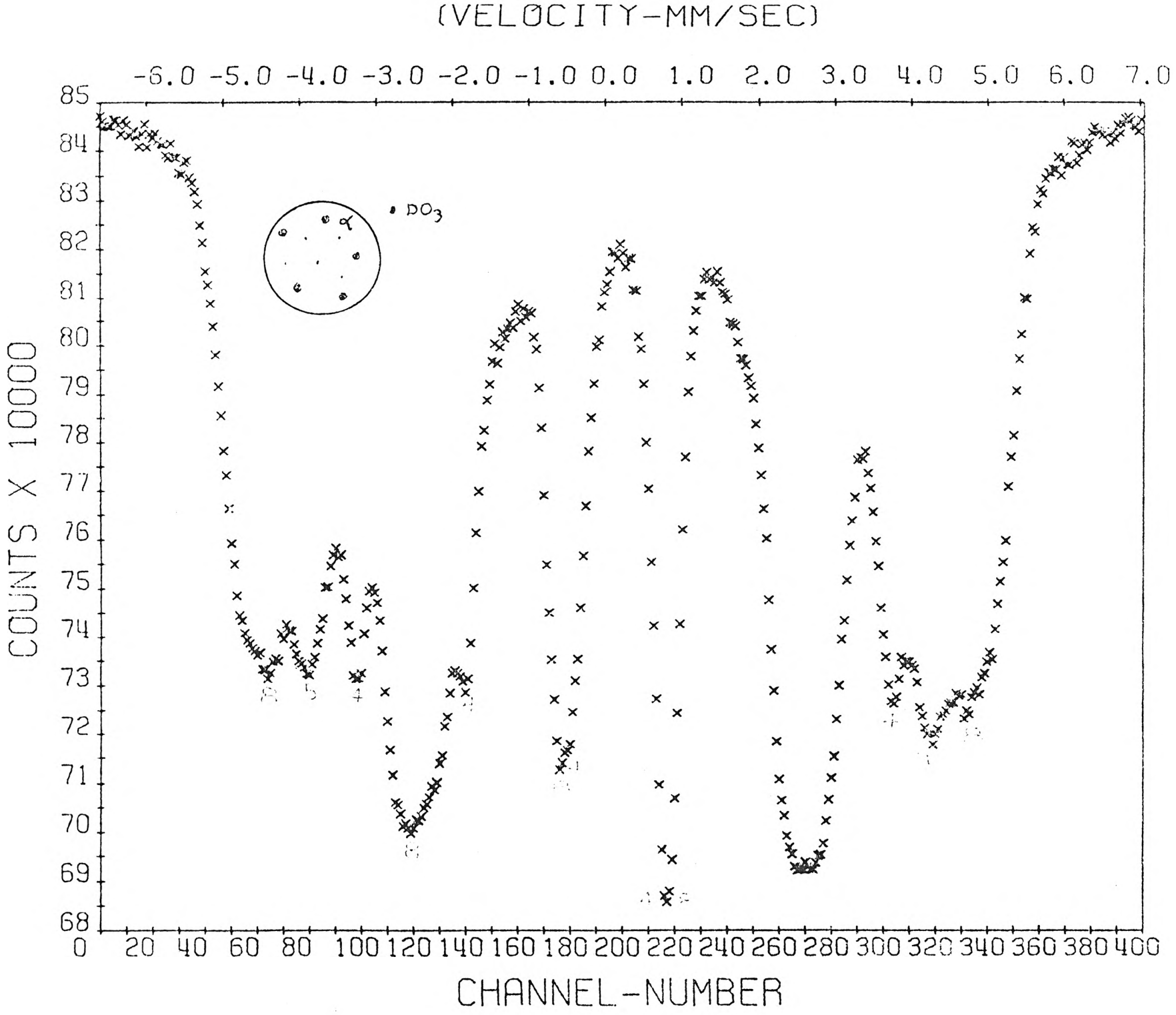

FIGURE 26

ANNEALED AT 200°C FOR 2 Hrs

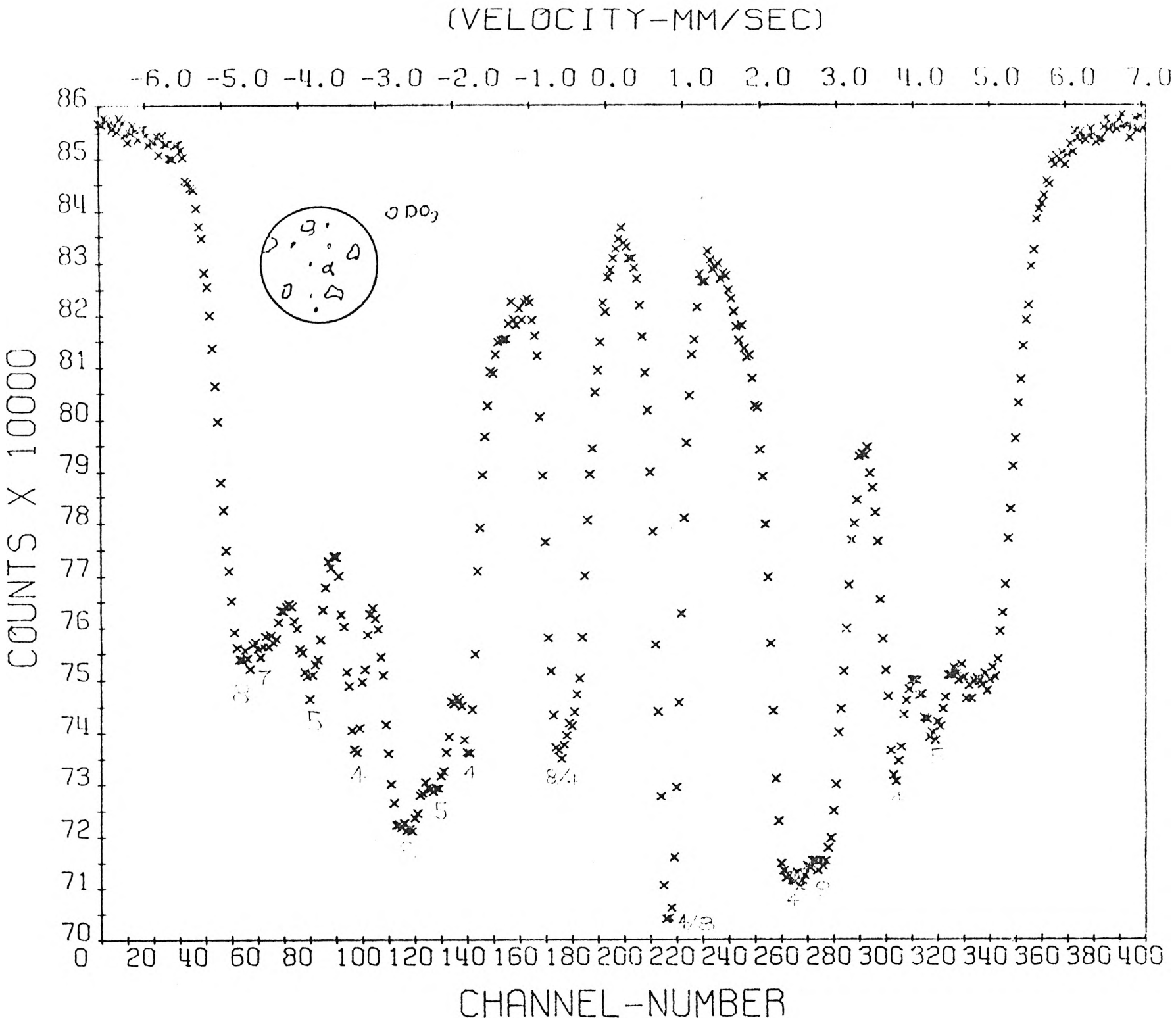

FIGURE 26 ANNEALED AT 200°C FOR 3 Hrs

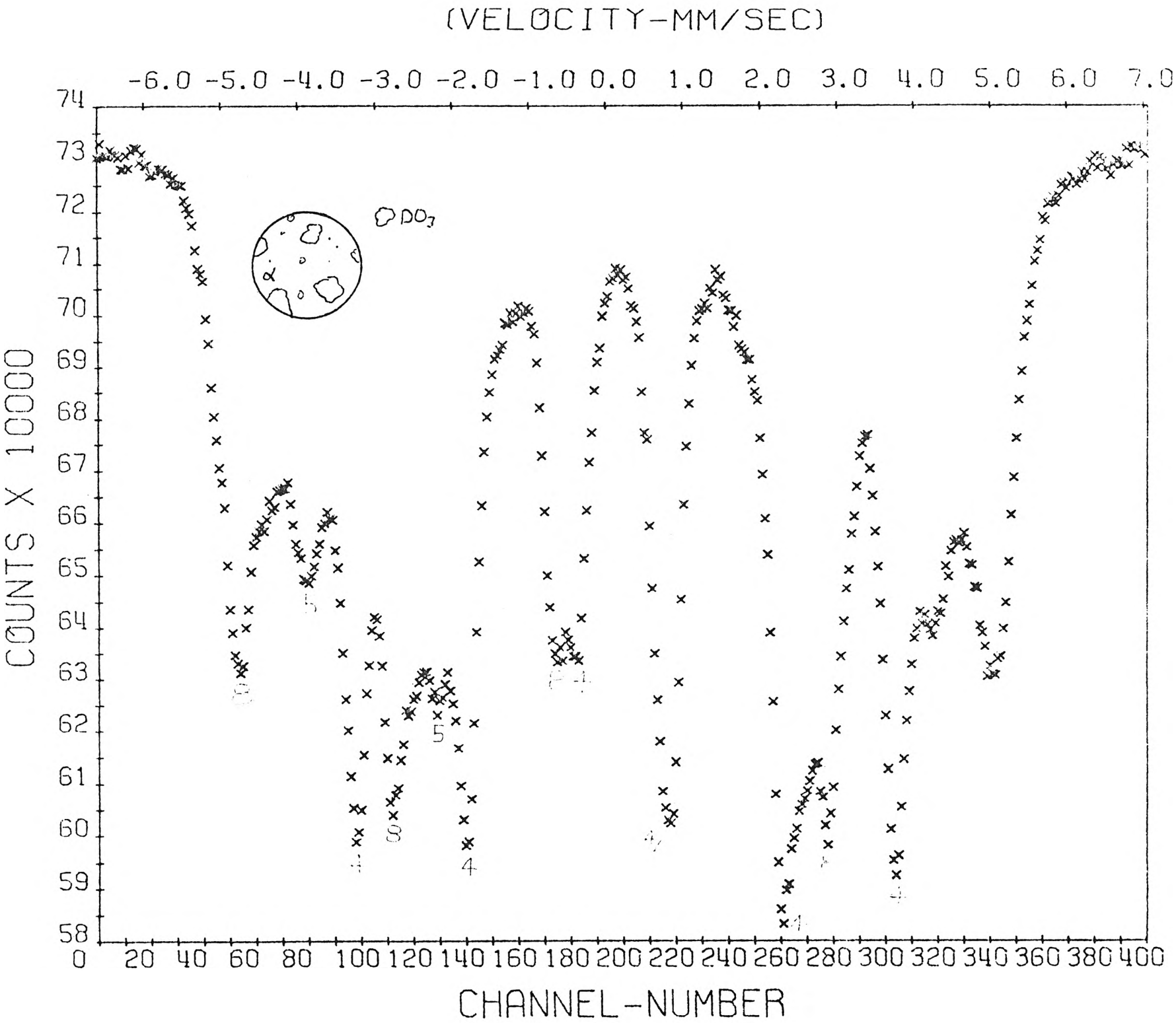

FIGURE 26 ANNEALED AT 200°C FOR 7 Hrs

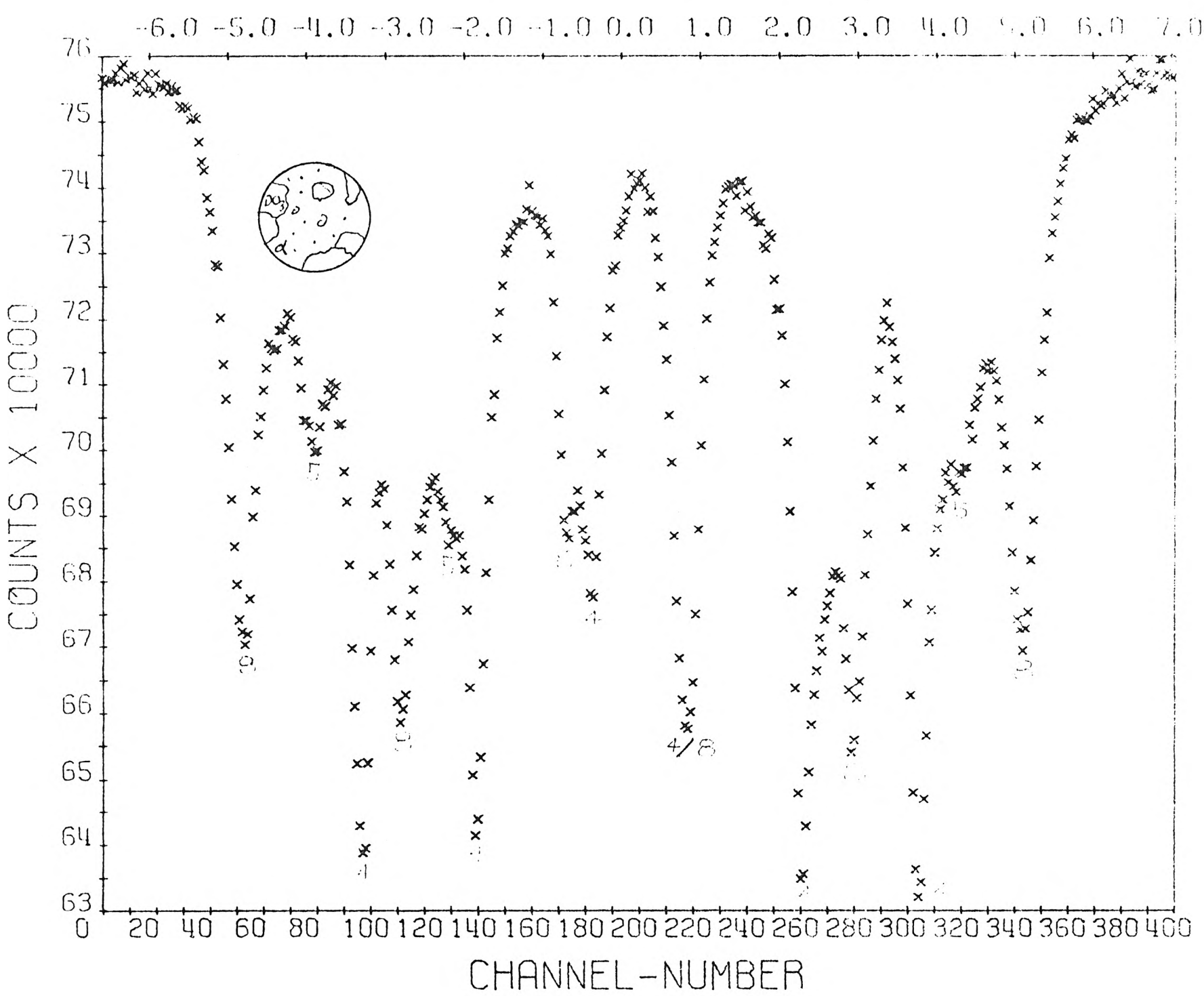

FIGURE 26

ANNEALED AT 200°C FOR 21 Hrs

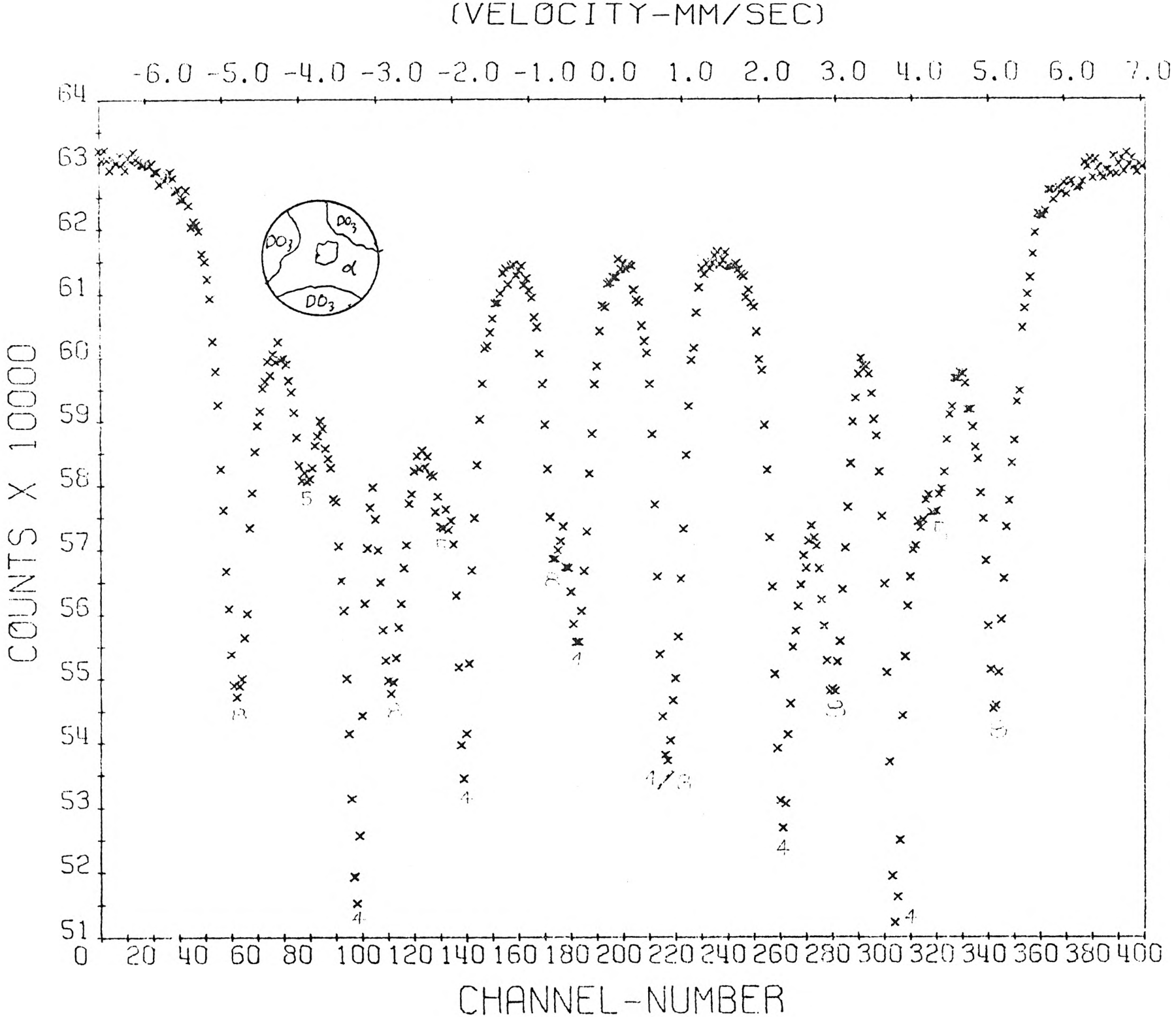

FIGURE 26

ANNEALED AT 200°C FOR 44 Hrs

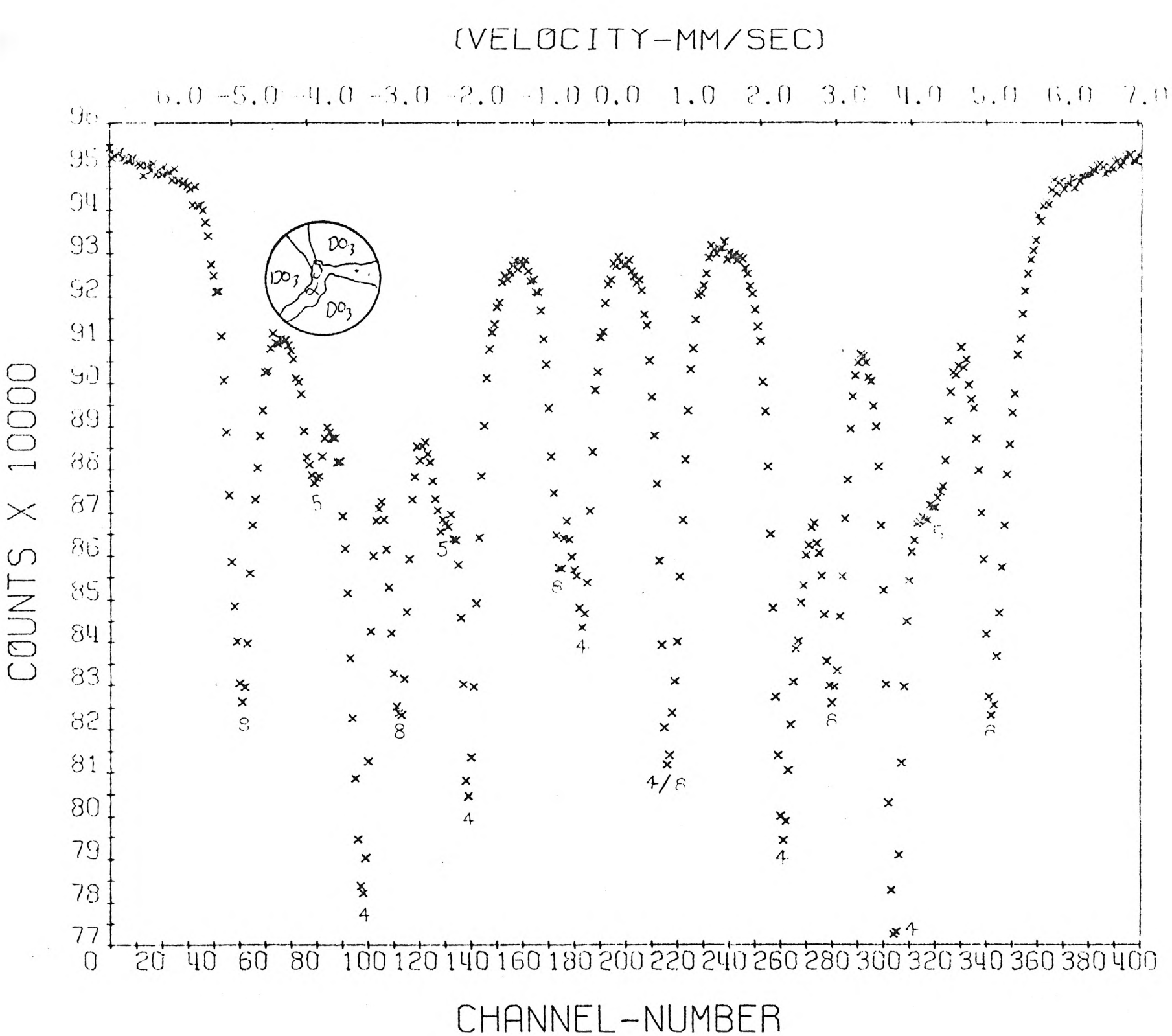

FIGURE 26 ANNEALED AT 200°C FOR 212 Hrs

parameter S_{31} covering the range of existance of the Fe_3Al phase may be introduced as exibited by equation 8. In this case the q, r, and 1-p are the probabilities of substitution of the Fe atoms of the γ, α, and β nodes, respectively; c is the Al concentration of the alloy; q and p may be represented by the formula as shown. Nonetheless, the theoretical amount of Fe_{nn} components have not been elucidated.

EQUATION 8

$$S_{31} = 2(1-q+p-2c) = r+p-1 \qquad S_{31} = \text{Long Range Order Parameter}$$

$$q = c(S_{31} - 1) \qquad p = c(3S_{31} + 1) \quad \text{FOR c less than 25 at\% Al}$$

Using the binomial law of atom distribution along the lattice sites in the first nearest neighbor coordination sphere, and considering the number of α, β, and γ sites surrounding a given site in the lattice of an Fe-Al alloy of arbitrary composition, a formula is obtained for the relative number of Fe atoms in the α, β and γ nodes with different numbers (m1) of Fe_{nn}. Equations 9,10 and 11 presents this idea.

EQUATION 9

$$N_\gamma(m1) = \frac{q}{2(1-c)} \left[\sum_{K}^{(-)} \frac{4!\,(1-q)^{4-k} q^k 4!\, p^{4-m1+k} (1-p)^{m1-k}}{(4-k)!\,k!\,(4-m1+k)!\,(m1+k)!} \right] \qquad (10)$$

EQUATION 10

$$N_\alpha(m1) = \frac{r}{4(1-c)}\, q^{m1}(1-q)^{8-m1}\, \frac{8!}{(8-m1)!\,m1!} \qquad m1 = 0,1,2,\cdots 8$$

$$(0 \le k \le m1 \text{ IF } m1 \le 4)$$

EQUATION 11

$$N_\beta(m1) = \frac{(1-p)}{4(1-c)}\, q^{m1}(1-q)^{8-m1}\, \frac{8!}{(8-m1)!\,m1!} \qquad (m1-4 \le k \le 4 \text{ IF } m1 \ge 4)$$

The formula $N_\gamma(m1)$ is in error. Upon rederivation, the (m1+k)! shown in the denominator should be (m1-k)!. Personal correspondance confirmed this change.[11]

By the addition of each (m1) Fe_{nn} for each site, the above formula

reduces to the following set as listed in table 1. These equations when applied to a 22 at% Al sample produces the graph shown by figure 27.

The probability study shows the 6 Fe_{nn} component as not representative of the disordered state but rather the 3,4,5,6,7 and 8 Fe_{nn} components. The full impact is felt when the Mössbauer spectra are analyzed for the percentage effect of each component using the computer least squares fitting procedure. Originally, the peaks were believed to be an additive composite of only the 4 and 8 Fe_{nn} component for the well ordered specimens and the 6 Fe_{nn} component for the disordered specimens and the 4, 8 and 6 for points between. However, the well ordered specimen is currently shown to be a composite of the 4, 8 and 5 Fe_{nn} components; the disordered a composite of the 3,4,5,6,7 and 8 Fe_{nn} components. Although the work performed in attempting to analyze the spectra by utilizing the computer least squares fitting procedure was a major part of the experimental procedure, the computer program will not be discussed in detail. Let it suffice that we were unsuccessful in producing a working computer fitting procedure; however, this is a solvable problem and for further reference see Bent,[8] et al. Nonetheless, this shortcoming did limit the feasibility of utilizing the Mössbauer effect for the study of the kinetics of ordering of the DO_3 from the disordered α phase in view of other methods.

The above probability study forced a radical change of thinking and created an interest in the possibility of other component spectra being observed in the spectra. M. R. Lesoille and P. M. Gielen[12] assign a component contributed from a second phase of $Fe_3Al(C)$. However, this seemed unlikely for our consideration due to the small amount of carbon in our specimens; 0.01 wt% Carbon. Nonetheless, a sample was carburized

TABLE 1

THEORETICAL PERCENTAGE EFFECT FOR EACH IRON

NEAREST NEIGHBOR COMPONENT

$$N(8) = \frac{1}{4(1-c)} \left[q^9 + 2q^5(1-p)^4 + (1-p)q^8 \right]$$

$$N(7) = \frac{1}{4(1-c)} \left\{ 8q^8(1-q) + 8(1-p)(1-q)q^7 + 2q \left[4(1-q)(1-p)^4 q^3 + 4(1-p)^3 q^4 p \right] \right\}$$

$$N(6) = \frac{1}{4(1-c)} \left\{ 28q^7(1-q)^2 + 27(1-p)(1-q)^2 q^6 + 2q \left[6(1-q)^2(1-p)^4 q^2 + 16(1-q)(1-p)^3 q^3 p + 6(1-p)^2 q^4 p^2 \right] \right\}$$

$$N(5) = \frac{1}{4(1-c)} \left\{ 56q^6(1-q)^3 + 56q^5(1-q)^3(1-p) + 2q \left[4(1-q)^3(1-p)^4 q + 24(1-q)^2(1-p)^3 q^2 p + 24(1-q)(1-p)^2 q^3 p^2 + 4(1-p)q^4 p^3 \right] \right\}$$

$$N(4) = \frac{1}{4(1-c)} \left\{ 70(1-p)(1-q)^4 q^4 + 70(1-q)^4 q^5 + 2q \left[(1-q)^4(1-p)^4 + 16(1-q)^3(1-p)^3 qp + 36(1-q)^2(1-p)^2 q^2 p^2 + 16(1-q)(1-p)q^3 p^3 + q^4 p^4 \right] \right\}$$

$$N(3) = \frac{1}{4(1-c)} \left\{ 56q^4(1-q)^5 + 56(1-p)(1-q)^5 q^3 + 2q \left[4(1-q)^4(1-p)^3 p + 24(1-q)^3(1-p)^2 qp^2 + 24(1-q)^2(1-p)q^2 p^3 + 4(1-q)q^3 p^4 \right] \right\}$$

FIGURE 27

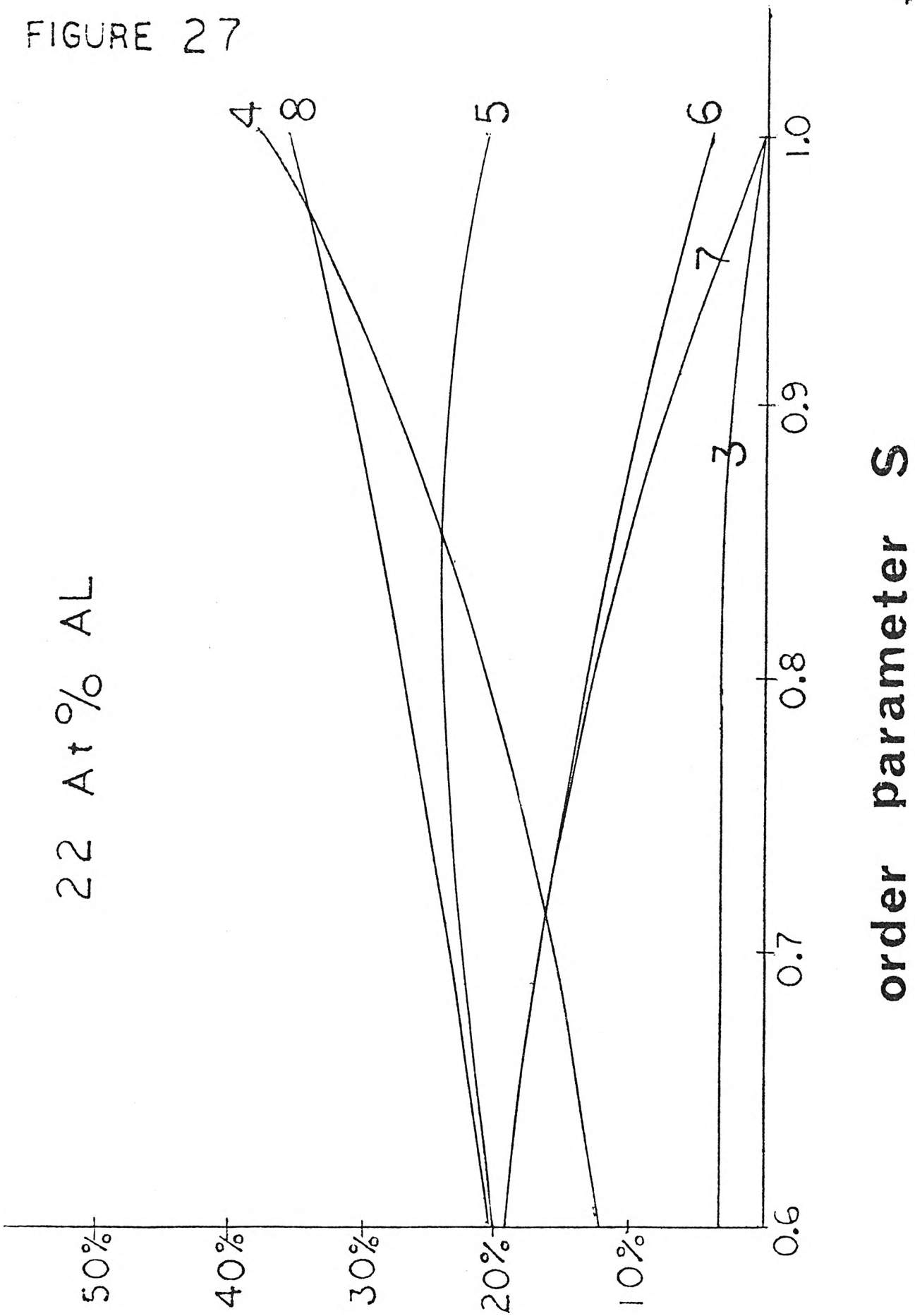

at 1100°C and quenched into room temperature water. A definite component arising from carburizing was observed as presented by figure 28,and the peaks do come in as Lesoille and Gielen state. However, this component was not observable from the Mössbauer work performed upon the normal samples, although it may have been unresolved and thereby not observable.

A further question arose as to the affect of the antiphase boundaries upon our spectra. P. R. Swann[5] et al. attribute an added 5 Fe_{nn} component from fine antiphase domains on the boundaries of which most Fe atoms have 5 Fe_{nn} and secondly to the presence of a second phase $Fe_{13}Al_3$ with ordered structure having Fe atoms with only 8 and 5 Fe_{nn}. Kuz'min and Losiyevskaya[10] attribute an added 5 Fe_{nn} component to concentration disordering. They show that with fine antiphase domains which one gets by quenching, one would achieve a larger 5 Fe_{nn} component than with large domains; i.e., a 5 Fe_{nn} component from fine antiphase domains. If Swann's $Fe_{13}Al_3$ phase does exist than the mechanism in which the 5 and 8 Fe_{nn} component acts in the ordering process is complicated, i.e., is the ordering α - DO_3 - $Fe_{13}Al_3$? Kuz'min and Iosiyevskaya show that the change in the hyperfine values of the 4 and 8 Fe_{nn} components with Al concentrations is inexplicable if the alloys are assumed to consist of two phases. Also, despite the extensive work performed by M. B. Stearns[15] a second phase of $Fe_{13}Al_3$ was not detected.

In concluding the above discussed considerations, a few words will be said about the problems encountered with the Mössbauer effect fitting procedure. The intent of the computer fitting procedure is to create a theoretical Mössbauer functional spectrum for each Fe_{nn} component. By varing each component's percentage effect i.e., area under each component, quadrupole splitting, center shift, and approxiamately nine other experimentally and theoretically obtained parameters, the individual component

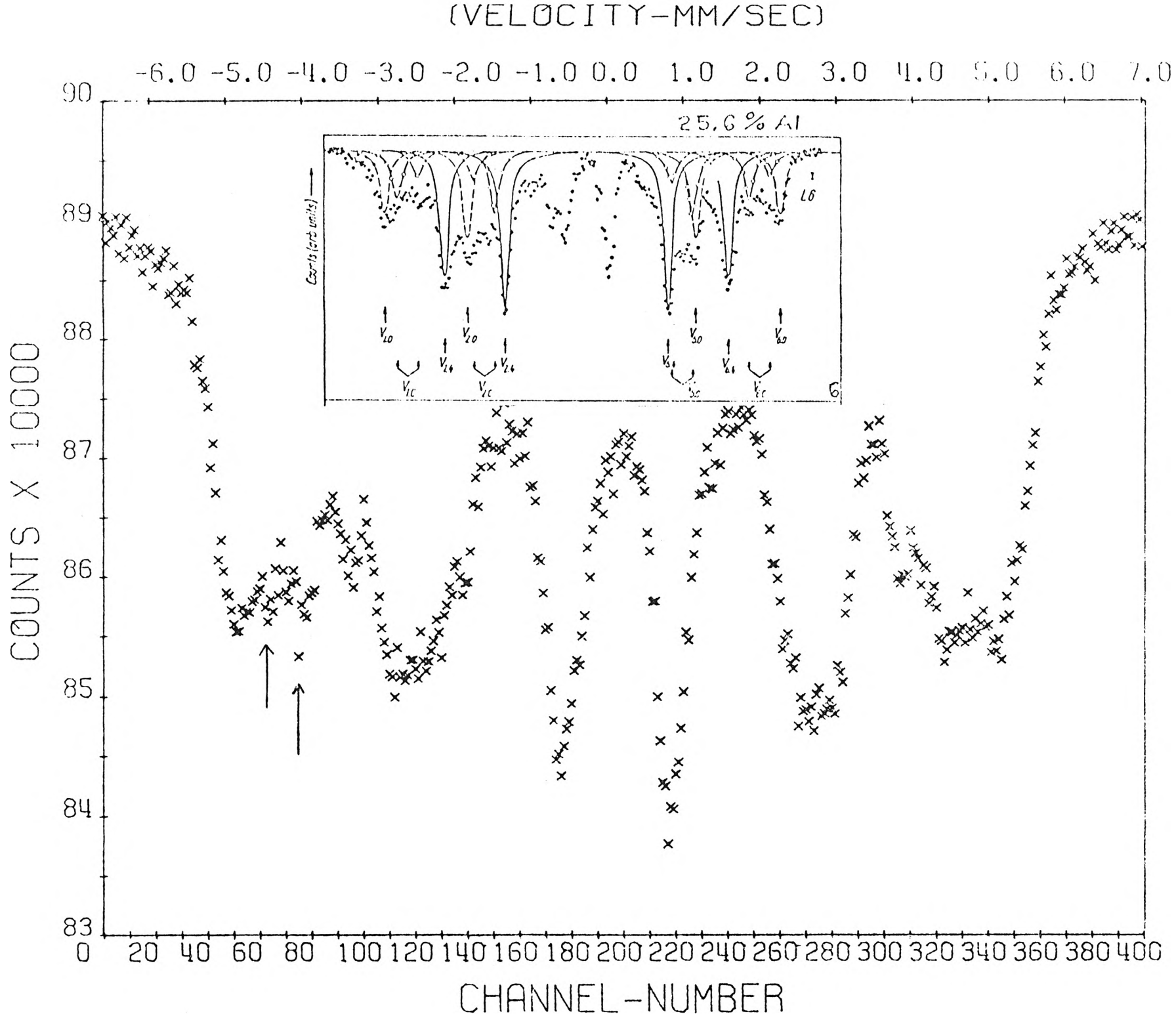

FIGURE 28 CARBURIZED AT 1100°C AND WATER QUENCHED

spectra were added and compared to the actual experimentally obtained spectrum. This procedure was repeated until a best fit with the experimental spectrum was obtained. From the best fit, each Fe_{nn} component percentage effect, which is dependent upon the relative number of Fe_{nn}, could be obtained.

As already realized, the fitting procedure must now consider the 3,4,5,6,7 and 8 Fe_{nn} components and this added considerable complication over the originally believed 4,8 and 6 Fe_{nn} components. The computer fitting required the imput parameters mentioned above; however, many Fe_{nn} components are hidden within the spectra, especially for the disordered spectra, and are not resolved enough to calculate the quadrupole splitting and center shift. Also, to imput the first 'guess' for the percentage effect for each Fe_{nn} component, the theoretical amounts as calculated earlier for an intelligently guessed long range order parameter was assumed. However, this would not be correct for the 5 Fe_{nn} component in light of the antiphase boundary contributions. To circumvent this handicap, a hand unfolding of the spectra was attempted by plainametric means to acquire the center shift, quadrupole splitting and percentage effect of each component. For the well ordered specimens spectra, this proved realitively successful, but no success was encountered for the disordered specimens.

To overcome the above problem, a procedure was devised using X-Ray analysis to obtain the long range order parameter for each time of anneal and thus knowing the exact theoretical percentage effect, an unfolding technique as before would be utilized for the 3,4,6,7 and 8 Fe_{nn} components and the remaining area of the spectrum would be attributed to the 5 Fe_{nn} component. This procedure was not used due to a consideration that up to this point was not taken into account.

Referring to the anneal series shown earlier by figure 26, the invisioned microstructure shows that during the room temperature quench, fine DO_3 domains are formed surrounded by the disordered α' phase. After the first time increment of anneal, the DO_3 domains exist in the equilibrium state of order which may be obtained for that particular temperature using figure 29. As the annealing process proceeds, the DO_3 domains grow absorbing each other and nearby disordered material until the equilibrium amount of each phase is encountered as predicted by the phase diagram. For the 22 at% Al alloy, the equilibrium structure at 200°C consists of both α' and DO_3 phases.

Realizing that the disordered α' phase of long range order degree close to zero also contributes a certain probability of percentage effect for each Fe_{nn} component and that the Mössbauer spectrum shows but the sum total of each Fe_{nn} component, dispite what phase it arises, the analysis of the spectrum for each Fe_{nn} component for each phase becomes extremely difficult. Theoretical consideration for the probability of each Fe_{nn} component for order degree zero is presented in table 2.

TABLE 2

Fe_{nn}( )	PERCENTAGE EFFECT
Fe(8)	13.70
Fe(7)	30.91
Fe(6)	30.24
Fe(5)	17.22
Fe(4)	6.06
Fe(3)	1.37

THEORETICAL

FIGURE 29

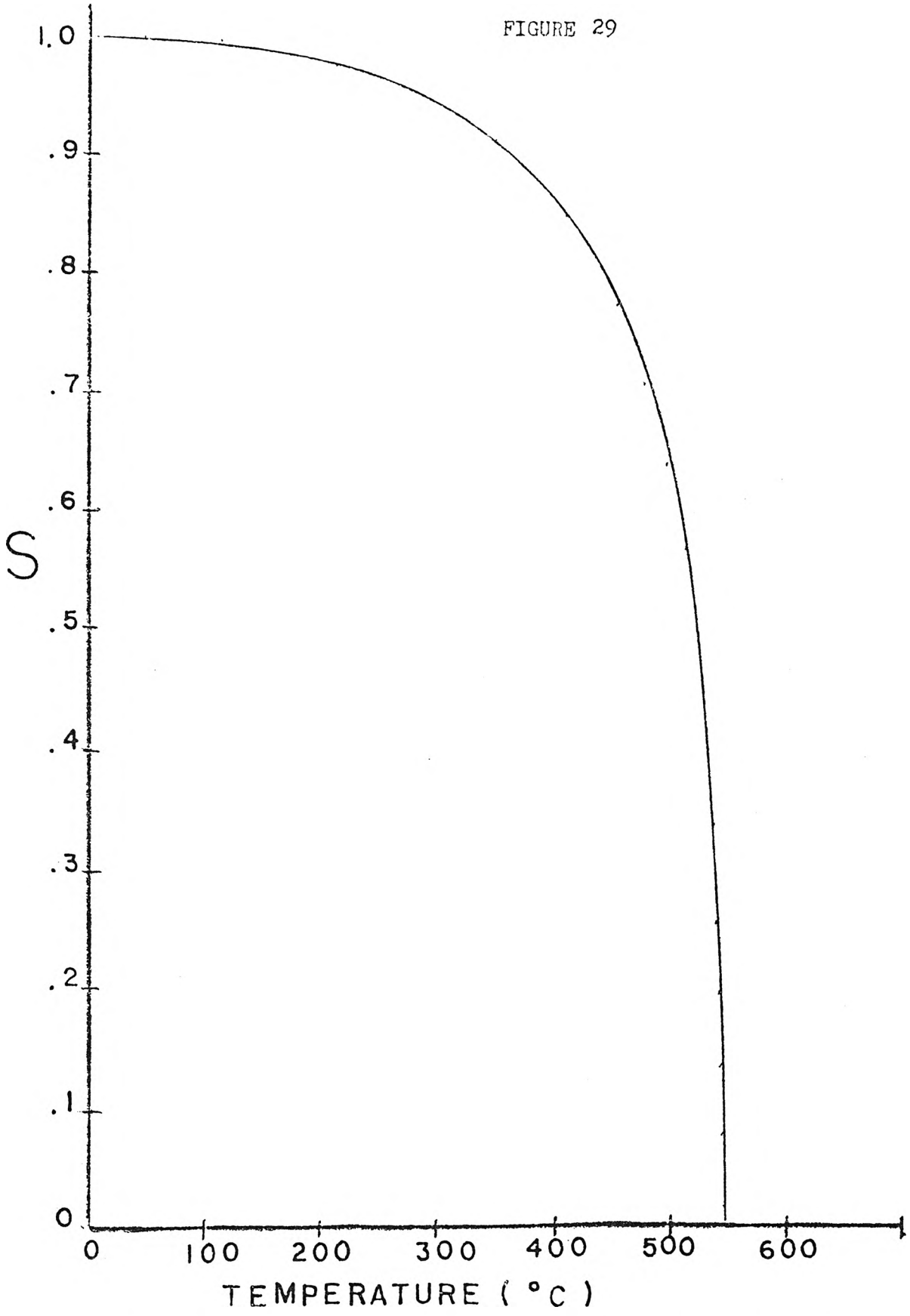

Equilibrium Degree of Order as a Function of Temperature as Determined by Rauscher (16)

Previously shown by figure 27 and table 2 are the theoretical probabilities of percentage effects that should be observed if and only if the specimens consists of either 100% α or 100% DO_3. However, this is not the case for our samples. At the time of the quench some DO_3 is present with α and at equilibrium some α exists with DO_3. Consequently, the observed percentage effect will be a composite of the α and DO_3 and be a function of their relative amounts. For example:

TIME OF QUENCH ----- 3% DO_3 97% α $S_{DO_3} = 0.94$ $S_\alpha = 0.0$

Iron nearest neighbor	Theoretical Percentage Effect DO_3 (100%)	α (100%)
Fe(8)	33.00	13.70
Fe(7)	4.30	30.91
Fe(6)	7.00	30.24
Fe(5)	23.00	17.22
Fe(4)	30.60	6.06
Fe(3)	1.50	1.37

Expected Percentage Effect

Fe(8)	(33.0%)(3%) + (13.70%)(97%)	14.28%
Fe(7)	(4.3%)(3%) + (30.91%)(97%)	30.11%
Fe(6)	(7.0%)(3%) + (30.24%)(97%)	29.54%
Fe(5)	(23.0%)(3%) + (17.22%)(97%)	17.39%
Fe(4)	(30.6%)(3%) + (6.06%)(97%)	6.80%
Fe(3)	(1.5%)(3%) + (1.37%)(97%)	1.37%

This process can be extended to other possible degrees of order and relative amounts of each phase. However, an added complication arises when the differences in Al concentrations between the disordered

α and ordered DO_3 phases is considered. The ordered DO_3 domains formed have Al concentrations of 25 at% Al and therefore the disordered α phase is depleted of Al atoms as the amount of DO_3 domains increases. Therefore, the Fe_{nn} components arising from the disordered α phase change with time due to concentration variations. Also, possibly a point is reached near equilibrium where the DO_3 domains have consumed most of the disordered α and therefore the DO_3 domains now must change its Fe_{nn} components due to the lack of Al atoms to fulfill the desired configuration.

The computer analysis of the spectra yields only the total percentage effect of each component. As outlined earlier, the kinetics of DO_3 ordering from disordered α was to be determined by noting the change of the DO_3 Fe_{nn} components percentage effect with ordering; however, the percentage of the total observed Fe_{nn} components that actually belong to the DO_3 phase is unknown. One may consider the theoretical as in the example before, but this is not correct in view of antiphase boundaries. Other complications arise when the possibility of supersaturation of Al during the quench is considered. If this happens, the probabilities of the Fe_{nn} components of the α phase change with annealing due to the composition change. Also, if it is incorrect to state that the DO_3 domains when formed during the growth process is at the equilibrium degree of order for that temperature of anneal, then the DO_3 domains must be considered to be ordering to a higher order as it grows.

In conclusion, when considering that a computer fitting procedure may be perfected for the analysis of these extremely complicated overlapping spectra, the need to know the relative amounts of each phase at each time of anneal in order to calculate the theoretical or the exper-

imental rate of DO_3 ordering, actually the growth of DO_3 domains from the disordered α phase, makes the use of the Mössbauer effect infeasible for this particular problem in view of other more straightforward techniques. Ideally, the observation of the change of the DO_3 Fe_{nn} components with ordering would produce direct evidence of the growth of the DO_3 domains. However, the Mössbauer effect spectra reveal the total Fe_{nn} components despite what phase they may arise; therefore, the DO_3 Fe_{nn} components cannot be separated from the total component without resorting to theoretical means which was shown to be in partial error.

The ordering process discussed is actually only a growth of the DO_3 domains from the disordered α phase and X-Ray diffraction techniques provides a basic means for the acquiring of the desired information. Briefly, diffraction patterns for a disordered alloy would be as normally predicted for any metal, whereas for the ordered alloy diffraction pattern, new lines arise known as superlattice lines. Experimentally, the intensity of these superlattice lines are dependent upon the degree of long range order present within the alloy. The advantage of X-Ray techniques over the Mössbauer technique for this particular concern lies with the consideration that only the ordered structure, DO_3, is observable with the use of superlattice intensities; the intensity increasing with the amount of DO_3 domains. The disordered α phase acts as any normal metal alloy producing normal fundamental lines whose intensity remains the same for both ordered or disordered alloy. Diffraction techniques will also produce results revealing the variations in the size of ordered domains. Therefore, the desired information may be obtained without the use of the Mössbauer effect merely by observing the change of the degree of long range order with the DO_3 domain growth. Kensuke Oki[17] et al. have determined the kinetic behaviors of

ordering for Fe_3Al alloys using X-Ray diffraction techniques with large success.

Investigating the feasibility in obtaining the kinetics of ordering for the DO_3 structure from the disordered α for the 25 at% Al alloy will be the next concern. Using the same experimental response as before utilizing the Mössbauer spectrometer, the impossibility of this problem is immediately realized from the work of Swan[13] et al. who showed that even at a quenching rate of 50,000°C per second through the B2 or FeAl region to room temperature from the disordered α region did not retain the α phase but resulted in fully 100% fine domain sized B2 structure. Therefore, DO_3 ordering from disordered α will never exist at this composition or for our experimentally used quenching rates. Nevertheless, the ordering rate of DO_3 from a B2 structure may be determined.

Acknowledging that DO_3 domains grow from B2 domains as a nucleation and growth process,[14] one would expect to see the DO_3 Fe_{nn} components to grow in at the expense of the B2 Fe_{nn} components when viewing an anneal series as before. However, the same problems arise as before; the relative amounts of each phase at each time of anneal is needed to be known in order to detect the change in the DO_3 Fe_{nn} components with ordering. A further complication arises beyond the previous example's problem; the B2 domains are also growing as the DO_3 domains are growing and consuming the B2 ordered structure. The work of K. Oki[17] supports this statement by the following observation as expressed by figure 30 and 31.

The required information before the spectra may be analyzed for the percent change of the DO_3 structure Fe_{nn} components as a function of time include the relative amounts of each phase with time and the degree of

FIGURE 30

ISOTHERMAL CHANGE IN DEGREES OF ORDER FOR DO_3 and B2 at 383°C

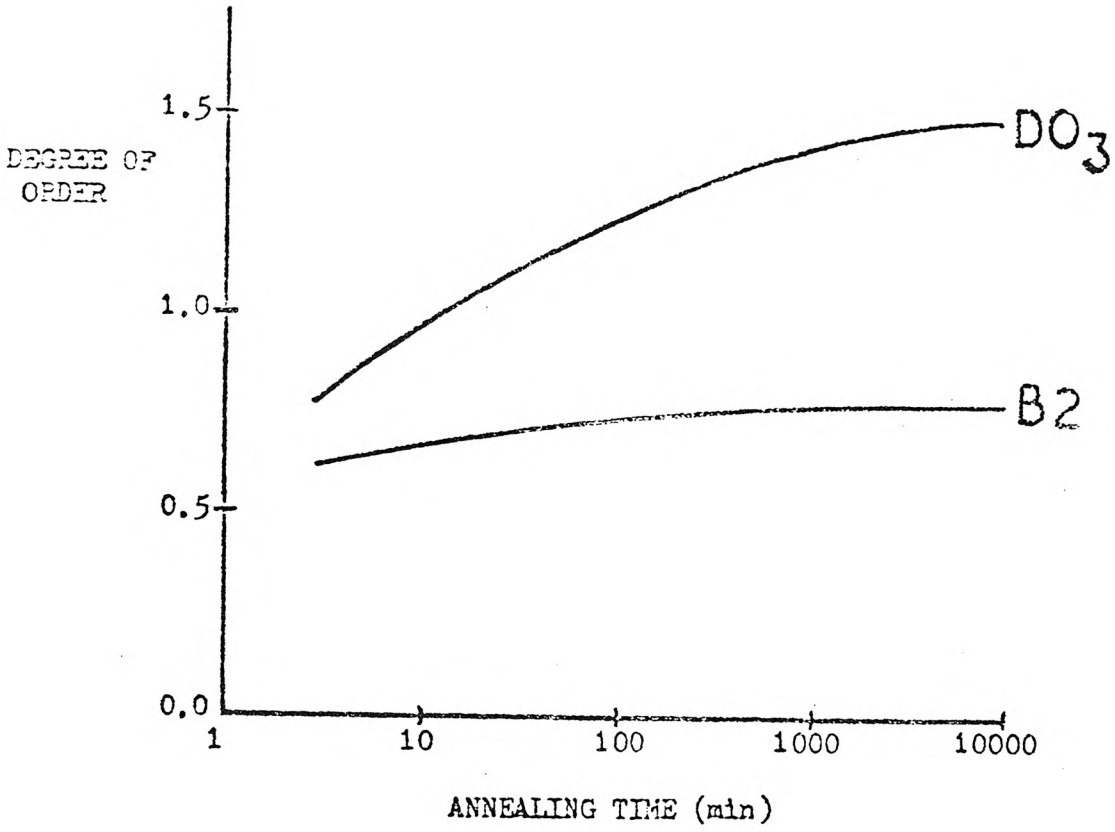

FIGURE 31

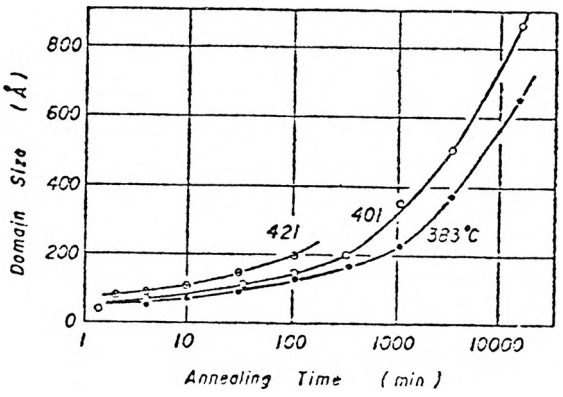

DOMAIN GROWTH OF DO_3 TYPE ON ISOTHERMAL ANNEAL

long range order for the B2 structure. This last information is required in order to calculate the theoretical percentage effect for each B2 Fe_{nn} component and with the knowledge of the relative amount of each phase, subtract these B2 components from the analyzed total spectra Fe_{nn} components thereby leaving the true DO_3 Fe_{nn} components. However, this technique is not accurate because as already observed, the actual Fe_{nn} component percentage effects do not follow theoretical considerations.

The previous concepts may be extended to other two phase ordering systems to find them to be equilly infeasible with the Mössbauer effect for the acquisition of the rate of ordering. There does exist a possibility of obtaining the kinetics of ordering of a phase from a more disordered state of that same phase; investigating the 25 at% Al alloy will elucidate this idea.

Based upon the equilibrium order degree Vs temperature diagram shown earlier by figure 29 for the 25 at% Al alloy, the degree of order is higher when lower temperatures are used to achieve equilibrium order. Therefore, if a specimen is ordered until equilibrium is reached at 500°C and subsequently ice water quenched to room temperature, thereby retaining the order state of 500°C (S=0.60) and subsequently performing isothermal anneals for various temperatures below 500°C but high enough so diffusion can take place readily (160°C), one may obtain the rate of the DO_3 ordering from more disordered DO_3 in the same manner as outlined previously. A question arises as to the possibility of observing a significant change in the Fe_{nn} components between the disordered and the ordered state to determine this change with the Mössbauer spectrometer. Consequently, the theoretical probabilities of various Fe_{nn} components was calculated for degrees of order for the 25 at% Al alloy.

Figure 32 is a graph for the probabilities for the Fe_{nn} encountered for different degrees of order for the 25 at% Al alloy. As previously determined, at 500°C, the equilibrium degree of order was determined to be 0.60 and at 160°C, the order degree is 0.99. Based upon a theoretical approach, a significant difference exists at the two extremes; however, any annealing above 350°C creates questionable concerns, especially for the 3,5,6 and 7 Fe_{nn} components. Presently, only the end points of the ordering process has been considered; however, the changes between the various stages of annealing at ony one temperature may not be significant enough to be readily observable.

The Mössbauer spectra analysis would proceed as before utilizing a computer fitting procedure to obtain the percentage effect change for each Fe_{nn} component. For this single phase ordering process, the components arise only from the DO_3 ordered structure and all previous complications are absent if the assumption is made that no B2 ordered structure exists after ordering at 500°C.

Despite the limitations placed upon the utilization of the Mössbauer effect for the quantitative study of ordered systems, the Mössbauer effect offers a major advantage over diffraction or other techniques. The Mössbauer effect will yield more information via the observation of the change in nine different Fe_{nn} component percentages. X-Ray diffraction techniques yield only one article of information; intensity of the superlattice lines. The implication of using the various changes in the Fe_{nn} component percentages may be extended to study the effects of various treatments upon the different sublattices upon the imposition of various appropriate limitations.

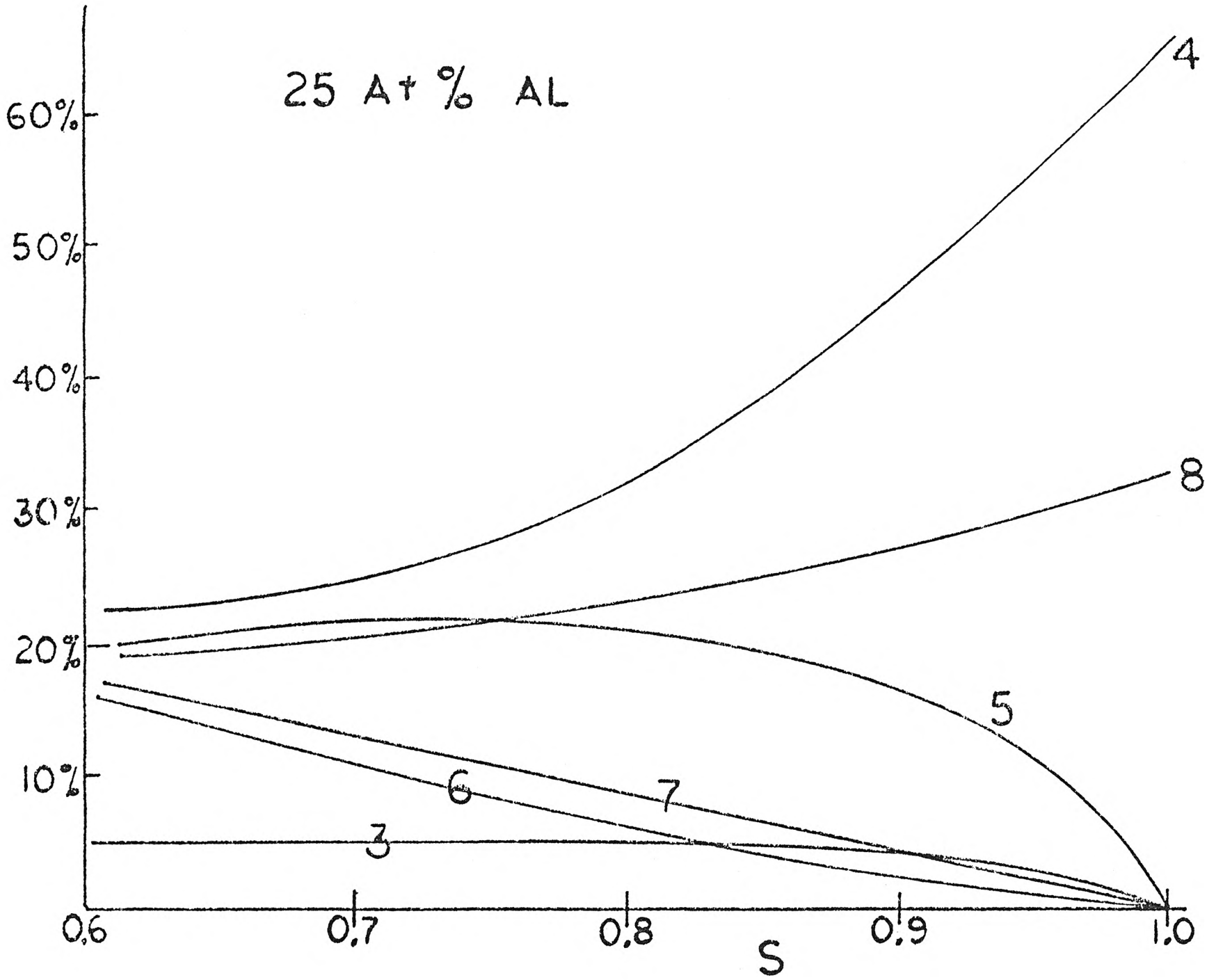

FIGURE 32

EXPERIMENTAL PROCEDURE

The alloy was obtained from the Naval Ordnance Laboratory in sheet form approximately 0.038 inches thick. The composition of the alloy was reported as 25 atomic percent aluminum and remainder iron. However, subsequent chemical analysis revealed the alloy to be 22 atomic percent aluminum.

In preparing the disordered alloy specimens, the alloy is air hot rolled to produce a sheet 0.008 inches thick. At this point, the 22 atomic percent aluminum alloy is water quenched from 1100°C after holding for four hours for equilibrium to be achieved producing a disordered α structure. This thickness and resulting oxide coating is unsatisfactory for Mössbauer effect work; therefore, the specimens are sand blasted to remove the oxidized layers of metal and subsequently chemically thinned to 0.002 inches using a 70% phosphoric acid, 15% nitric acid, and 15% water solution heated to 68°C.

The isothermal annealing as a function of time was performed utilizing a silicon oil bath with temperature control valid to $\pm$ 1.0°C. For the stopping of the ordering at any particular time of anneal, the specimen is rapidly quenched into water. Subsequent Mossbauer effect spectrum is obtained for each time of anneal as shown be figures 26 and 33.

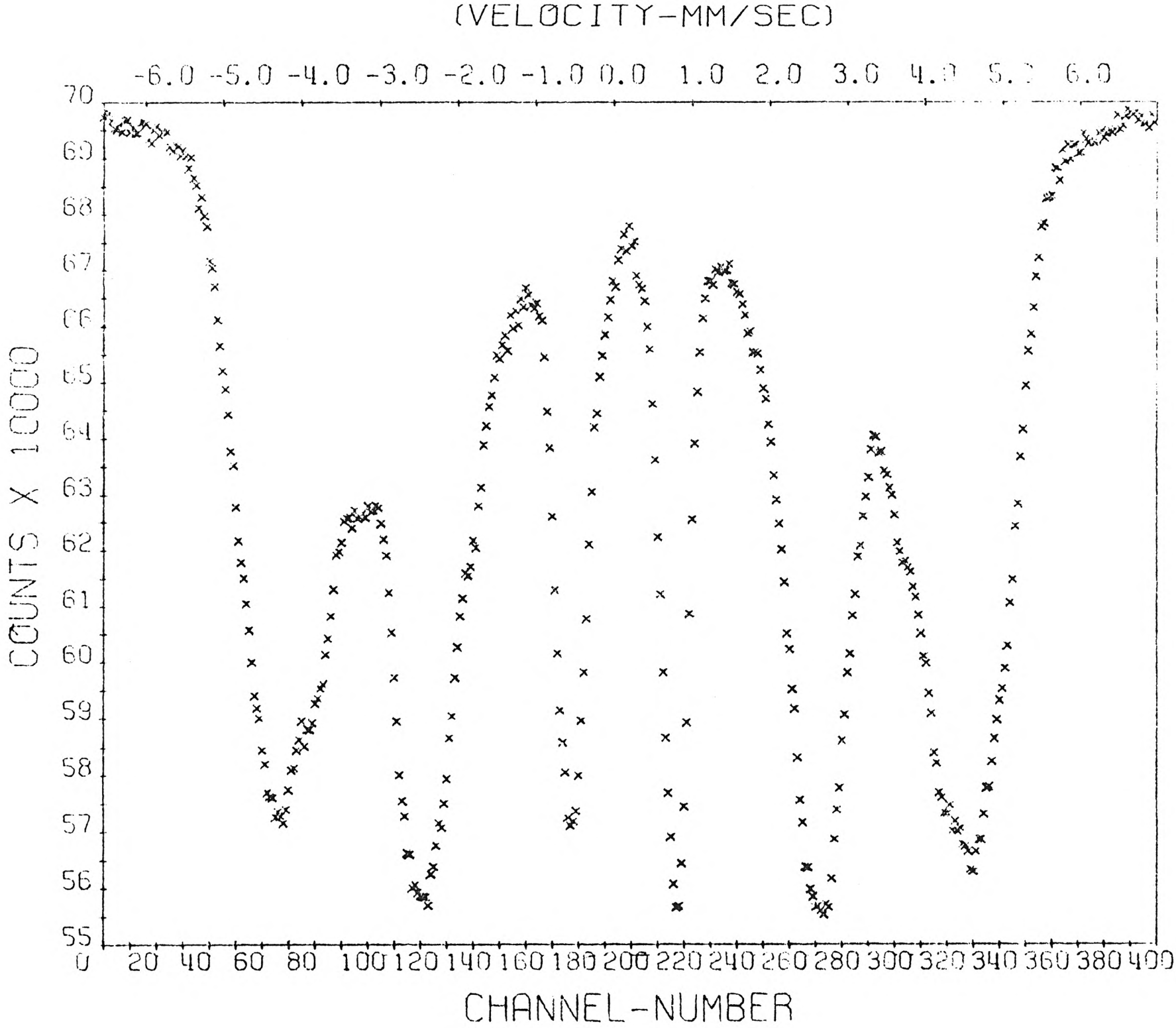

FIGURE 33 WATER QUENCHED FROM $1100^{0}C$

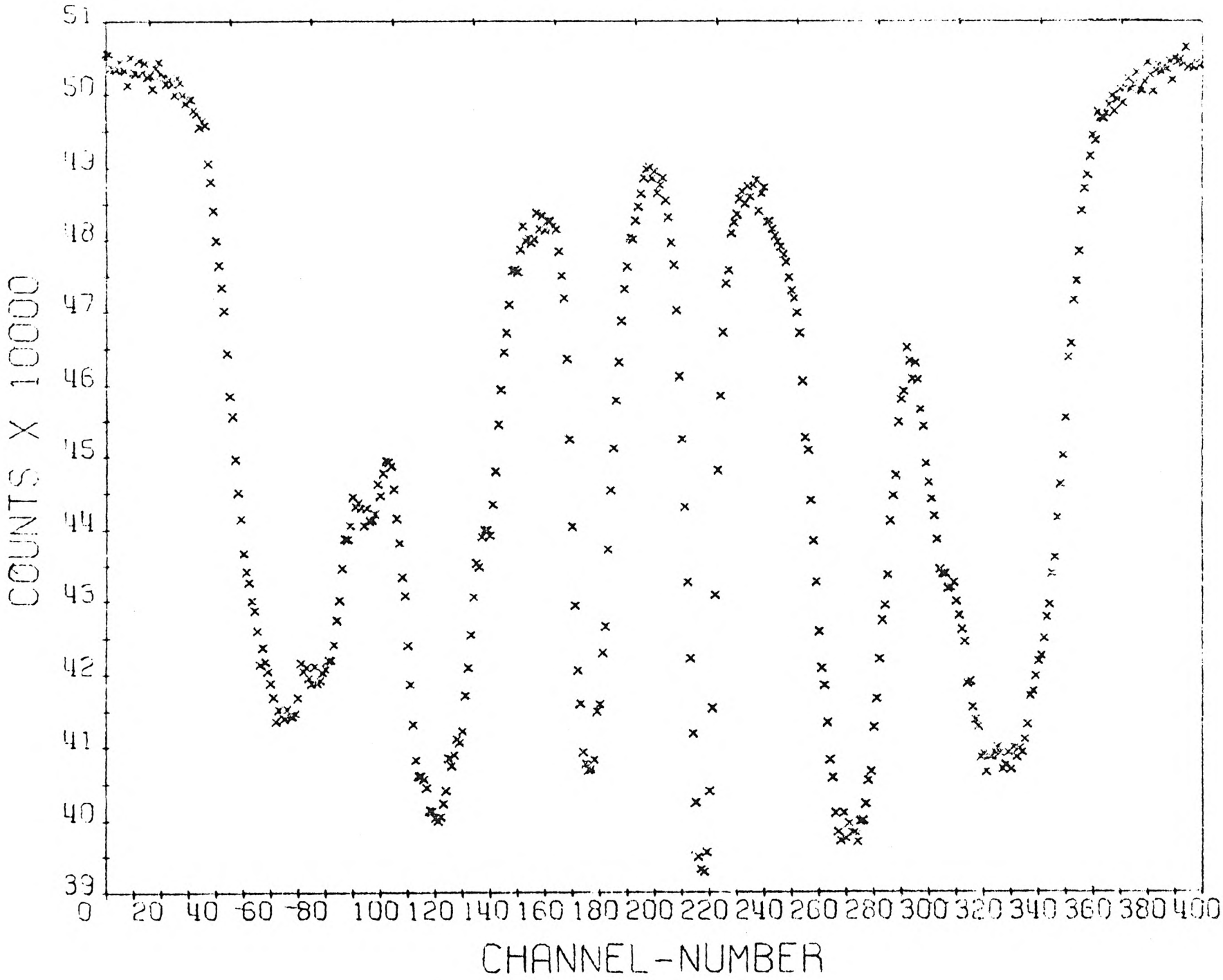

FIGURE 33

ANNEALED FOR 4 MINUTES AT 240°C

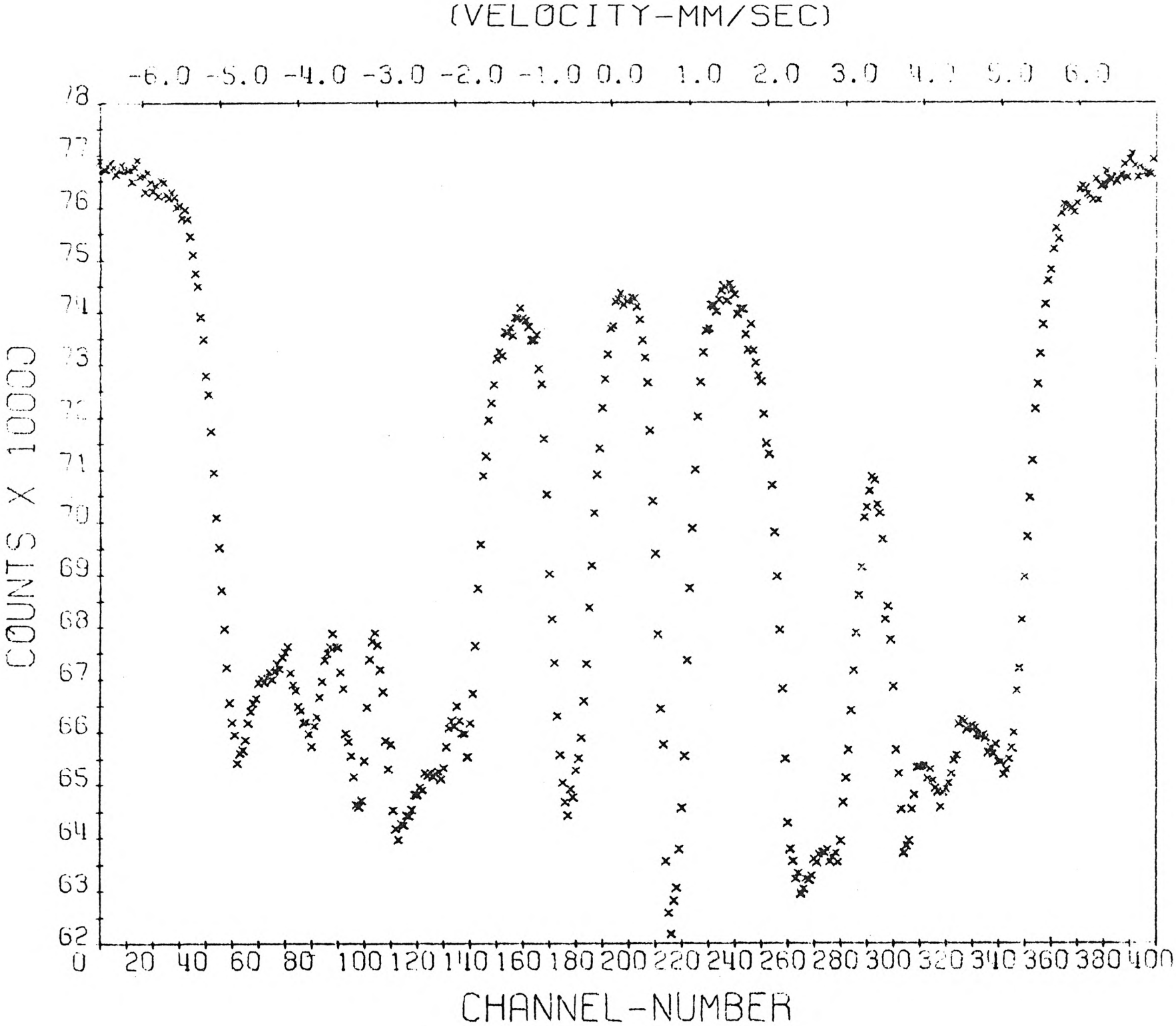

FIGURE 33 ANNEALED FOR 17 MINUTES AT 240°C

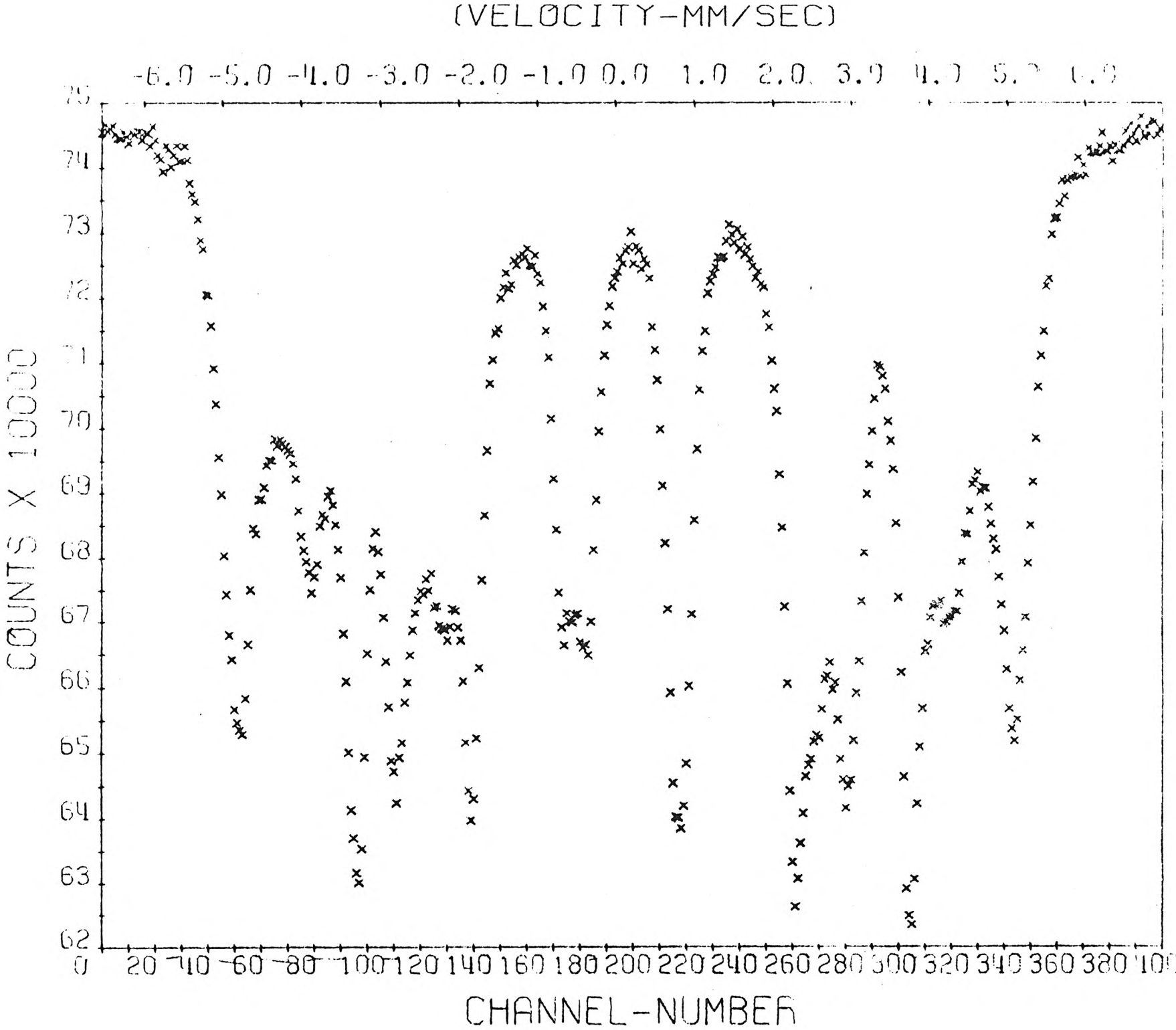

FIGURE 33 ANNEALED FOR 1 HOUR AT 240°C

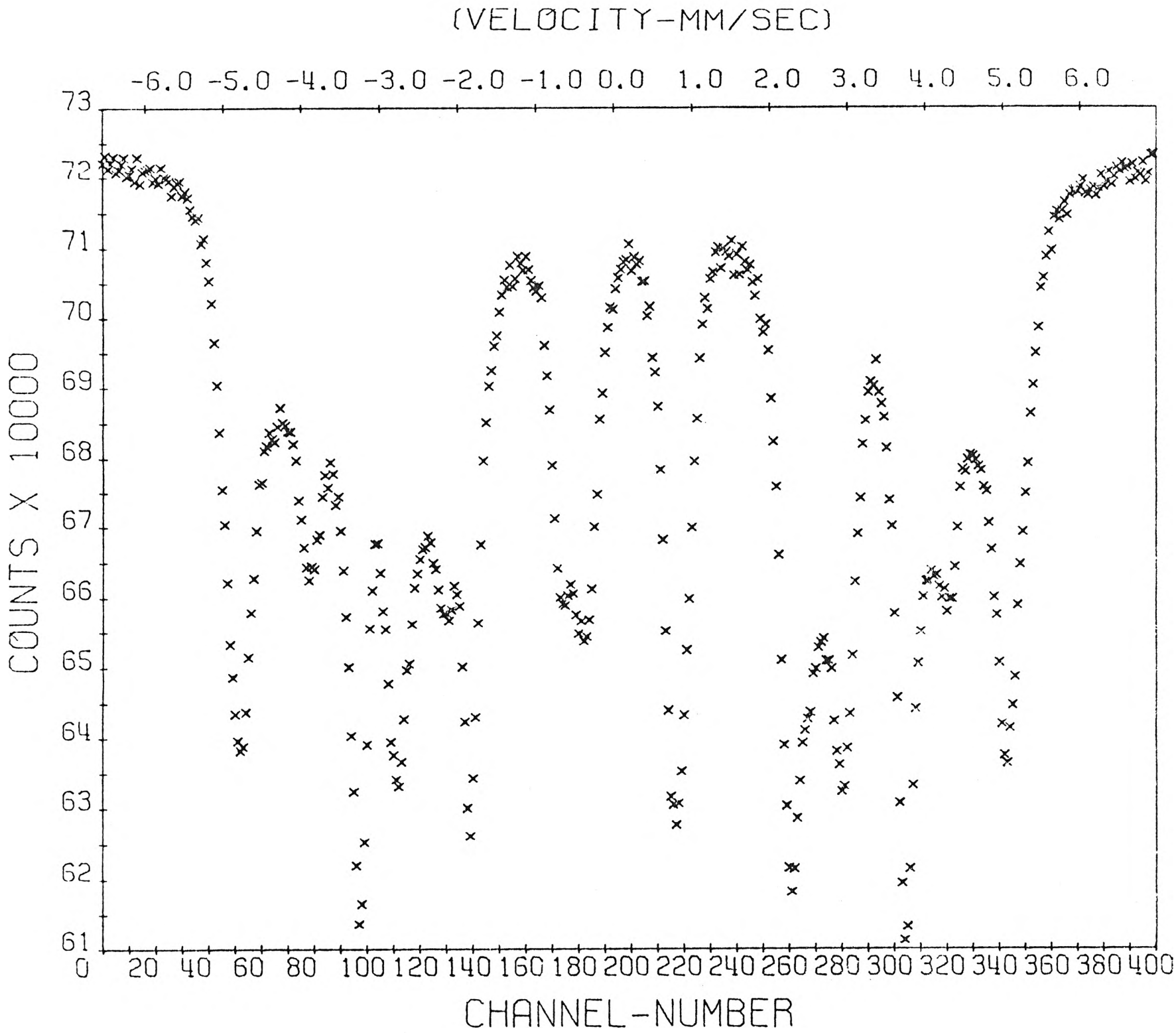

FIGURE 33

ANNEALED FOR 4 HOURS AT 240°C

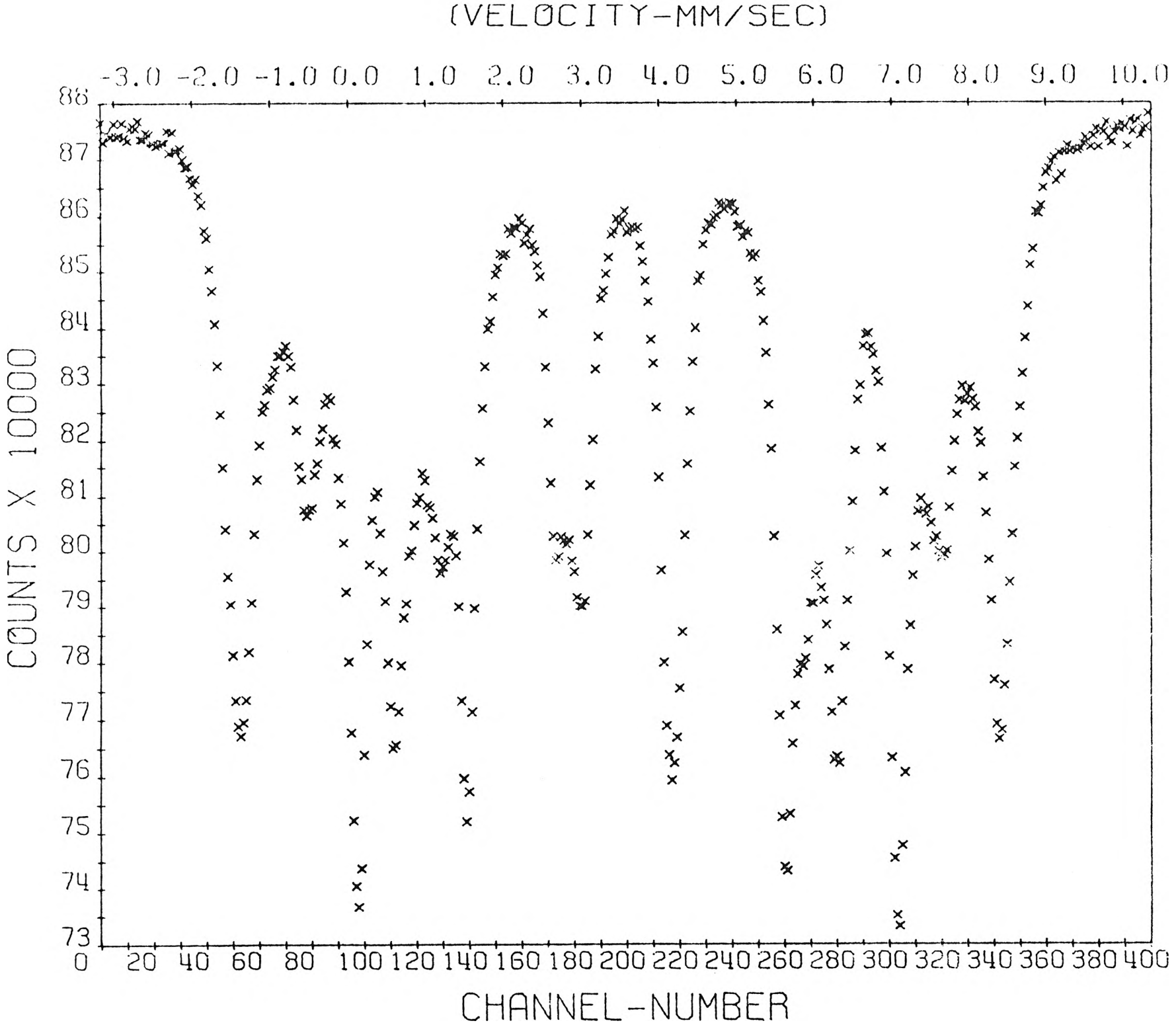

FIGURE 33 ANNEALED FOR 22 HOURS AT 240°C

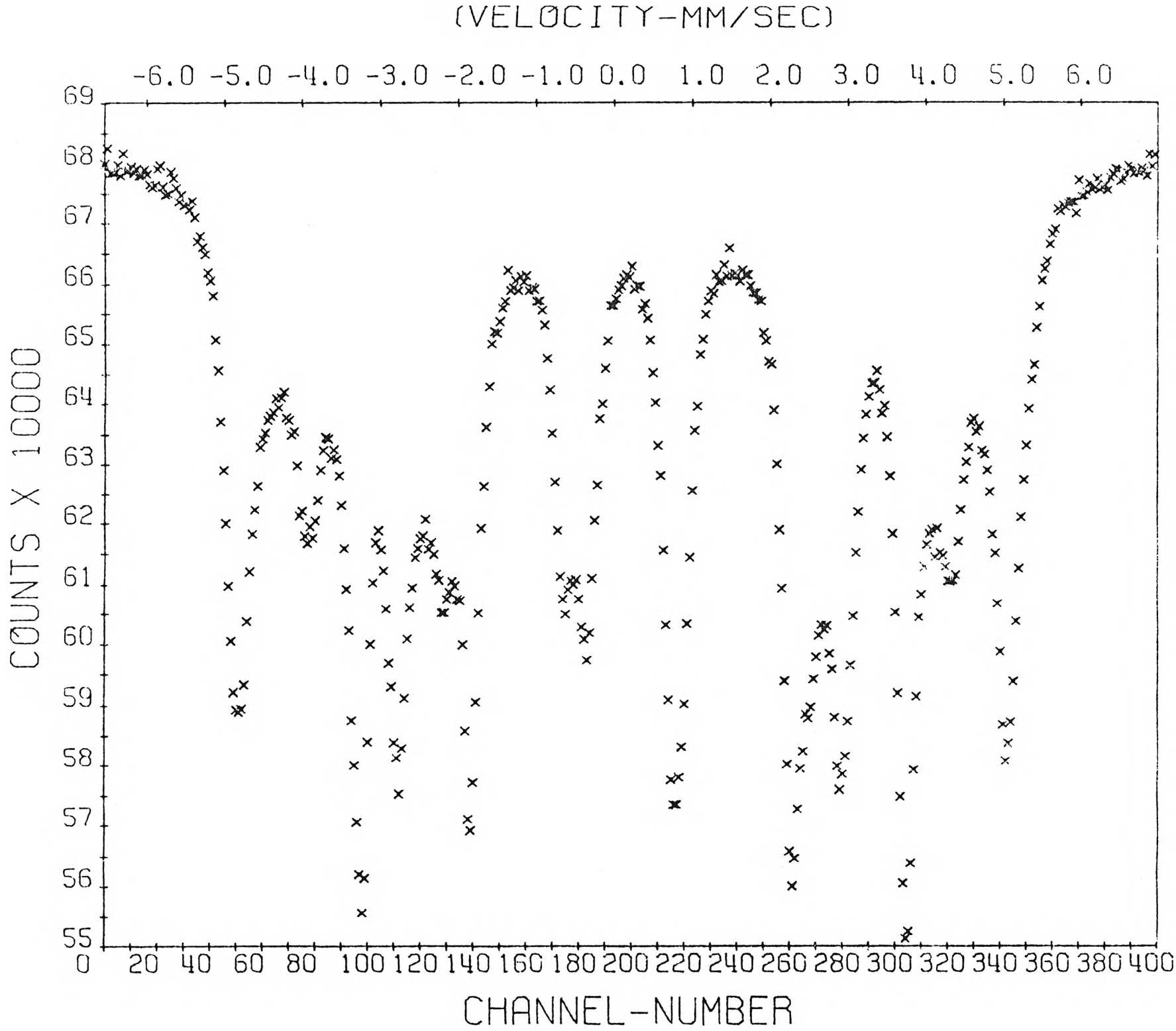

FIGURE 33 ANNEALED FOR 40 HOURS AT 240°C

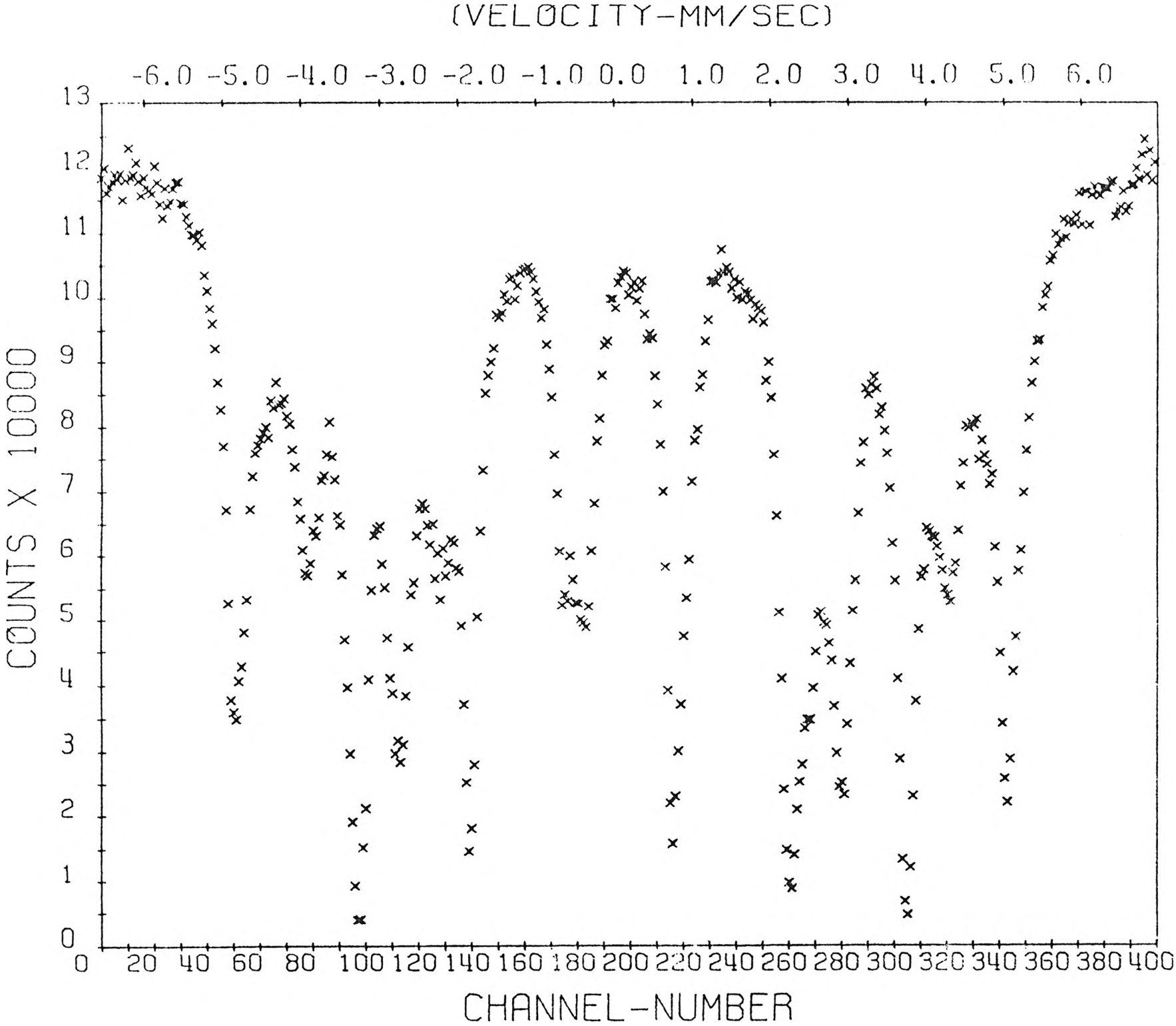

FIGURE 33 ANNEALED FOR 43 HOURS AT 240°C

EXPERIMENTAL RESULTS

A Determination of Alloy Composition

The Mössbauer effect peak assignments and percentage effect for each Fe_{nn} component for the 200°C anneal series did not agree with other researchers for the 25 at% Al alloy. However, a good agreement was noted if the alloy was 22 at% Al. Figure 34 presents the spectrum associated with a specimen that was quenched from 510°C after achieving equilibrium. If the alloy was 25 at% Al, a different spectrum from the 1100°C quenched specimen would be seen due to the DO_3 order present. The spectrum did not illustrate a difference just as a 22 at% Al alloy would be expected not to show a difference. From this data, a chemical analysis was justified which revealed the alloy to be 22 at% Al.

B Order Induced by Gamma Irradiation

An interest persisted as to if gamma irradiation could be used to produce order in a thermally disordered iron-aluminum alloy. Figure 35 and 36 presents spectra for gamma irradiated 22 at% Al specimens that were irradiated for 167.2 hours at 2.34×10^5 R/Hr, and 171 hours at 2.34×10^5 R/Hr respectively. No difference between the disordered and irradiated spectra were observable.

C Mössbauer Effect Spectrum Line Broadening

The possibility of observing a change in the Mössbauer effect spectrum Fe_{nn} component peak widths with the annealing out of vacancies existing from the water quench was investigated. A water quench was performed from 1100°C for a 22 at% Al specimen and low temperature anneals were per-

formed and any change in peak width noted. Figure 37 presents such an anneal series.

This procedure proved to be in error because the Mössbauer effect is very sensitive to many types of lattice defects and no means was devised to separate the defect effects upon the spectrum. Also, the Fe_{nn} component peaks would need to be studied and not the observed peaks because the observed peak widths are a function of the percentage effect of hidden Fe_{nn} components. Therefore, the computer fitted spectrum peak widths was needed but the fitting procedure was not perfected.

D Disorder by Mechanical Deformation

Figure 38 presents the Mössbauer effect spectrum for the 22 at% Al alloy that was disordered by producing fine alloy fillings. The spectrum is unresolved and is due to magnetic effect considerations.

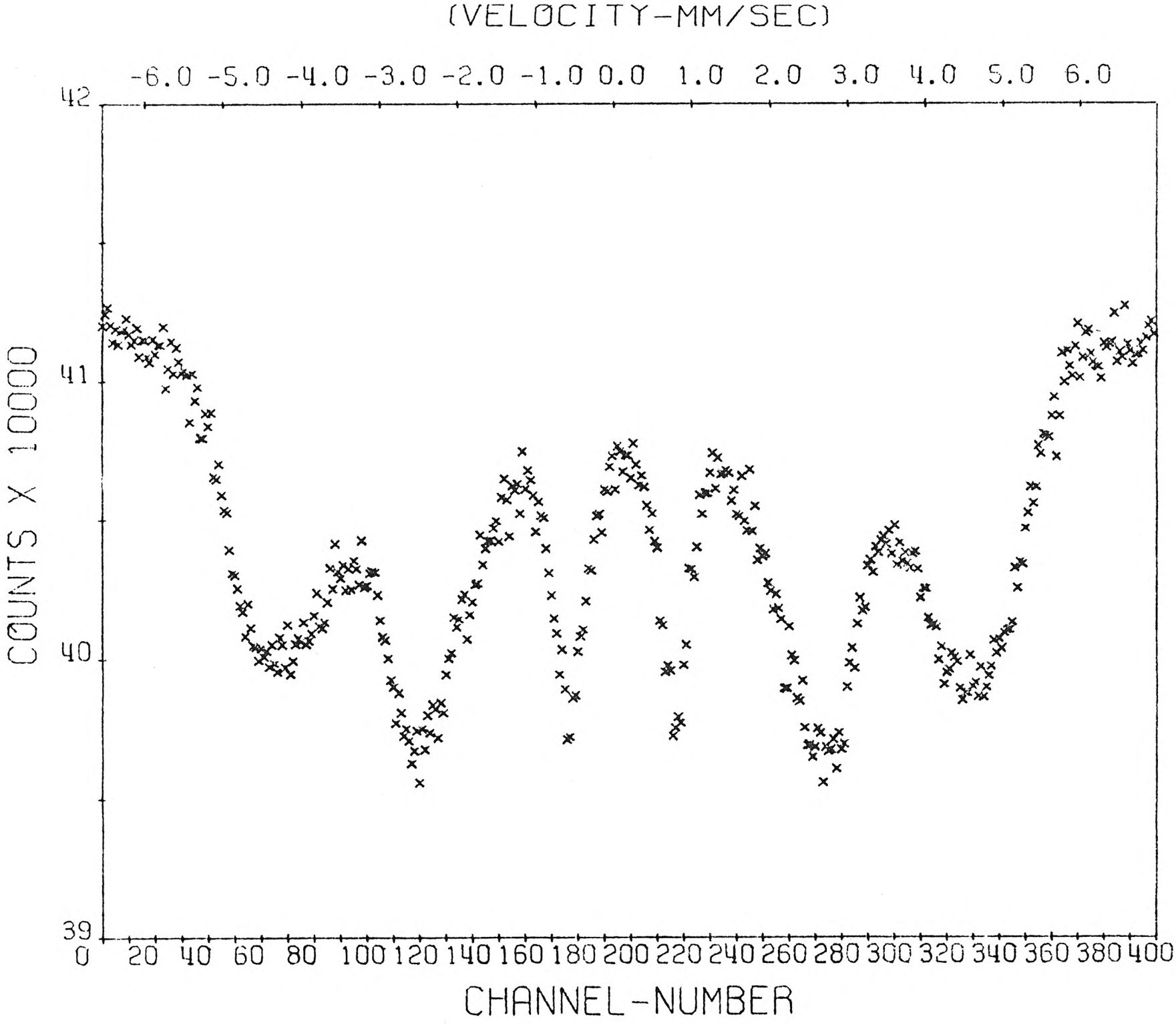

FIGURE 34 QUENCHED FROM 510°C

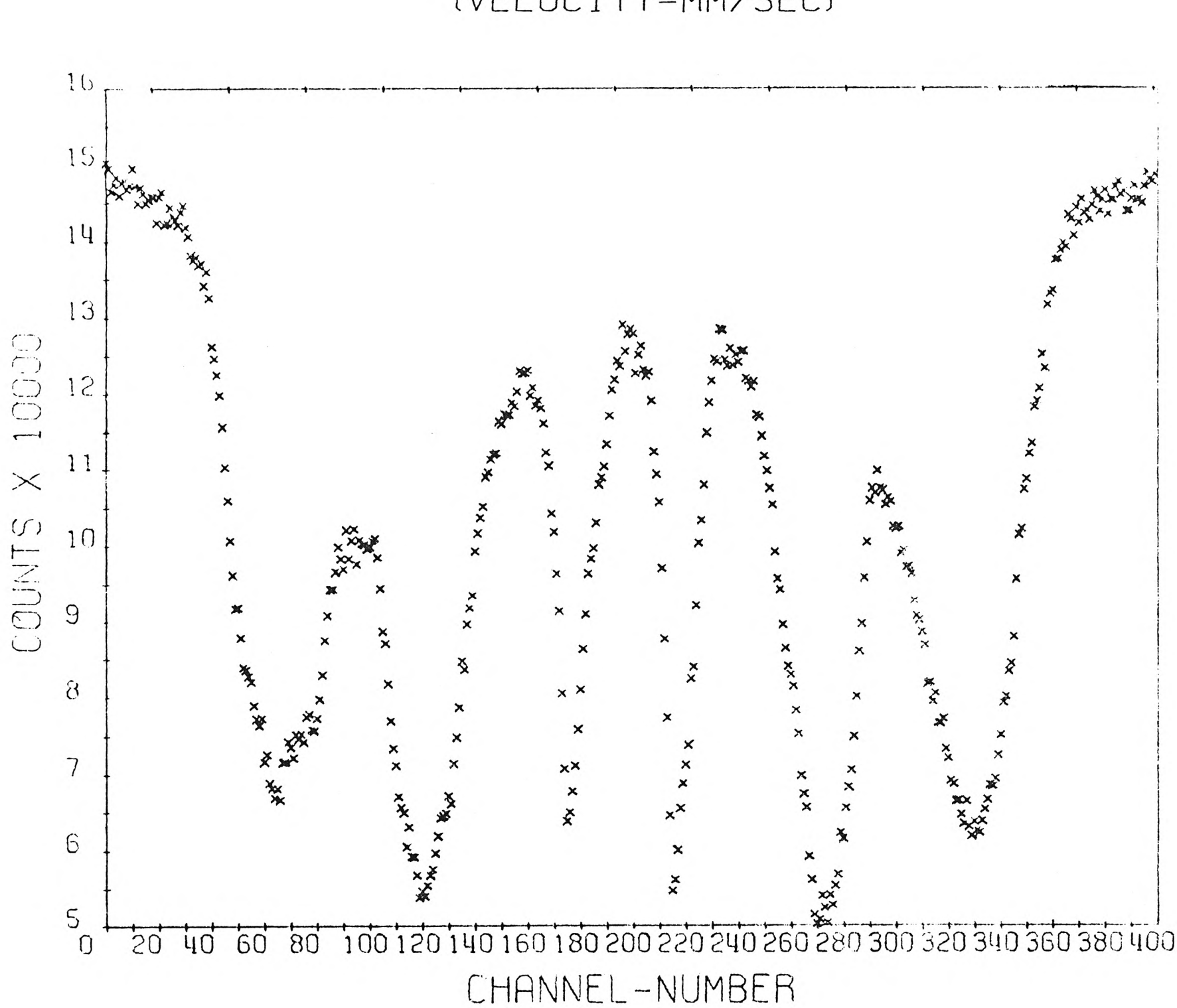

FIGURE 35 QUENCHED FROM 1100°C

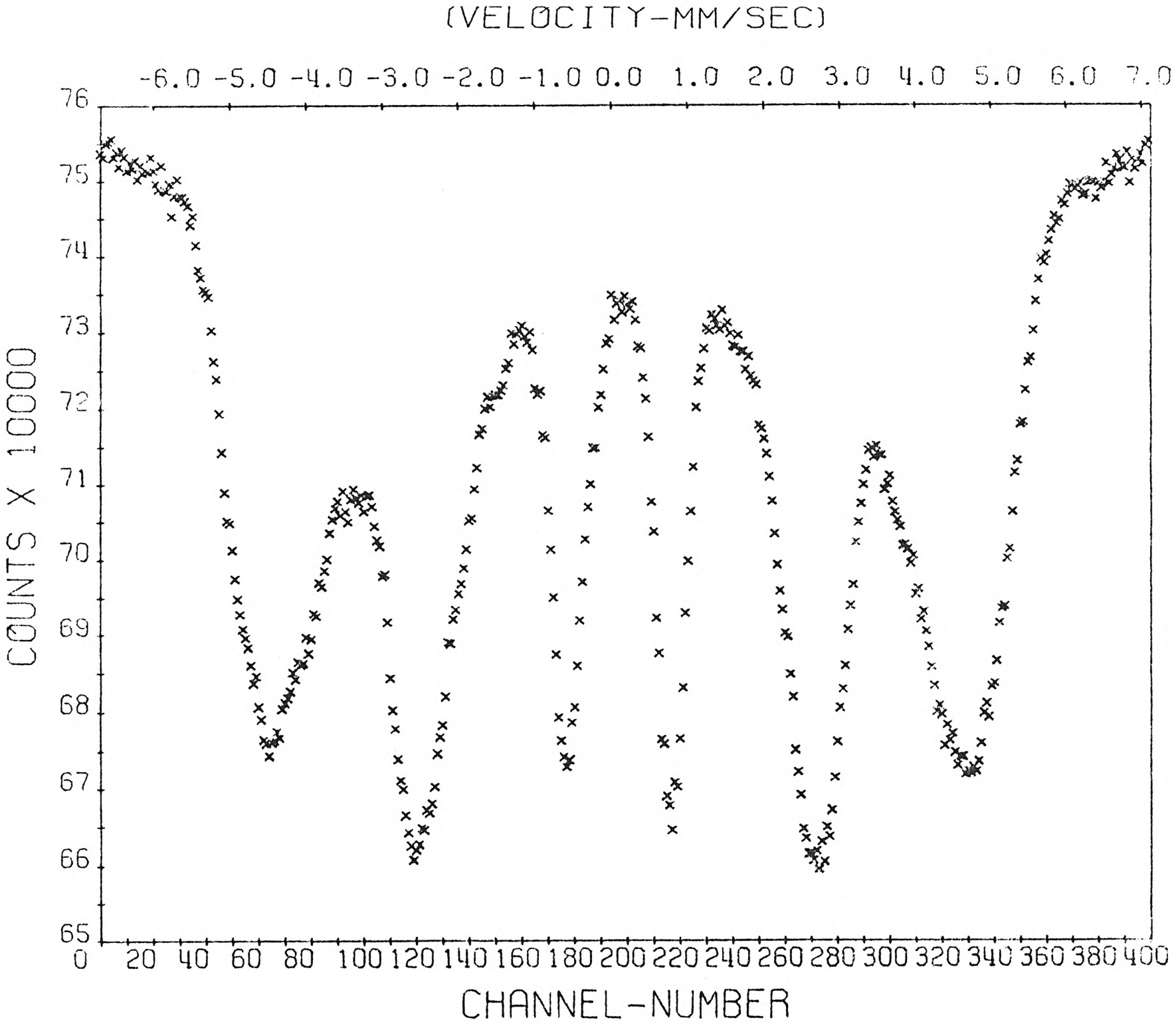

FIGURE 35 GAMMA IRRADIATED FOR 167.2 HOURS at 2.35×10^5 R/Hr

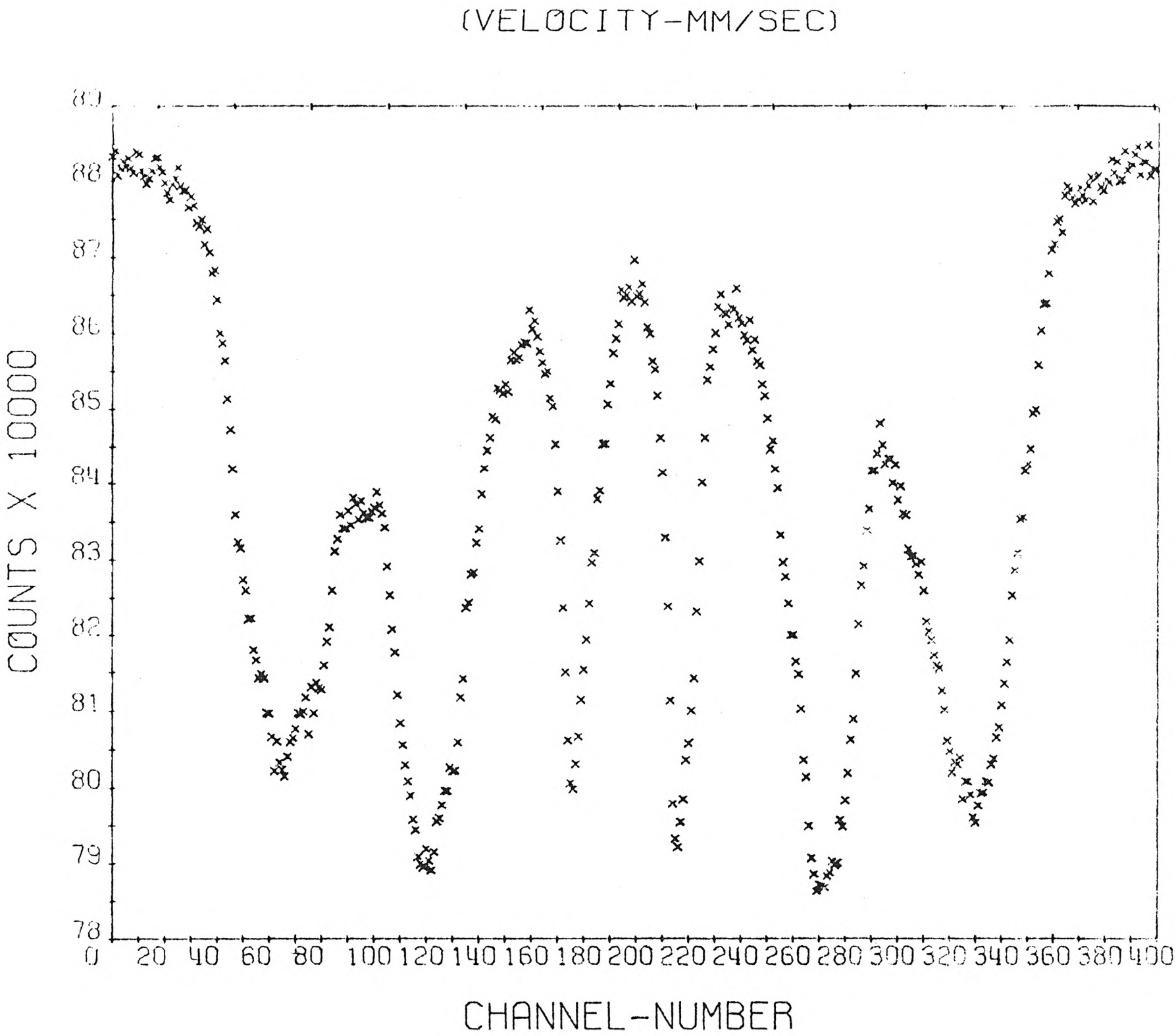

FIGURE 36 QUENCHED FROM 1100°C

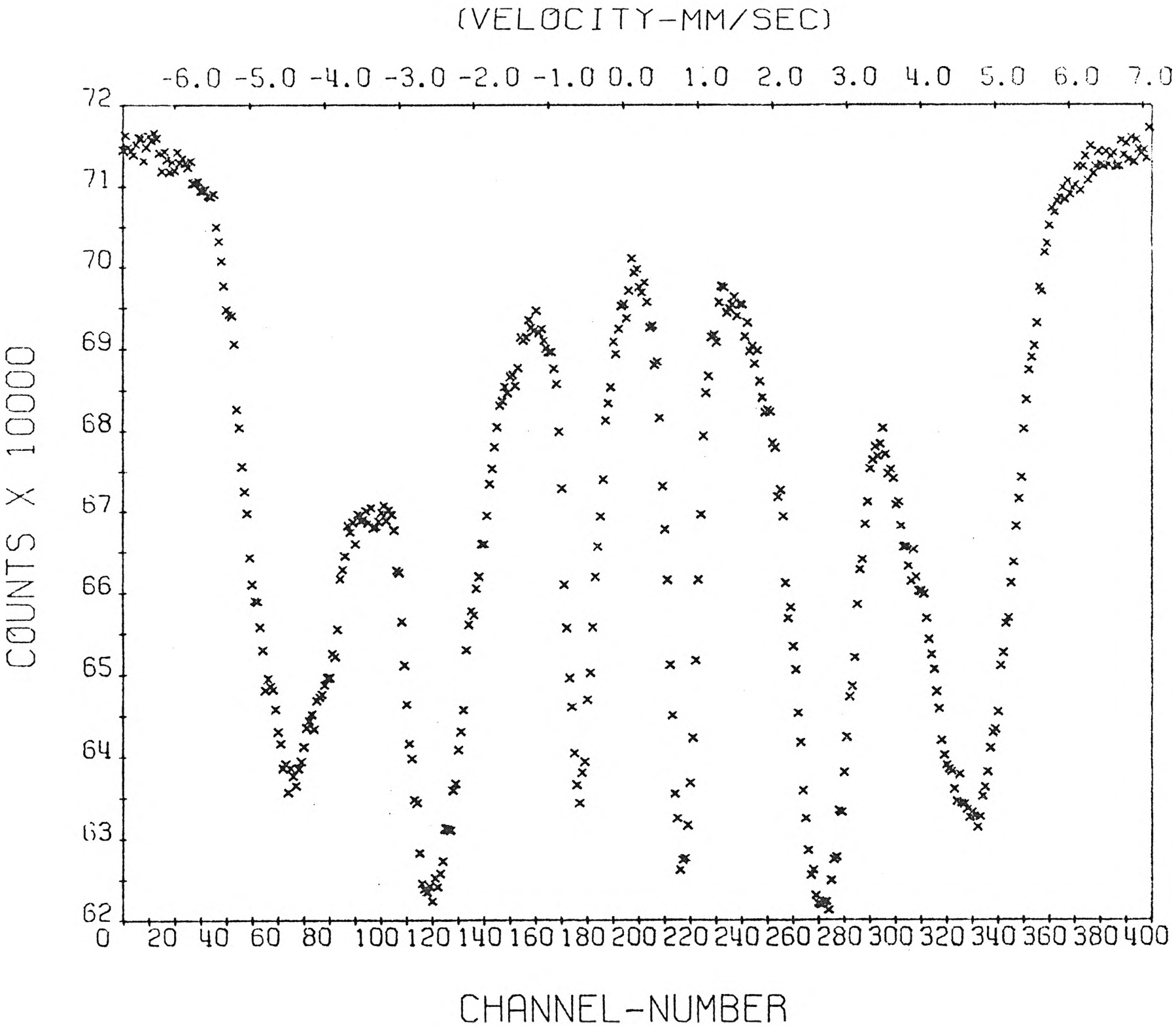

FIGURE 36 GAMMA IRRADIATED FOR 171 HOURS at 2.34×10^5 R/Hr

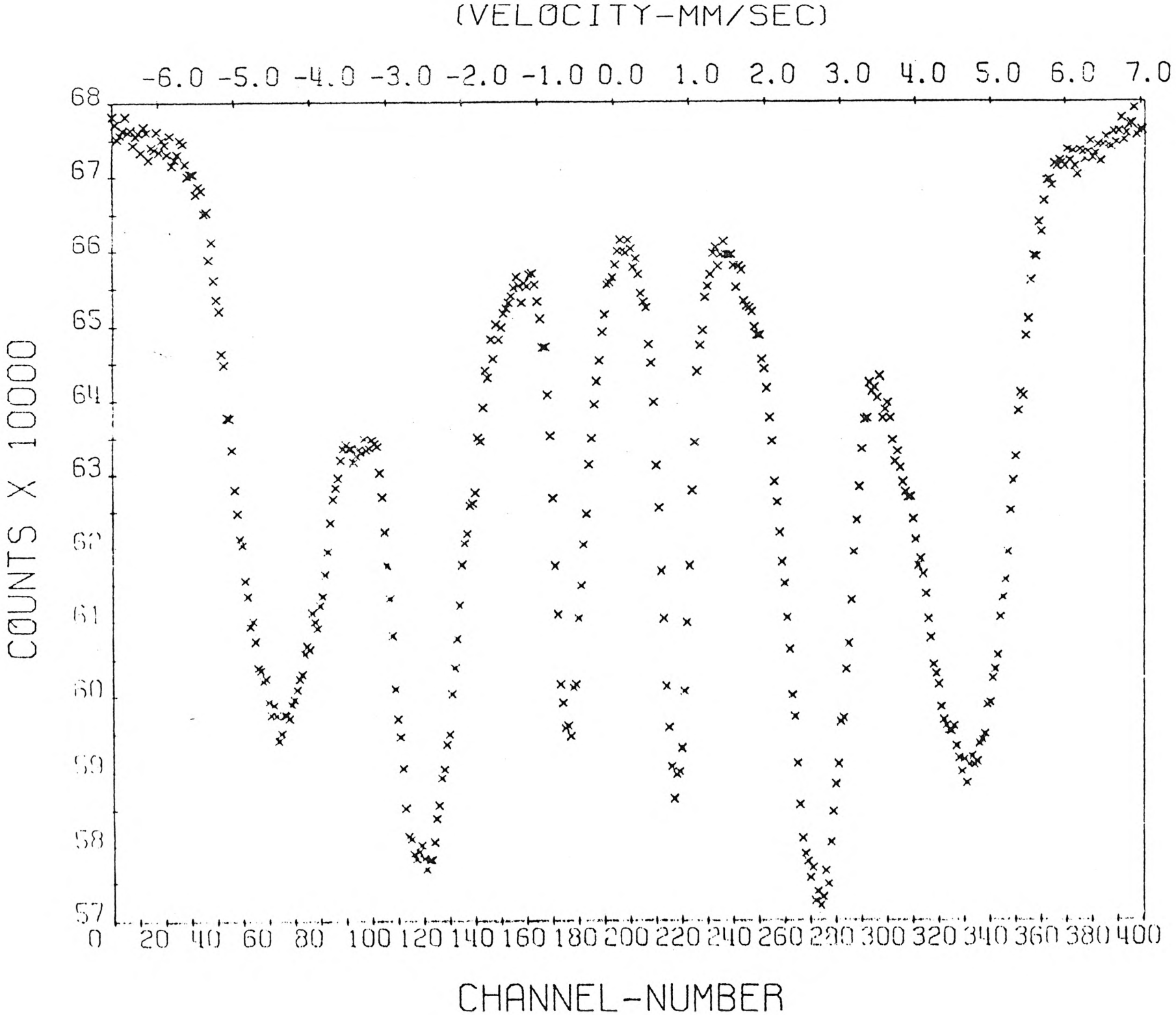

FIGURE 37

BRIEF CONCISE

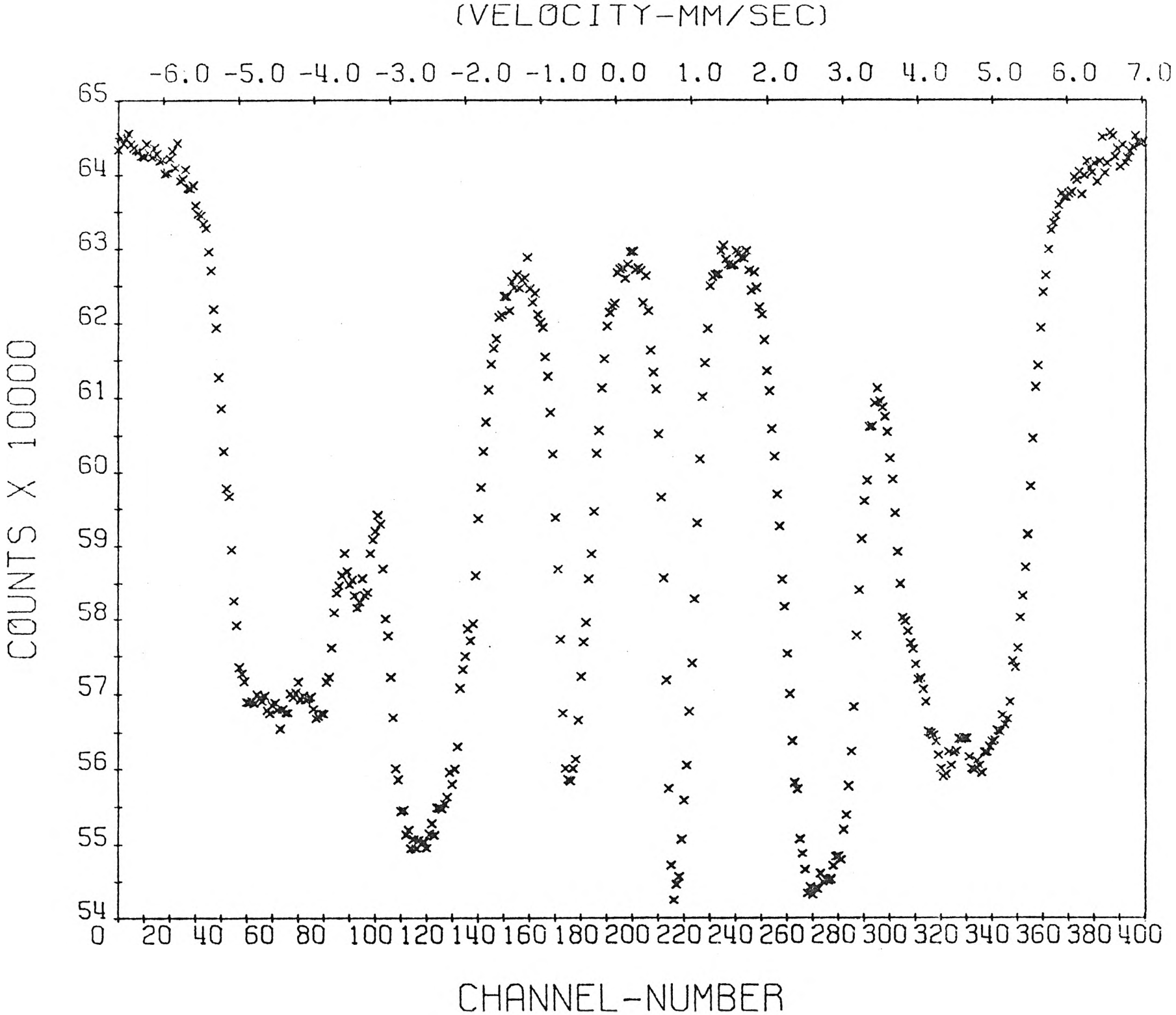

FIGURE 37 ICE BRINE QUENCHED ANNEALED FOR 1 HOUR AT 160°C

FIGURE 37 ICE BRINE QUENCHED ANNEALED FOR 7 HOURS AT 160^{0}C

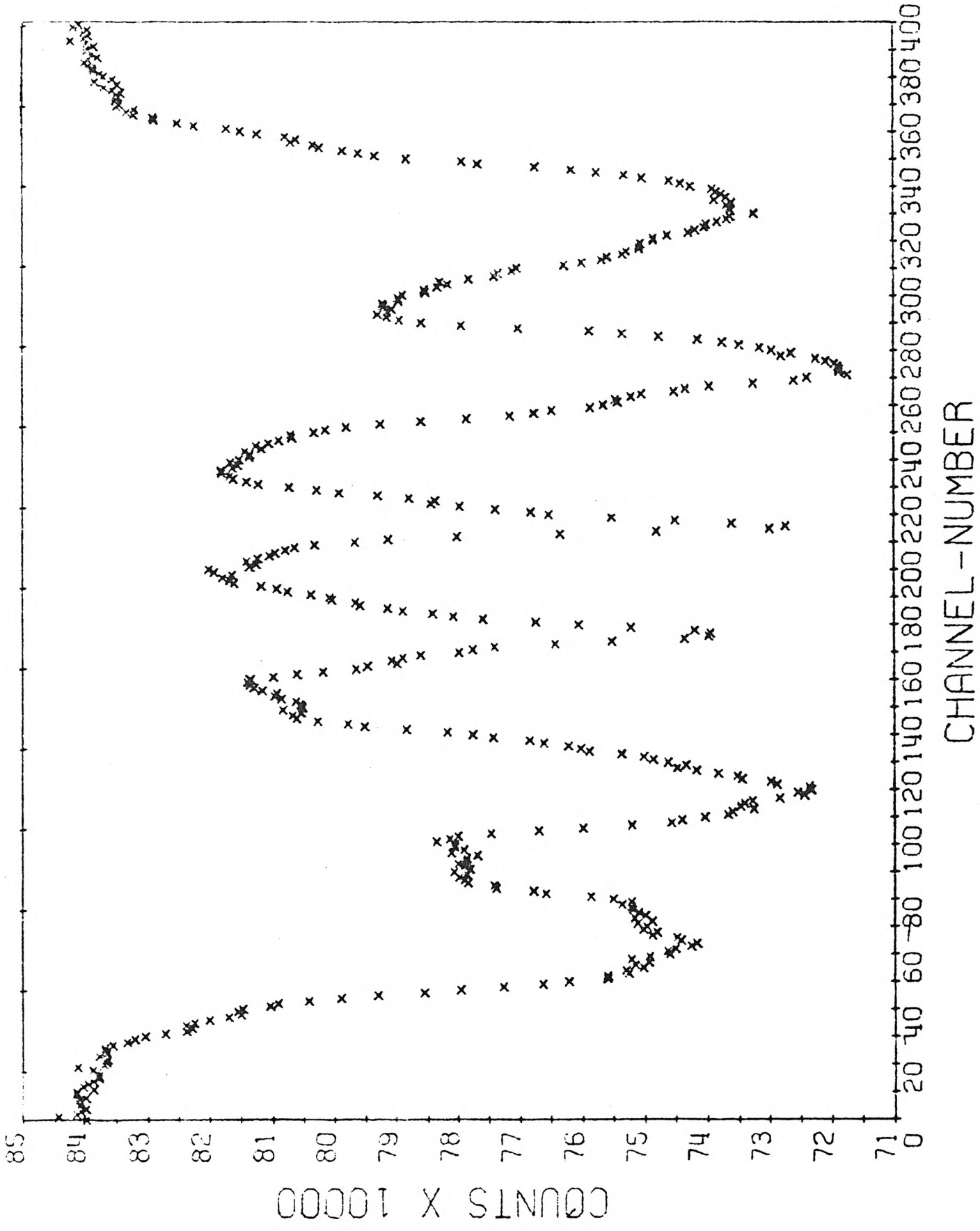

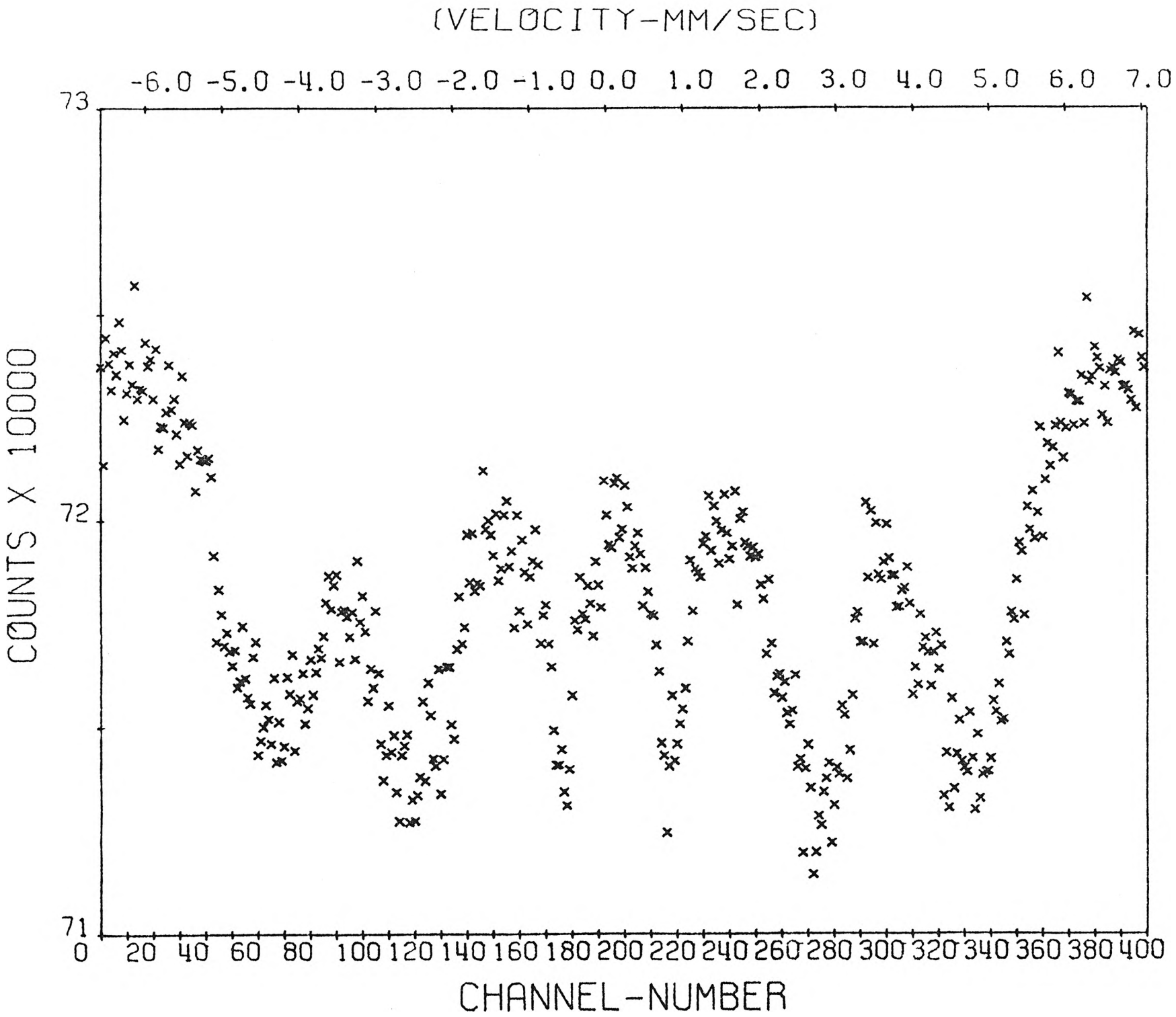

FIGURE 38 IRON - ALUMINUM FILLINGS DISORDERED BY COLD WORKING

CONCLUSION

From theoretical and experimental considerations, the utilization of the Mössbauer effect for the acquisition of the kinetics of ordering for any two phase order system by noting the change in one phase's absorbing nuclide's environment is infeasible.

The infeasibility arises from the Mössbauer effect sensitivity to all absorbing nuclides, and therefore its inability to distinguish between the two phase order.

BIBLIOGRAPHY

1. H. J. Lipkin, Ann. Phys. Vol. 9, No. 332 (1960); Vol. 18, No. 182 (1962).

2. R. N. Kuz'min and S. A. Losiyevskaya, Fiz. Metal. Metalloved., Vol. 29, No. 3, 569-577, 1970.

3. L. Haggstrom, L. Granas, R. Wappling and S. Sevanarayanan, Physica Scripta, Vol. 7, 125-131, 1973.

4. Mossbauer Effect Data Index (1969 to 1974), IFI PLENUM, New York.

5. P. R. Swann, W. R. Duff, and R. M. Fisher, Tran Metal Society of AIME, Vol. 245, 851-853, 1969.

6. H. J. McQueen and G. C. Kuczynski, Trans. of Metal Society of AIME, Vol. 215, 619-622, 1959.

7. L. Rimlinger, Compt. Rend. Acad. Sci., Vol. 261, No. 4090, 1965.

8. Michael F. Bent, Borje I. Persson and David G. Agresti, Computer Physics Comm., Vol. 1, 67-87, 1969.

9. Denjiro Watanabe, Journal Phy. Soc. of Japan, Vol. 29, No. 3, 1970.

10. S. A. Losiyevskaya and R. N. Kuz'min, Russian Met., Vol. 3, 141-145, 1971.

11. Personal Correspondance with S. A. Lesiyevskaya and R. N. Kuz'min.

12. M. R. Lesoille and P. M. Gielen, Phys. Stat. Sol., Vol. 37, No. 127, 127-139, 1970.

13. P. R. Swann, W. R. Duff, and R. M. Fisher, Metal. Trans., Vol. 3, 409-419, 1972.

14. Mary Beth Stearns, (1964) Spin density measurements and the spin susceptibility of the 4s-conduction electrons in Fe, Presented at Magnetism Conference at Minneapolis

15. G. P. Rauscher, (1962) A study of the superlattice transformations in iron-aluminum alloys. Thesis, University of Denver, 71 p.

16. Kensuke Oki, Masayuki Hasaka and Tetsuo Eguchi, Trans. JIM, Vol. 15, 143-149, 1974.

17. Kensuke Iki, Masayuki Hasaka and Tetsuo Eguchi, Trans. JIM, Vol. 14, 1973.

VITA

The author was born on October 13, 1951, in Springfield, Missouri. He has received his college education from Southwest Missouri State College in Springfield, Missouri, and the University of Missouri-Rolla. He received a Bachelor of Science degree in Metallurgical Engineering from the University of Missouri-Rolla in June 1973.

He has been enrolled in the Graduate School of the University of Missouri-Rolla since August 1971.